UNIVERSITA' DEGLI STUDI DI PADOVA

Sede Amministrativa: Università degli Studi di Padova

FACOLTA' DI FARMACIA
DIPARTIMENTO DI SCIENZE FARMACEUTICHE

SCUOLA DI DOTTORATO DI RICERCA IN SCIENZE MOLECOLARI

INDIRIZZO SCIENZE FARMACEUTICHE

XXI CICLO

TESI DI DOTTORATO

SYNTHESIS, QUALITY CONTROL AND PHARMACOLOGICAL STUDIES OF ^{99m}Tc- AND ^{188}Re-RADIOPHARMACEUTICALS FOR IMAGING AND THERAPY

Direttore della Scuola: Ch.mo Prof. MAURIZIO CASARIN

Supervisore: Ch.mo Prof. ULDERICO MAZZI

Dottoranda: ELENA ZANGONI

31 GENNAIO 2009

INDEX

SUMMARY - *RIASSUNTO*

The most important goal of the research in the radiopharmaceutical field is the development of radioactive isotopes containing drugs, suitable for the application in diagnosis and therapy.

Technetium-99m is a γ-emitter with optimal characteristics widely employed in Nuclear Medicine for imaging, and it is readily available as pertechnetate from the $^{99}Mo/^{99m}Tc$ generator.

Rhenium-188 appears to be promising as a candidate for the treatment of neoplasia for its β^- emission, available as perrhenate from a $^{188}W/^{188}Re$ generator, facility that makes it suitable for clinical use.

For the development of site-directed diagnostic and therapeutic radiopharmaceuticals, a biomolecule (hormones, peptides i.e.) with high affinity for a receptor-target should be labelled to deliver the radionuclide in a specific body region.

Labelled biomolecules must exhibit *in vivo* stability and retain receptor affinity after administration. The labelling protocol is therefore optimised depending on the structure of the desired biomolecule, then receptor binding studies and in vivo biodistribution studies on the labelled species must be performed to confirm the ability to accumulate on target cells or organs.

This work relates on the production of target-specific radiopharmaceuticals focusing on two types of biomolecules, somatostatin analogues and hyaluronic acid.

The first part of this work involves the indirect labelling of two somatostatin dicarba-analogues, named CIF and CIN, conjugated to the chelating agent PN_2S. Chapter 2 describes the adopted labelling protocols, which were carried out using two different metal cores: ^{99m}Tc-oxo for the CIN-PN_2S peptide, and ^{99m}Tc–tricarbonyl for the CIF-PN_2S peptide. Afterwards, stability studies and biodistribution studies in animal models were performed on the obtained complexes, which results are debated in chapter 3. In particular, [CIF-PN_2S-$^{99m}Tc(CO)_3$-DMTC] complex demonstrated to maintain its specificity for somatostatin-receptor expressing organs.

The second part of this work is focused on the direct labelling with ^{188}Re of the liver targeting agent hyaluronic acid. In order to evaluate the possible therapeutic use of the

obtained complex, stability studies and pharmacokinetics of ^{188}Re-HA were carried out, as reported in chapter 4. Afterwards, toxicity and dosimetry of the radiolabelled compound were evaluated, and finally therapeutic effect on animal models with induced liver cancer was studied. The encouraging results obtained, reported in chapter 5, prompted us to consider hyaluronic acids with different molecular weights (5, 10, 200 and 500 kDa), in order to determine if they can provide some advantages in liver uptake with respect to the HA previously studied. As reported in chapter 6, high molecular weight HAs were directly labelled with ^{188}Re and tested to evaluate their stability. Biodistribution studies in healthy mice showed that liver uptake was higher with respect to the 70 kDa HA used in the previous chapter. Therefore these high molecular weights ^{188}Re HAs seem to be promising agents for the treatment of liver cancer, since they enable a further reduction on the exposition of non target tissues to radiation damage.

RIASSUNTO - *SUMMARY*

La ricerca nella disciplina radiofarmaceutica ha come obiettivo primario lo sviluppo di composti contenenti isotopi radioattivi per applicazioni di tipo diagnostico e/o terapeutico.

Il tecnezio-99m è gamma emettitore dotato di ottime proprietà sia chimiche che nucleari, che ne giustificano l'enorme impiego nella diagnostica per "imaging" in medicina nucleare. E' inoltre disponibile nella specie pertecnetato grazie al generatore $^{99}Mo/^{99m}Tc$, che per la sua reperibilità ed economicità è presente in quasi tutti gli ospedali.

Il renio-188 invece è un radionuclide beta-meno emettitore, particolarmente interessante per il potenziale trattamento radioterapico dei tumori. Anch'esso viene prodotto mediante un generatore, rendendo dunque possibile un suo impiego nei reparti di medicina nucleare.

La marcatura con un tracciante radioattivo di biomolecole con affinità recettoriale si inserisce nel settore della produzione di radiofarmaci target-specifici. In particolare questa strategia deve portare all'ottenimento di specie stabili *in vivo* e non deve alterare la loro biospecificità. Il metodo di marcatura deve quindi essere studiato in funzione della biomolecola in esame, e successivamente devono essere effettuati studi di binding recettoriale e di biodistribuzione *in vivo* per confermare la capacità della specie marcata di accumularsi a livello dell'organo o delle cellule bersaglio.

Questo lavoro di tesi affronta la produzione di radiofarmaci recettore-specifici attraverso lo studio di due biomolecole, derivati della somatostatina e acido ialuronico.

La prima parte del lavoro riguarda la marcatura indiretta di due dicarba-analoghi della somatostatina, CIF e CIN, derivatizzati con il set chelante PN_2S. Nel capitolo 2 vengono riportati i due protocolli di marcatura adottati, che prevedono l'impiego di due diversi centri metallici: ^{99m}Tc-oxo per il peptide CIN-PN_2S e ^{99m}Tc –tricarbonile per il peptide CIF-PN_2S. Successivamente sui complessi ottenuti sono stati eseguiti gli studi di stabilità e biodistribuzione in animali, i cui risultati sono discussi nel capitolo 3. Il complesso [CIF-PN_2S-$^{99m}Tc(CO)_3$-DMTC] ha dimostrato mantenere la specificità per gli organi esprimenti recettori per la somatostatina.

La seconda parte di questo lavoro invece si è concentrata sulla marcatura diretta con ^{188}Re di acido ialuronico quale agente direzionante per il fegato. Al fine di valutare il possibile impiego terapeutico del complesso ottenuto, sono stati eseguiti studi di stabilità e

farmacocinetiche di ^{188}Re-HA riportate nel capitolo 4. Successivamente, sono state prese in esame la tossicità e la dosimetria legate alla somministrazione del composto marcato, per poi studiarne l'effetto terapeutico su modelli animali con tumore epatico. I risultati incoraggianti di questo studio, riportati nel capitolo 5, ci hanno indotto a prendere in esame acidi ialuronici a diversi pesi molecolari (5, 10, 200 e 500 kDa), per verificare se potessero offrire dei vantaggi rispetto all'HA precedentemente utilizzato dal punto di vista dell'accumulo nell'organo bersaglio. Come riportato nel capitolo 6, i derivati ad elevato peso molecolare una volta marcati direttamente con ^{188}Re, sottoposti ai successivi studi di stabilità e di biodistribuzione in animali sani, hanno evidenziato come l'accumulo di HA a livello epatico sia maggiore rispetto all'acido ialuronico (70 kDa) utilizzato nei trattamenti terapeutici, risultando così vantaggiosi poiché permettono di ridurre ulteriormente l'esposizione dei tessuti non target al danno da radiazione.

1

INTRODUCTION

1.1 DIAGNOSTIC AND THERAPEUTIC RADIOPHARMACEUTICALS

Radiopharmaceuticals are radionuclide containing drugs, and are employed as diagnostic or therapeutic agents. They are used routinely in nuclear medicine for the diagnosis (Imaging) and therapy (Radiotherapy) of various diseases [1]. The nuclear characteristics of the radioisotopes, such as chemical properties, mode of decay and half life, determine their potential application in medicine.

Since radioisotopes selection is essential for successful imaging and therapy, and for reducing whole body irradiation, great attention must be paid to this aspect [2]. Moreover, the stability of the radiopharmaceutical molecule must exceed the radioisotope half-life in vivo, thus isotopes with a generally short half-life (typically not more than 2-6 days) are preferred [3].

Radiodiagnostics are useful tools for supplying information about several medical problems such as cancer, infection, cardiological and neurological disorders, bone, kidneys and liver abnormalities.

Radiotherapeutics are designed for the treatment of neoplasia. Unfortunately, there are still a limited number of compounds employed for clinical use, but a great interest in the research led to many promising therapeutic radiopharmaceuticals, that are at various stages of development [4].

1.1.1 Imaging

Imaging is an essential part of medical practice, mainly in oncology, with a crucial role in screening programs, diagnosis and staging of established disease. Generally a clinical sign or symptom leads to many investigations as plain X-Ray, computed tomography (CT) scan or ultrasounds scan, which evidence abnormalities related to malignancy. The next step for an accurate diagnosis is the management of the patient to provide important prognostic information, such as the location of the tumour, its size and nature, in order to select the treatment with curative intent.

CT and magnetic resonance imaging (MRI), with high soft tissue resolution, have made a significant contribution in terms of morphological definition. Unfortunately they are not able to provide functional information, which are essential in detecting tumour type and also for comparing the results of clinical trials during treatment. Furthermore the assessment of disease status based on anatomical measurement is not the correct modality to perform a cancer diagnosis. Tumour size can not be associated with the viability of malignant cells and changes in the dimension of solid tumours are frequently seen only over a period of months depending on the course of chemotherapy. Consequently the development of imaging tools, able to detect functional changes soon and after starting treatment as well as morphological images, is an important aim in Molecular Imaging research.

Molecular Imaging is "the *in-vivo* characterisation and measurement of biological processes at the cellular and molecular level" [5]. The most employed and studied modalities belong to nuclear medicine, but MRI with specific contrast agents and Fluorescence Spectroscopy are also currently under investigation. A great advantage of all these techniques is determined by the fact that they are non-invasive, avoiding the potential hazards of surgical procedures (i.e. tumour biopsy).

Nuclear medicine techniques are by far the most developed and improved procedures to obtain functional images, carried out by administering small amount of a radioactive compound (diagnostic radiopharmaceuticals or radiodiagnostics having differential accumulation in the diseased tissue) and detecting radiations escaping from the body. For diagnostic imaging purposes the radiation must be able to penetrate the tissues of the patient and be detected by external instrumentation. Imaging modalities widely used in

nuclear medicine include Gamma Camera Scintigraphy, Single Photon Emission Computed Tomography (SPECT) and Positron Emission Tomography (PET).

Gamma Scintigraphy and SPECT ideally require radiopharmaceuticals containing a pure γ-emitting nuclides with a suitable emission-energy, typically 100-250 keV. Radioisotopes that decay with energy lower than this range produce scattering effects while those with higher energy are difficult to collimate. In both cases low quality images are collected. The defined optimum energy range for the medical facilities currently present in hospitals is 100-200 keV. Table 1 shows a selection of gamma radiometal-isotopes with nuclear characteristics and methods of production.

Isotope	$T_{½}$ h	γ-Radiation (keV)	Production
^{99m}Tc	6.02	140	Generator
^{111}In	67,9	245, 172	Cyclotron
^{67}Ga	78,3	91, 93, 185, 296, 388	Cyclotron
^{201}Tl	72	135, 167	Cyclotron

Table 1 Selected gamma-metal-radionuclides for diagnostic applications

The technetium-99m (^{99m}Tc), thanks to its excellent nuclear properties and availability (as reported in the following chapters), is the radioisotope of choice in nuclear medicine for the scintigraphy and SPECT [6].

PET was initially developed in the 1960s but has largely been used as a research tool. This technique requires a radiopharmaceutical labelled with a positron-emitting radionuclide (β^+, Table 2).

During emission the positron traverses a few millimetres before combining with an electron (annihilation), converting it into energy with the production of two 511 keV photons travelling 180° apart. The radioactivity is detected outside of the patient by a circular array of cameras with coincidence circuits, and subsequently used to reconstruct tomographic images of regional distribution.

Fluorine-18, often associated with the compound fluorodeoxy-glucose (FDG), is the most employed tracer with PET technique since it allows imaging in a large variety of malignant tumours and metabolism diseases.

Isotope	$T_{½}$	Radiation (KeV)	Production
^{11}C	20.4 m	max β^+-960, γ-511	Cyclotron
^{13}N	10 m	max β^+-1190, γ-511	Cyclotron
^{15}O	122 s	max β^+-1720, γ-511	Cyclotron
^{18}F	110 m	max β^+-935, γ-511	Cyclotron
^{62}Cu	9.8 m	max β^+-2910, γ-511	Generator
^{64}Cu	12.9 h	max β^+-656, γ-511, β^-–573	Reactor
^{68}Ga	68.3 m	max β^+-1880, γ-511	Generator

Table 2 Selected positron-radionuclides for diagnostic applications (γ-radiation after annihilation)

Despite the high technology cost for both production and instrumentation PET is one of the most important developments in nuclear medicine. The unique characteristics of β^+ decay, associated with modern high-performance commercial PET scanners, allow excellent resolutions (3-4 mm vs 5-10 mm of SPECT) making PET the most interesting technique at present. These scintigraphic and tomographic analyses, even providing important biological and biochemical information, are limited by meagre anatomical definitions. Nevertheless nowadays nuclear medicine departments have been carrying out new SPECT-CT and PET-CT thus combining the functional information (pathologic situation) with the morphologic aspect, as depicted in figure 1.

Fig. 1 PET-CT in a nuclear medicine department and morphological-functional images

1.1.2 Therapy

Therapeutic radiopharmaceuticals are designed to deliver cytotoxic doses of ionizing radiation to tumours with high specificity, thus minimising normal tissue-damage.

The doses normally administered for routinely diagnostic PET and SPECT analysis are pathologically insignificant, since tumour cell destruction requires radionuclides decaying by particle emission (as α, β^-, and Auger electrons) which can induce cell apoptosis [7]. Ideal radioisotope properties for an application in therapy are still not well established [2], and total tumour eradication is rarely achieved by radiopharmaceuticals. An exception is reported for haematological malignancies such as non-Hodgkin's lymphomas [8].

Neoplasia size, morphology and intratumoural biodistribution (due to the heterogeneity of isotope deposition) basically determine the choice of radionuclide to be used for radiotherapy. In addition physical half-life is a critical consideration in therapeutic radiopharmaceuticals design. A slow delivery of radioactivity to the tumour and a prolonged localisation in situ and body residence (such as in the case of labelled monoclonal antibodies), requires the choice of a long half-life radionuclide [9]. On the contrary, if tumour uptake and clearance from the blood are rapid, radioisotopes with short half-life should be preferred [10]. The radioisotope should be densely concentrated and localised in the tumour to reach a successful treatment, since its radiation will damage primarily tumour cells. The number of ionisations per unit caused when a radiation traverses a cell or tissue, is called linear energy radiation transfer (L.E.T.). The concept involves lateral damage along the path, in contrast to path length or penetration capability. For single cell tumours, such as lymphomas and micrometastases, a very short-range emission is required to ensure an effective dose with minimal damage to normal tissues. For large carcinomas longer-range medium L.E.T. radioisotopes are preferred.

Actually β^--emitters (Table 3) are the most studied isotopes for radiotherapy, since they are highly radiotoxic but without causing the problems connected to the relevant cytotoxicity over the healthy cells typical of the α-emitters. Furthermore, Auger emitters such as Iodine-125 are interesting because of their capability to kill cells when deposited very close to nuclear structures, but this implyes that ^{125}I-radiopharmaceuticals must be internalised into the cell to achieve therapeutic response.

Therefore, monoclonal Antibodies (MoAb) or receptor specific molecules, depending on their capability to be internalised, can be associated with radioisotopes causing

apoptosis both from the interior and exterior of a cell. This strategy led to ZEVALIN® (Ibritumomab Tiuxetan), an immunoconjugate resulting from a stable covalent bond between the monoclonal antibody Ibritumomab and the linker-chelator tiuxetan, a restricted chelation site for Yttrium-90. ZEVALIN and BEXXAR (tositumomab labelled with ^{131}I), are the two FDA-approved radioimmunotherapies for patients with relapsed or low-grade B-cell recurrent non-Hodgkin's lymphoma (NHL).

Isotope	$T_{½}$ d	Radiation (KeV)	Production
^{153}Sm	1.9	β^--800, γ-103 (29%)	Reactor
^{89}Sr	50.5	β^--1460	Reactor
^{131}I	8.0	β^--810, γ-364 (81%)	Reactor
^{90}Y	2.7	β^--2270	Generator
^{64}Cu	0.52	β^--570, γ-511 (38%)	Cyclotron
^{111}Ag	7.5	β^--1050, γ-342 (6%)	Cyclotron
^{166}Ho	1.1	β^--1060, γ-810 (6.3%)	Reactor
^{186}Re	3.8	β^--1070, γ-137 (9%)	Reactor
^{188}Re	0.7	β^--2110, γ-155 (15%)	Generator

Table 3 Selected radionuclides for therapeutic applications

1.2 RADIOMETAL-BASED RADIOPHARMACEUTICALS

The ideal diagnostic and therapeutic radiopharmaceuticals would likely be physiologic molecules where a common constituent atom (such as carbon, nitrogen or oxygen) is replaced by a related radioactive isotope (^{11}C, ^{13}N or ^{15}O). The organism is therefore unable to recognize the labelled compound which maintains proper biodistribution. An alternative strategy is represented by the incorporation of monoatomic radiohalogens ^{18}F and $^{125\text{-}131}I$ into bioorganic molecules by means of a covalent bond formation, but these reactions may be very difficult. However the radionuclides with the best nuclear properties suitable for an application either in diagnosis or therapy are predominantly metals. These elements under normal conditions are not present in our bodies and must be stabilised by a suitable chelation system, which usually involve multiple heteroatom coordination. Once stabilised, the radiometal biodistribution can be determined by the properties of the total

coordination compound leading to an "essential or first generation radiopharmaceuticals", or by biological affinity of a carrier molecule bound to the stabilised metal in a "second generation radiopharmaceuticals" approach. In the first case size, charge and lipophilicity of the complex establish affinity to specific tissues, while in the second one the targeting ability resides in a biologically active molecule (BAM). This difference is marked in chapter 2.4 where some examples are also reported for technetium and rhenium. The use of radiometallic isotopes offers many opportunities for designing new pharmaceuticals by modifying the environment around the metal and allowing different in vivo behaviours. The design of radiometal-based compounds requires deep knowledge of both the physical and chemical properties of the chosen metal, but also of the physical properties of the radiometal complex. Knowing information such as redox properties, stability, stereochemistry, charge, and hydro-lipophilicity of the complex can help predict the in vivo behaviour, such as excretion pathway. For example, it is known that negatively charged compounds tend to clear through the kidneys, while positively charged ions accumulate in the heart, and an overall neutral complex is required for crossing the blood-brain barrier. Lipophilic complexes are usually cleared through the hepatobiliary system and may accumulate in fatty tissues.

1.3 TECHNETIUM AND RHENIUM

Among the range of metallic radionuclides suitable for clinical applications, technetium-99m and rhenium-186/188 play a fundamental role in the production of radiopharmaceuticals for diagnosis and therapy, respectively [11]. Most of diagnostic nuclear medicine imaging studies is carried out worldwide using technetium-99m. Rhenium-186 is used as bone pain palliative agent while the 188-isotope appears to be promising for preparing new compounds in the treatment of cancer.

1.3.1 ^{99m}Technetium

The element technetium (from the Greek word *technetos*, meaning artificial), and which presence was first predicted by Mendeleev, was discovered in 1938 by Carlo Perrier and Emilio Segrè [12]. Technetium is situated in the middle of the second-raw transition series

(Z = 43) and has no stable isotopes. There are currently more than 20 known isotopes, all radioactive.

The chemistry of this element was significantly developed after the 1970s because its metastable (m) ^{99m}Tc isotope had become the mainstay of diagnostic nuclear medicine. At present, nearly 80% of all radiopharmaceuticals used in nuclear medicine department are ^{99m}Tc-labeled compounds. The nuclear properties of ^{99m}Tc are virtually ideal for diagnostic imaging: it has a 6.02 h half-life and gamma–ray emission energy of 141 keV with 89% abundance. The decay is long enough to allow a radiochemist to carry out the preparation, quality control, administration of labelled compound to the patient and all nuclear medicine practitioners to collect images with commercial gamma cameras. At the same time the absence of tissue-damaging radiation allows the injection of activities higher than 30 mCi with low time exposure for the body. ^{99m}Tc in fact has not primary beta emission but only low energy Auger electrons, which are practically inoffensive to the tissues.

Another reason of the wide clinical use of this nuclide and that changed the field of nuclear medicine, was the development of the ^{99}Mo/^{99m}Tc generator by Walter Tucker and Margaret Greene (Brookhaven National Laboratories) in the early 1950s. Technetium is available as pertechnetate ($^{99m}TcO_4^-$) at low cost from this commercial generator, which is commonly present in every department of nuclear medicine. ^{99m}Tc is produced from a parent nuclide ^{99}Mo, as molybdate, a fission product with a 2.78 days half-life. Molybdate is absorbed to an alumina column in the generator and pertechnetate is formed by decay and eluted with saline (Figure 2).

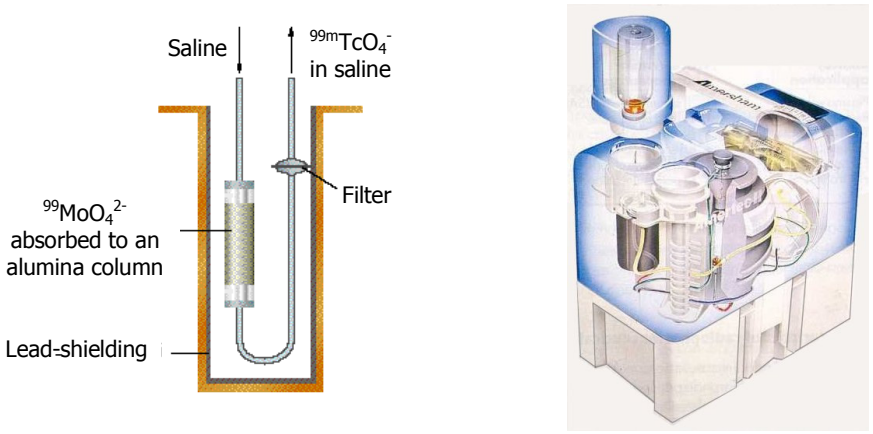

Fig. 2 ^{99}Mo/^{99m}Tc generator

The ^{99m}Tc eluted from the generator is not carrier-free since a small percentage of ^{99}Mo decays directly to the long-life isotope ^{99}Tc ($t_{1/2}$ = 2.13 x 10^5 years), which is also the single decay product of ^{99m}Tc. The specific activity of the eluted pertechnetate is very high and dependent upon prior-elution time. Generally the total concentration of the eluted species from the generator is in the range 10^{-7}-10^{-8} M.

A few years ago the preparation of two techenium-94 radioisotopes was carried out by the irradiation of molybdenum-94 in a cyclotron. Both ^{94m}Tc and ^{94g}Tc are positron emitters opening an interesting a useful application of the knowledge over ^{99m}Tc for PET imaging.

1.3.2 Rhenium

The element rhenium (from the Latin word *rhenus*, meaning river) was discovered in 1925 by Noddacks I. Tacke and O. Berg and located in the periodic table below technetium (Z = 75). It is one of the rare elements occurring naturally as a mixture of two non-radioactive isotopes ^{185}Re (37.4%) and ^{187}Re (62.6%). The nuclear medicine interest for rhenium has been stimulated by potential applications of two of its radioactive isotopes, ^{186}Re and ^{188}Re, for tumour therapeutic purposes thanks to the β^--emission and medium half-lives (Table 3) [13]. Rhenium-186 is already employed as a bone metastases palliative agent and its emission range (5 mm) suggests an application for small tumours, while the 188-isotope is suitable for large masses for its higher emission range (11 mm) and max. emission-energy. In addition to electron emission ^{186}Re and ^{188}Re decay with minor gamma emissions of 137 keV (9%) and 155 keV (15%) energy respectively, which allow the evaluation of in vivo biodistribution of rhenium-radiolabelled compounds with commercial gamma cameras.

^{188}Re is one of the most promising isotopes for therapy in the near future. It is conveniently produced in high specific activity, as a non-carrier added perrhenate ($^{188}ReO_4^-$) by using a commercial ^{188}W/^{188}Re generator. Perrhenate, formed by the radioactive decay of tungsten-188, is separated by an analogous chromatographic method of that used for ^{99m}Tc and eluted in saline solution at 10^{-11}M concentrations. Commercial generators charged with 0.5 Ci of ^{188}W are available and able to provide therapeutic treatments to hundreds patients over their 2-6 months lifetime.

1.3.3 Comparison between the chemistry of technetium and rhenium

The $^{99}Mo/^{99m}Tc$ and $^{188}W/^{188}Re$ generators are based on the analogous chemistries of both the group VIB (Mo and W) and VIIB (Tc and Re) congeners. In both generators the highest oxidation state of the parent nuclides are tightly bonded and retained by the alumina support, while the more negatively charged decay products can be eluted. The "lanthanide contraction" causes technetium and rhenium to have comparable radii and ensures that the analogous complexes display very similar coordination parameters and physical properties (size, lipophilicity, dipole moment, formal charge etc.), making their chemistry the same or nearly identical in many cases [14]. This provides a noteworthy example of Tc and Re behaving as a "matched pair" of elements, thus suggesting that the development of ^{99m}Tc-radiopharmaceuticals for tumour imaging paves the way for therapeutic radiopharmaceuticals.

Despite the analogies in terms of physical properties, the chemical properties between Tc and Re are expected to be different. Technetium complexes are simple to prepare starting from $^{99m}TcO_4^-$ because they are easier to reduce (less reducing agent, as $SnCl_2$, is required). On the other hand $^{188}ReO_4^-$ is harder to reduce (higher standard reduction) than the rhenium complexes obtained, thus confirming that this metal complexes are more stable in their higher oxidation state than their technetium analogues. This behaviour has practical consequences in nuclear medicine applications since reduced rhenium radiopharmaceuticals have thus a greater tendency to re-oxidized back to perrhenate than their technetium analogues to re-oxidize to pertechnetate. However this may be an advantage because it provides an ultimate elimination route of the non-targeted radioactivity via the urinary pathway. Furthermore rhenium complexes are more kinetically inert to substitution than technetium ones. These are some of the reasons why, despite the availability of $^{186/188}$Re starting materials, these radionuclides have been used less than other isotopes, such as ^{131}I or ^{90}Y, to formulate therapeutic radiopharmaceuticals.

1.3.4 Technetium and rhenium coordination chemistry

Technetium and rhenium belong to transition or *d* block elements, and give rise to multiple oxidation states (from –I, d^{10}, to VII, d^0). The starting materials in preparing radiopharmaceuticals are the respective permetallates $^{99m}TcO_4^-$ and $^{188}ReO_4^-$ that exhibit the highest oxidation number (VII) and also the most stable electronic conditions for the

metals, whereas most of the technetium- and rhenium-based radiopharmaceuticals contain the nuclide in a reduced form. Lower oxidation states are generally stabilized by complexation with a variety of inorganic and organic compounds (named ligands) resulting in complexes having various coordination geometries (from 4 to 9). However the synthesis of transition metal complexes requires a subtle interplay of thermodynamic and kinetic considerations. If Tc/Re (VII) species are reduced the final complexes depend upon the nature of reducing agents, the employed ligands and reaction conditions as reported in the works of Baldas et al. [15]. Rhenium is harder to reduce than technetium but it can quickly expand its coordination shell from 4 to 6, thus displaying better affinity than its congener to lead complexes with carboxylated donors such as citrate, tartrate and oxalate. Table 4 shows some Tc/Re cores, namely the form in which the metal is present in a complex.

Oxidation state	Cores
VII	MO_4^-
VI	MN^{3+}
V	MO^{3+}, MO_2^-, $M_2O_3^{4+}$, MN^{2+}, MS^{3+}
IV	M^{4+}, MP_2^{4+}, $MO(OH)^+$, $M(OH)_2^{2+}$
III	MP_3^{3+}, M^{3+}
II	M^{2+}
I	M^+, MP_6^+, $M(CNR)_6^+$
O	M, M_2
-I	M^-

Table 4 Oxidation states and metal cores for rhenium and technetium (M = Re, Tc)

The V^{th} is probably the most important oxidation state for medical application and usually has a metal-oxygen bond, named oxo-core, giving a five-coordinate structure and a tetragonal pyramidal geometry (four donor atoms in the basal plane and the oxygen in the apical position). However more oxygen can be bound to the metal which may be stabilised by a wide class of ligands, generating a variety of oxo-metal (V) complexes (MOL_n, MO_2L_n, $M_2O_3L_n$ etc.). The metal (III) and (I) complexes are known to have the ligand coordinated to the metal alone, being the core a "naked" Tc/Re metal atom (i.e., ML_n, M_2L_n, etc.), whereas the metal IV can exhibit both metal-oxo and "metal-naked" cores.

Low oxidation states are known to exist mainly in the organometallic field and have only recently started to receive considerable attention, after the introduction of $^{99m}Tc^{I}$ $[MIBI]_6^+$ (see chapter 2.4.1). A convenient aqueous synthesis for the cations *fac*-$[Tc/Re^{I}(H_2O)_3(CO)_3]^+$ and synthon $[Tc(N)(diphoshine\text{-}ligand)]^{2+}$ introduced the novel concept of *metal fragment* for the design of new radiopharmaceuticals (see chapter 2.7.2). The other oxidation states are less common (i.e.-I, II, and VI) or derivatives of the $Re^{0}_2(CO)_{10}$, as starting material to prepare other organometallic complexes.

The metal core determines the design of the ligand(s) framework and the choice of the donor atoms, which coordinate the metal centre. A stable complexation of the desired metal centre by using suitable ligands is essential for an application in vivo, providing products with high thermodynamic stability and kinetic inertness. It is well-known that, for a particular metal centre, ligands with higher denticity lead to high stability complexes, and this is a general rule followed in the research and development of new chelating set (an exception is $^{99m}Tc[MIBI]_6^+$). Therefore, ligands with high denticity should be of particular value for in vivo applications. In the case of technetium and rhenium, most of the complexes involve tetradentate open chained ligand systems containing nitrogen and/or sulphur as donor atoms.

The thiol group, but also carbamates, ditiocarbamates and ditiosemicarbazones, typically has great affinity for transition metals, and provide a strong coordination site in the ligand for the radionuclide [16]. On the other hand ligands containing the thiol group are instable because of their high sensitivity to oxidation. Therefore, thiol is generally protected with groups such as benzoyl, acetamido methyl or trityl, which is quickly removed before complexation.

Nitrogen containing groups (as amines, amides or heterocyclic containing N) generally do not suffer instability and display optimal stabilising performance both for rhenium and technetium [17]. It has to be pointed out that proteins are rich in these potential coordinating groups, thus giving a theorycal explanation for the “direct labelling method” for preparing radiopharmaceuticals as reported in chapter 2.5. On the other hand some donor groups present in the blood pool can partially or totally remove the selected ligand in the stabilisation of the metal, compromising both the stability and biodistribution of the labelled compound with a “transchelation effect”.

As a result, some non-conventional heteroatomic chelating systems have been under investigation for many years. Phosphine phosphorous is an excellent candidate because it possesses great bonding capability with early transition metals. The σ phosphorous-metal interaction, which uses the lone pair electrons on the P^{III} atom and a vacant orbital on the metal centre, can be associated to a synergic π back-donation form non-bonding $d\pi$ pair of electrons on the metal centre to the vacant $3d\pi$ orbital on the phosphorous [18].

Finally, the formation of isomers is not desired but usually occurs in many complexation reactions, and this possibility should be considered at the development stage because isomers can have different physical properties. In fact they can have a significant impact on the pharmacological behaviour of radiopharmaceuticals like organ accumulation, blood clearance and receptor binding. It is remarkable that minimal potential isomerism, using stabilising chelating agents, is required.

1.4 TECHNETIUM AND RHENIUM RADIOPHARMACEUTICALS

Functionally, all radiopharmaceuticals may be conveniently classified into two broad categories:

- radiopharmaceuticals whose biological distribution is determined strictly by blood flow and perfusion, named essential or perfusion agents. The target systems usually are glomerular filtration, phagocytosis, hepatocytes, clearance and bone absorption.
- radiopharmaceuticals whose biodistribution is determined by specific interactions, such as receptor binding, transporting or enzymatic interactions, thus targeting low-capacity sites. These are called second generation agents or target-specific radiopharmaceuticals.

The rapid expansion of using technetium in diagnostic nuclear medicine is related to the diffusion of a low cost commercial $^{99}Mo/^{99m}Tc$ generator available in every nuclear medicine department and to the contemporary development of single vial kits containing both reducing agent and chelating agent. These so-called instant kits afford to high-yields radiopharmaceutical in one step upon the addition of pertechnetate. The same $^{99m}TcO_4^-$ was

approved as agent for thyroid scanning in routine clinical use in the 1960. But now the routine clinical use can take advantage by employing several commercial ^{99m}Tc-radiopharmaceuticals.

1.4.1 First generation technetium radiopharmaceuticals (perfusion imaging)

Brain imaging

Regional cerebral blood flow can be determined by using ^{99m}Tc-complexes that can penetrate the intact blood-brain-barrier (BBB) in response to blood flow. Brain imaging agents are useful in detecting stroke and in general large zone with depleted flow. Many ligands were developed to form mononuclear, neutral, lipophilic and stable complexes. After administration they have a rapid uptake and wash out in the brain, but a significant amount of radiotracer is retained by enzymatic conversion, producing a fixed biodistribution and allowing SPECT imaging.

Ceretech (with hexamethylpropyleneamineoxime proligand, ^{99m}Tc-HMPAO, Figure 3-A), and Neurolite (with ethylenecysteinediester ligand, ^{99m}Tc-ECD) represent two examples of brain imaging agents.

Heart imaging

It was postulated that lipophilic unipositively charged complexes would accumulate in heart tissue using the Na/K ATPase mechanism as K^+ ion mimetics. This concept prompted to the development of some complexes and achieving the first approved myocardial perfusion agent was Cardiolite (^{99m}Tc-$[MIBI]_6^+$), depicted in Figure 3-B. This labelled compound accumulated via a diffusion mechanism and electrostatic binding due to the high mitochondrial membrane potential. Cardiotec (^{99m}Tc-teboroxime) the first neutral agent and ^{99m}Tc-NOET demonstrated that cationic charge is not essential.

The use of the cited compound, and others as Myoview (^{99m}Tc-Tetrofosmine), exhibit different distribution properties such as providing supplementary information for clinical imaging.

Kidney imaging

^{99m}Tc-Gluceptate (glycero-glucoheptonate) and ^{99m}Tc-MAG_3 (^{99m}TcO-mercaptoacetyl-triglycine, Figure 3-C) are employed for renal function imaging. They have a rapid wash out from the blood stream containing free carboxylic groups that prompt efficient renal excretion, involving kidney accumulation on the proximal convolute tube. The passage into and through the organs provides a measure of renal functioning.

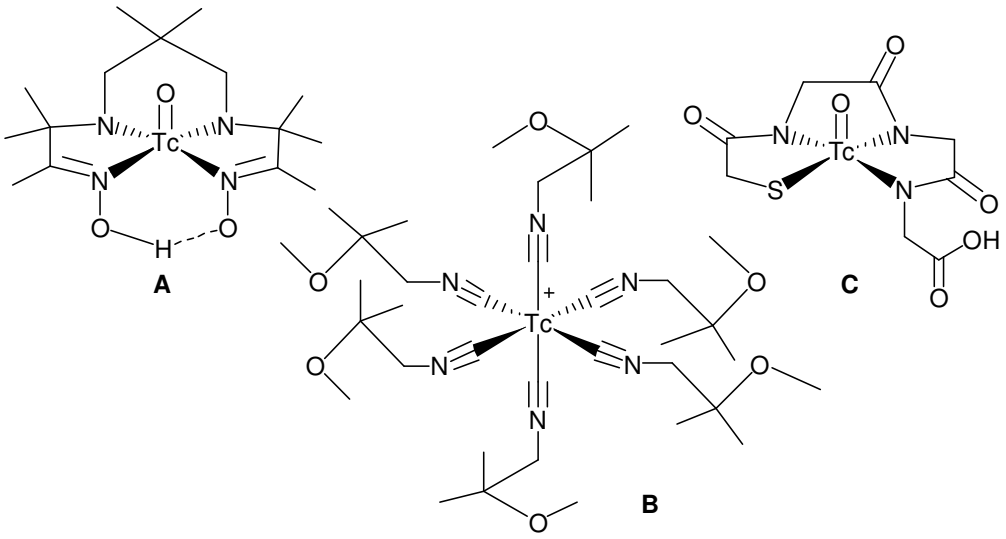

Fig. 3 Technetium essential radiopharmaceuticals Ceretech (A), Cardiolite (B) and MAG_3 (C)

Bone Imaging

A number of phosphonate ligands have been developed for the complexation of technetium for bone-imaging, and important agents are ^{99m}Tc-MDP (methylene diphosphonate, TechneScan) and ^{99m}Tc-HEDP (hydroxyethilene diphosphonate). The mechanism of absorption on bone is believed to be via integration of the labelled molecules to the bone surface due to the similarity to hydroxyapatite. Since stressed bone has a higher concentration of calcium ions, these areas appear as “hot spots” on the images, providing information on lesions which may not be visible by conventional X-Ray methods (i.e. metastases).

Liver imaging

Some technetium complexes have shown to be suitable for imaging the hepatobiliary system. Choletec (^{99m}Tc-Mebrofenin), Hepatolite (^{99m}Tc-Disofenin), TechneScan HIDA, (^{99m}Tc-Lidofenin), ^{99m}Tc-albumin colloid and ^{99m}Tc-sulphur colloid are usually employed to monitor the liver functionality.

1.4.2 Second generation or target-specific technetium radiopharmaceuticals

The growing demand for radiopharmaceuticals more specific than the "essentials" has prompted the development of a new class of labelled compounds. Despite enormous research efforts to achieve a useful and routinely applicable ^{99m}Tc-target-specific radiopharmaceutical, there are very few compounds with FDA approval in clinical use [19]. These can be classified according to the receptor site or biological function, and gave rise to the research field "molecular imaging".

The labelled compound once administered is first distributed by the blood stream, then uptake and retention rely on specific interactions. Labelling of a biologically active molecule (BAM) that binds with high affinity and specificity for a receptor is the most common example. The bioactive molecule acts as a vehicle, which carries the radionuclide to the receptor site at the diseased district. The uptake must be selective and depends on the concentration of the target receptor. Therefore the over-expression of cell surface or nuclear receptors in malignancy is a premise for receptor-based radiopharmaceuticals. First the relation between a disease and the receptor expression must be described both on chemical and clinical grounds. Then the receptor concentration in the target has to be determined and be sufficiently high to discriminate the ill from healthy tissue. The last identified selective biomolecule must be able to recognise the target with high affinity and specificity both before and after labelling. Finally, the non-bound labelled compound has also to be quickly removed from the body to give an optimal target / non-target ratio, thus providing good quality images.

The carrier or vehicle class involve a large range of biomolecule: from high molecular weigh polypeptides, such as monoclonal antibodies, to small peptides, peptido-mimetics, hormones and other non-peptide receptor ligands.

Some examples of routine clinical target-specific agents can better explain this concept.

^{99m}Tc-Nofetumomab merpentan and ^{99m}Tc-Arcitumomab are labelled murine monoclonal antibody Fab fragment for the imaging of tumours, particularly small cell lung cancer (SCLC) and colonrecto metastases. ^{99m}Tc-TRODAT (a cocaine derivative with selectivity for dopaminergic sites) has been tested for several years in the diagnoses of Parkinson's disease. Apomate (^{99m}Tc-HYNIC-annexin-V) is a promising molecular agent that identifies concentrated sites of apoptosis associated with cancer therapy, myocardial infarction, and atherosclerotic plaques. ^{99m}Tc-HYNIC-Octreotide and Lanreotide are important tools for the in vivo localisation of somatostatin receptor–positive tumours.

1.4.3 ^{188}Rhenium radiopharmaceuticals

Rhenium-188 is a radionuclide with excellent specific properties that has been used to label many therapeutic molecules, including monoclonal antibodies and peptides. One potential advantage over other radionuclides is its routine availability because of the ^{188}W/^{188}Re generator, but the more simple chemistry of yttrium-90 or lutetium-177 may be the cause for which ^{188}Re is still less used in clinical practice. Nevertheless, preclinical and clinical studies have demonstrated favourable pharmacokinetic and dosimetric properties for several ^{188}Re-based therapeutics.

Current internal radionuclide therapy in humans is based almost exclusively on beta-particle-emitting radionuclides. Because of the low LET of beta particles, the use of rhenium-188 as a therapeutic agent requires a high radionuclide concentration within the target tissue and the traversal of several thousand electrons per mammalian cell nucleus. Since the maximum range in soft tissue of each rhenium-188 beta particle is 10.4 mm, the cross-fire effect is possible, a consequence that avoids the need to target every cell within the tumour and to internalize the radionuclide in each targeted cell [20].

At present, ^{188}Re is one of the most common radionuclides used in clinic for radioimmunotherapy (RIT), and it was used for example in the labelling of the monoclonal antibody (MoAb) against CD66 antigen, a target of great interest in the case of leukaemia, in high-risk leukaemia patients. This labelled compound was employed as a strategy to destroy residual tumour cells in patients with limited tumour load prior to hematopoietic stem cell transplantation [21]. Also Rituximab, a chimeric monoclonal antibody directed against theCD20 antigen, approved by the FDA in 1997 for lymphomas, was efficiently labelled with ^{188}Re starting from lyophilized formulations [22].

Solid tumours are generally more radioresistant than, for example, lymphocytic tumors and to achieve tumour response require higher doses than those needed to obtain a response in hematological malignancies. The biodistribution, pharmacokinetics and dosimetry of ^{188}Re-labeled MN-14, an IgG anti-carcinoembryonic antigen monoclonal antibody, were reported in 1998 in patients with advanced gastrointestinal cancer, being the first time that ^{188}Re was used in RIT [23]. Several other MoAbs labelled with this radionuclide are currently under investigation for their application as RIT agents.

Another strategy in cancer targeted therapy is represented by the use of ^{188}Re-labeled peptides. ^{188}Re-labeled somatostatin analogues have been reported as radiopharmaceuticals with good properties for peptide receptor radionuclide therapy (PRRT) but until now they have only been evaluated in preclinical studies [24].

Finally, among the non-specific rhenium radiopharmaceuticals, ^{188}Re-lipiodol is now the agent of choice for radioembolization in patients with primary or secondary hepatocellular cancer (HCC) [25]. This malignancy is correlated to a very poor prognosis and a short survival time, but clinical trials with ^{188}Re-lipiodol, easily prepared using the bifunctional chelating agent 4 hexadecyl-1,2,9,9-tetramethyl-4,7-diaza-1,10-decanethiol (^{188}Re-HDD-lipiodol), revealed to be a safe and promising treatment for HCC.

1.5 TARGET-SPECIFIC RADIOPHARMACEUTICALS: LABELLING METHODS FOR TECHNETIUM, RHENIUM AND OTHER RADIOMETALS

The techniques to produce technetium and rhenium radiopharmaceuticals are generally classified into two main categories as “direct and indirect labelling methods”. There is also a third approach, which is elegant but practically unemployed, defined as integrated design [26].

1.5.1 Direct labelling approach

The direct labelling approach involves the coordination of the reduced metal (mainly technetium oxo-V) through donor atoms present in the targeting molecule or biomolecule, as represented in Figure 4. It was first performed more than 20 years ago on HMW (high molecular weight) proteins and antibodies with technetium, when Buck Rhodes developed the first kit method using stannous chloride [27]. The candidates to stabilise the metal core are usually disulphide bridges, carboxylate, amido and other side chain functional groups.

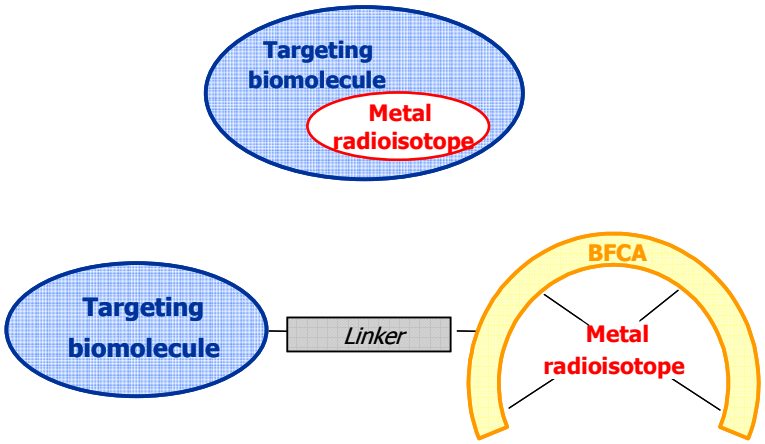

Fig. 4 Schematic representation of two strategies of target-specific radiopharmaceutical design: direct labeling (top) and bifunctional approach (bottom)

This is a convenient way to prepare radiolabelled compounds, since it is easy to carry out. However very little is known about the number of donor atoms and the coordination geometry around the metal centre, therefore this procedure is often not applicable to low molecular weight (LMW) peptides or small compounds in general, because it leads to a deep modification in the original structure that can be critical for maintaining biological properties. Furthermore, an in vivo dissociation of initially bound tracer is often observed. This is why only limited studies were performed to prepare ^{99m}Tc-macromolecules by the direct approach.

1.5.2 Indirect labelling approach

The alternative and most commonly employed method involves the attachment of strong chelating groups, named BiFunctional Chelating Agent (BFCA), to biologically active molecules (BAM), as depicted in Figure 4. The BFCA comprises a donor atom set

which strongly coordinates the radiometal and a functional group to be covalently attached to the targeting molecule, either directly or through a linker, thus producing a stable target-specific radiopharmaceutical with both in vitro and in vivo favourable characteristics. The binding affinity can be maintained by carefully selecting the coordination fragment and the conjugation site in the BAM backbone, chosen far from the receptor recognising motif. Moreover the coordination chemistry toward a selected metal can be developed and described without BAM with usual chemical techniques. Therefore it is not surprising that all the new target-specific radiopharmaceuticals approved or under clinical investigation use this method.

On the other hand, it must be considered that the "metal tag" is not totally innocent because the metal and coordination system may affect target uptake and biodistribution of the labelled compound. Especially for small BAM the nature (hydrophilic or lipophilic) and size of the BFCA-radiometal complex can be critical factors for maintaining the biological affinity for their target, mainly if this is intracellular [28]. A strong chelation for the radiometal is essential, but it is not useful as a successful strategy if it greatly modifies biological behaviour.

Some problems may also involve HMW BAM, such as MoAb or macropeptides, during the introduction of suitable BFCA. This procedure may induce intramolecular cross-linking which reduces both stability and interaction with the target of the labelled compound, especially with chelating systems including thiols. Thus, thiol-free or thiol-protected (to be deprotected just before complexation reaction) ligands are preferred and investigated for metal stabilisation and HYNIC- (hydrazine-nicotinic) MAG_3- (for ^{99m}Tc and $^{186/188}$Re), DOTA-, DTPA- (for ^{111}In an ^{90}Y) based linkers are available conjugated to BAM with different sizes [29].

1.5.3 Integrated approach

A very smart and interesting approach is to integrate the receptor binding sites directly around the radiometal periphery, like a "trojan horse". A heterodimer of two different aminothiol derivatives was applied to prepare 99mTc-labelled steroid analogues, considering that the dimension and the shape of the metal sphere could replace the missing part of the BAM (Figure 5). As expected for the initial model receptor-binding affinity was found to be low, but the approach really makes for a good study [30].

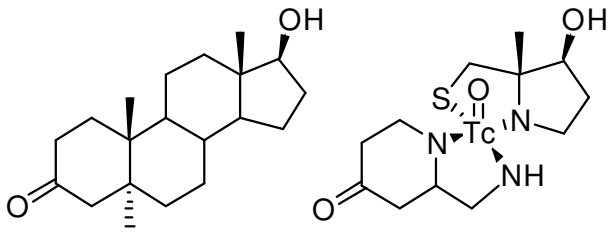

Fig. 5 Integrated approach for the design of a dihydrotestosterone (left) mimetic radiolabelled compound (right)

1.6 DESIGN AND DEVELOPMENT OF NEW TECHNETIUM AND RHENIUM TARGET-SPECIFIC RADIOPHARMACEUTICALS

As mentioned before the most popular approach to synthesise new labelled compounds with target-specific activity is the "indirect method". The radionuclide is linked to a BAM by using a BFCA suitable both to stabilise the metal and to realise the connection to the carrier molecule. The labelling reaction modality can be carried out applying two routes: pre-conjugation and post-conjugation labelling [31].

The pre-conjugation labelling approach involves formation of the ^{99m}Tc/$^{186/188}$Re complex with a BFCA and the following conjugation of the preformed complex to the biomolecule in a separate step at tracer level. The advantage of this approach is that the chemistry is well defined and potential coordinative groups of the selected BAM are less exposed to modification for the forcing condition used in the metal complexation step. However, this technique is often too complex and time-consuming for routine clinical use.

In the post-conjugation labelling approach the BFCA is first linked to the BAM forming the BFCA-BAM conjugate, which then undergoes the labelling reaction.

This approach combines the ease of direct labelling with the well-defined chemistry of the preformed chelate approach. The knowledge for the preformed BFCA-metal complex can be useful to define the preferred coordination modality without affecting the biological integrity of BAM.

This approach is by far the most common and, therefore, research is continuously producing new BFCA-BAM for different diagnostic and therapeutic radiometals. The development of a suitable ideal "building-block", or a "coordinated metal-fragment", to be tested first with the metal without the presence of a BAM and than conjugated to the BAM to study the behaviour in "post-conjugation direct labelling conditions", is the aim of many research groups [32].

There are several requirements for an ideal BFCA. It should selectively stabilise a defined metal oxidation state, thus avoiding further redox-reactions that are often accompanied by transchelation prompted by the chelating groups present both in the BAM and in the biological media. BFCA should also exhibit thermodynamic stability, kinetic inertness with respect to dissociation and minor tendency to produce isomers, because they often possess different biological and pharmacokinetic characteristics that can condition the BAM *in-vivo* behaviour. Furthermore, the BFCA must be easily conjugated to the BAM fragment selected.

From a structural point of view BFCA can be divided into three parts: a chelating group suitable for coordinating the metal, a spacer or linker that can also act as pharmacokinetic modifier, and the binding unit useful for conjugation to the BAM, as reported in Figure 4 (Chapter 2.5).

The development of a target-specific radiopharmaceutical for clinical use is a long and complicated process. Selection of the target (i.e. receptor or enzyme) and relative BAM is a priority, followed by the choice of a potential radionuclide-BFCA system to formulate a "start-up" diagnostic or therapeutic radiopharmaceuticals. Proof of the biological stability and efficacy in vitro and in vivo systems (i.e. by using malignant cell lines, healthy and diseased animal models) conclude the preclinical stage. Finally, the radiopharmaceuticals of choice must undergo a clinical evaluation (phase I-III) to assess their safety in addition to sensitivity and specificity to the target of interest [31].

1.7 BIFUNCTIONAL CHELATING AGENTS FOR THE MOST IMPORTANT ^{99m}Tc AND $^{186/188}$Re CORES

The choice of BFCA is largely dependent on the nature and oxidation state of the metallic radionuclide. It serves two purposes: to bind the metal radionuclide securely without dissociation in vivo and to provide structural appendance for BAM linkage maintaining maximal its biological integrity.

At present $[M^{V}O]^{3+}$ and some organometallic fragments, such as metal-tricarbonyl species, are the most interesting cores for the design of both new technetium and rhenium target-specific radiopharmaceuticals. The HYNIC system is another useful tool for labelling with ^{99m}Tc, and although not explored in this work still deserves an important mention. Since the method is versatile and the complexes very robust many LMW and HMW BAM were labelled. However the products are in general poorly characterised because the chemistry of coordination is quite complicated and so not well defined. Moreover this labelling strategy seems of little use for rhenium compounds, because of the instability of the resulting complexes.

1.7.1 BFCA for $[^{99m}TcO]^{3+}$ and $[^{186/188}ReO]^{3+}$ cores

The $[M^{V}=O]^{3+}$ or M^{V}-oxo (M= Tc, Re) core is the most frequently studied for the development of ^{99m}Tc and $^{186/188}$Re-labelled compounds, being very stable in the biological media. The desired M^{V}-oxo state can be achieved by reducing the permetallate solution eluted from the generator. Many reducing agents were tested but Sn(II) is the most commonly used for preparing technetium-99m commercial kits. This is due to the fast reduction kinetics when reacting with $^{99m}TcO_4^-$, avoiding harsh conditions that may decompose the BFCA. However Sn(II) often leads to significant problems, such as the formation of the insoluble colloids $Tc^{IV}O_2$ and $Sn^{IV}O_2$ that compromise radiolabelling yields.

The lower oxidizing power of perrhenate as compared with pertechnetate makes rhenium more difficult to reduce into lower oxidation states. The reduction of ReO_4^- is also generally accomplished by the addition of Sn(II) in acidic solution. However, due to the readily reversible redox reaction of Re(VII), Re(V) and Re(IV), a considerably higher amount of Sn(II) is required for radiolabelling with $^{186/88}$Re.

The strategy employed to limit the radioactive by-products is application of the "two-steps ligand exchange reaction". This method involves the reduction of the permetallates in presence of a weak chelating agent, such as gluconate, glucoheptonate or tartrate, able to stabilise the metal in the oxo-state. The intermediate complex [MO(exchange ligand)$_2$] is then reacted with the developed BFCA-BAM under mild conditions (pH, temperature etc.) to give the wanted ^{99m}Tc and $^{186/188}$Re-labelled compounds.

A variety of BFCAs with optimal in vivo stability and insignificant BAM bioactivity reduction have been developed over the last 20 years. Most of those reported in the literature are based on the $N_xS_{(4-x)}$ framework, such as N_2S_2 diaminothiols, diamidethiols and monoamidemonoaminodithiols (DADT, DADS, MAMA), N_3S triamidethiol and mercaptoacetylglycine (MAG_3), or N_4 propylene amine oxime (PnAO), as depicted in Figure 6 [33].

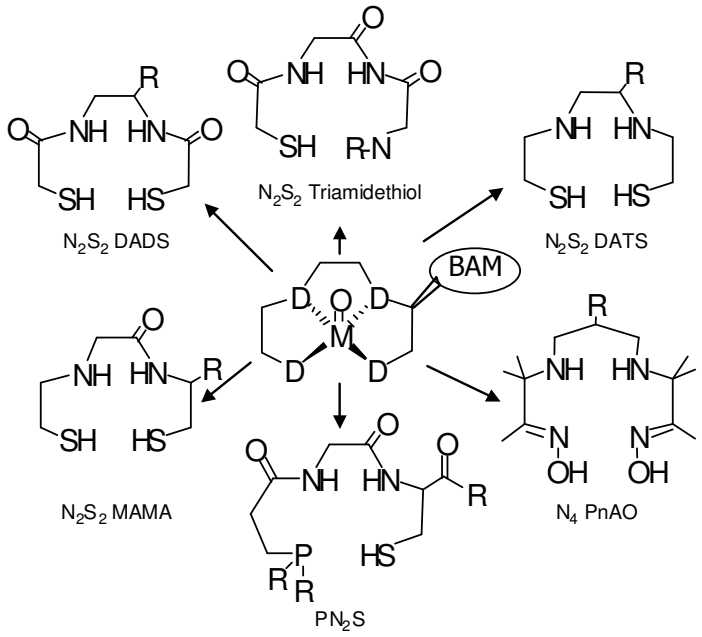

Fig. 6 BFCAs coordinating the $[M^V{=}O]^{3+}$ core (M= Tc, Re) useful for the design of target -specific radiopharmaceuticals (D = general coordinating atom)

Although these chelators are used in a large number of technetium-99m radiopharmaceuticals they are subject to certain limitations. The complexes resulting from coordination may be limited by enhanced size, lipophilic nature and reduced flexibility, altering the affinity of the labelled BAM for the target and prompting high liver uptake and

hepatobiliary excretion. Furthermore many of these chelating agents are asymmetrical producing two or more isomers with the oxo-metal core, often difficult to separate, displaying different behaviour in vivo.

Finally, some of these chelates, especially the bis amine-oximes, have limited stability *in vitro* and *in vivo* [34] and sometimes, harsh reaction conditions (e.g., high temperatures and extended reaction times) are required to form the corresponding complexes with high specific activity, or their labelling efficiency is low [35]. Consequently variations of the conventional $N_xS_{(4-x)}$, as N_xP_y, S_xP_y and $N_xS_yP_z$ sets were synthesised and tested [36]. For the last several years, there has been a growing interest in using small peptides, such as Gly-Ala- Gly-Gly and Gly-Ser-Cys, as BFCAs for Tc and Re labelling [37]. There are several advantages of using small peptides as BFCAs. First, the attachment of the BFCA can be easily achieved into solid-phase peptide synthesis. Second, these tripeptide chelating sequences usually form stable technetium complexes with the $[TcO]^{3+}$ core. Finally, the hydrophilicity of the technetium chelate can be tuned by changing side chains of the tripeptide or polypeptide chelating sequence. Our group recently proposed a PN_2S fashion with the presence of phosphine phosphorous for a tetradentate ligand as reported by Visentin et al. (Figure 6). This set exhibits high affinity for $[M^V{=}O]^{3+}$, and one of its advantages is that the radiolabelling reaction can be performed at ambient temperature. Moreover, this coordination set leads to complexes with good stability in plasma and in vivo and thus, can be considered a promising candidate for the design of new radiopharmaceuticals. Unfortunately the formation of two isomers, named syn and anti, is often observed [38]. An alternative strategy for the stabilisation of the M^V-oxo state by tetracoordination involves a mixed ligand set of a tridentate thiolate ligand of the type $[S\text{-}X\text{-}S]^{2-}$ (X=O, S, NR) and a monodentate thiolate, so named "3+1 mixed ligand approach" [39]. The main limit of this chelating system is its relative instability in biological media due to substitution of the labile monodentate coordinated ligand (transchelation).

1.7.2 BFCA for organometallic fragments

Great efforts are being made applying organometallic technetium and rhenium complexes to radiopharmaceutical design. Here two examples of metal fragments employed for tethering a BAM are reported in Figure 7.

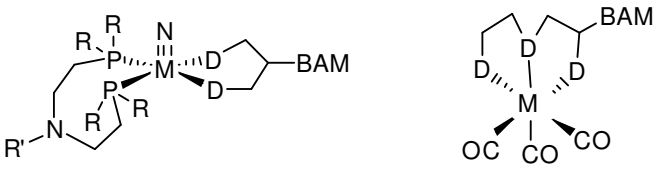

Fig. 7 $[M(N)(\text{diphoshine-ligand})]^{2+}$ and *fac*-$[M(CO)_3]^+$ organometallic cores (M= Tc, Re) for the design of target -specific radiopharmaceuticals (D = general coordinating atom)

Duatti et al. proposed a class of labelled compounds based on the metal-nitrido fragment. The Tc≡N precursor is quickly prepared using a currently available kit formulation, reducing $^{99m}TcO_4^-$ with Sn(II) and succinic hydrazide in the presence of a phosphate buffer and a Sn-chelating agent in a quantitative yield [40]. This moiety can be reacted then to form the versatile metal synthon $[Tc(N)(\text{diphoshine-ligand})]^{2+}$, which is an interesting basic motif for stabilisation by a BFCA-BAM system. Since soft π-donor bases containing S^- and O^-, such as amino acid cysteine (Cys), display optimal coordinating capabilities toward this fragment a number of Cys-derivatised ligands with small BAM (benzodiazepines and $5HT_{1A}$ receptor agonists for the study of central nervous system diseases) and medium BAM (i.e. distamycin for tumour imaging) were developed and tested [41].

Recently, the Tc and Re radiopharmaceutical development by using organometallic fragments has also been intensely stimulated by the fundamental contribution of R. Alberto, R. Schibli and P. A. Schubiger with the development of novel and simple methods for preparing the aquaions *fac*-$[^{99m}Tc(H_2O)_3(CO)_3]^+$ and *fac*-$[^{188}Re(H_2O)_3(CO)_3]^+$ [42]. These radioactive moieties are easily produced at tracer levels from pertechnetate in saline solution employing the commercially available "Isolink" kit (Mallinckrodt Med., BV Pettern, The Netherlands), and from perrhenate in slightly different conditions, paving the way for both diagnostic and therapeutic routine applications. The reactions involve the reduction and direct carbonylation of $^{99m}TcO_4^-$ (with $Na[H_3BCO_2H]$) or $^{186/188}ReO_4^-$ ($Na[H_3BCO_2H]$ and $NH_3{\cdot}BH_3$ as additional reducing agent) in saline and leads to quantitative yields. Moreover the water-soluble precursors are fully characterised in contrast to other organometallic fragments.

Interest in the design of radiopharmaceuticals with carbonyl ligands results from their

high thermodynamic stability, small size, kinetic inertia and in vivo stability, even for rhenium which is instable at low oxidation states. Furthermore the $[M(CO)_3]^+$ moiety allows the use of a wide range of ligand systems, facilitating the testing of many different chelating sets (Figure 8) [43].

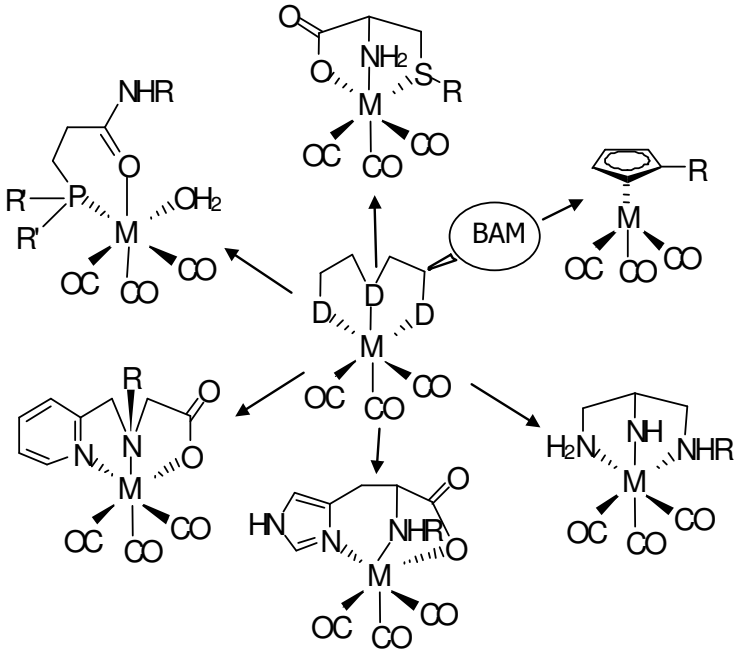

Fig. 8 BFCAs coordinating the *fac*-$[M(CO)_3]^+$ core (M= Tc, Re), (D = general coordinating atom)

The *fac*-$[M(H_2O)_3(CO)_3]^+$ stabilisation was first achieved employing soft sp^2 nitrogen or aromatic amines, such as histidine-BFCA derivatives or histidine residues in protein and peptides [44]. Also other amino acids chelates or synthetic amino acid analogues, with methionine or cysteine basic frameworks, triamines or (PADA) were tested with promising results, giving significant flexibility to target-specific radiopharmaceutical design using a variety of BAM (neurotensine, enkephalin, vitamin B12 and nuclear localising sequence, NLS) [45]. The complexes obtained have limited size, thus minimising the perturbation of the structure and function of the BAM, and once the diagnostic or therapeutic purpose is explained the BFCA can be metabolised by a normal amino acid recycling route. Histidine and single amino acids in general offer attractive bidentate and tridentate chelations, since they are present in a variety of naturally occurring biopolymers or peptides. On the other

hand the complexes resulting by this stabilisation mode may be susceptible to coordination competition by the natural amino acids present in the in vitro and in vivo systems, even leading to the "transchelation effect". To prevent this basic problem some considerations can be made during the design of new $[M(CO)_3]$-based radiopharmaceuticals. Very high stable species are required and, in addition, the occupation of all the three available coordination sites of the tricarbonyl metal core is preferred (i.e. by a tripodal BFCA). This situation generally exhibits better properties than complexes with mono- or bidentate sets, as reported in Schibli's work on the influence of denticity for tricarbonyl species in a biological media.

The full metal sphere fashion permits to reduce interactions with the native donor groups present in the blood pool, which may compromise both the integrity and biodistribution of the labelled compound typically represented by unspecific liver and kidney retentions [46].

Non-amino acid-BFCA derivatives were developed in order to obtain stable complexes not recognised or replaced by natural occurring chelating motifs [47] but despite a lot of attempts several research groups are currently still looking for an optimal BFCA, for the technetium and rhenium tricarbonyl species, useful in preparing an "ideal building block" for the design of diagnostics or therapeutics.

Complexation studies are still principally focused on the development of BFCAs to obtain tripodal mode of coordination (Scheme 1-A), for the reasons explained before.

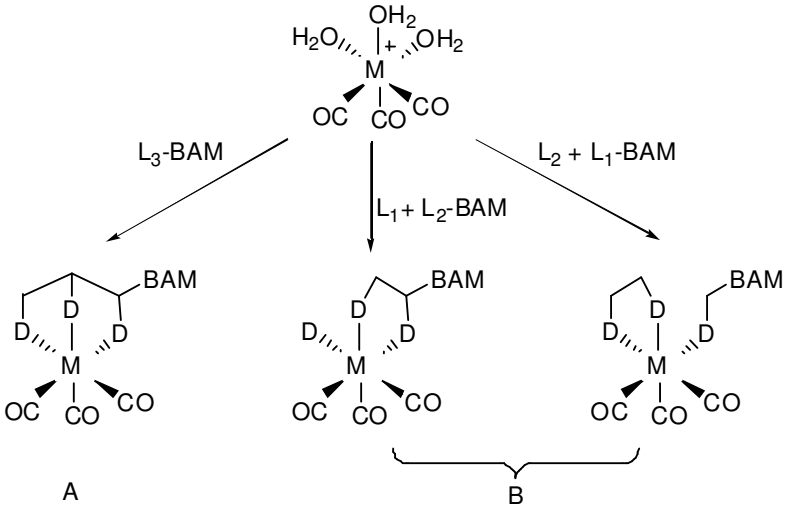

Scheme 1 Coordination strategies for the *fac*-$[M(CO)_3]^+$ (M= Tc, Re) , (D = general coordinating atom)

Tripodal BFCAs that lead to neutral complexes are the most commonly employed and efficient stabilising systems from a thermodynamically point of view, but they suffer several disadvantages, such as protection of the coordinating functionalities prior the BFCAs are introduced into the desired position of the BAM. Then, after conjugation, the protections have to be removed before labelling. Moreover the use of asymmetric ligands often leads to at least two structural isomers, because of their possibility to adopt two different orientations after coordination. These species are not always detectable and separable, and they may exhibit a substantial difference in the target selectivity.

Another strategy to achieve tricoordination is represented by using a mixture of two ligands, one bidentate L_2 and one monodentate L_1 (Scheme 1-B). In a bicoordinated complex $[M(H_2O)L_2(CO)_3]$ the coordination vacancy can be occupied by an appropriate monodentate ligand, such as in the imidazole or isocyanide groups, bearing the targeting biologically active molecule to produce the $[M(L_2)(L_1\text{-BAM})(CO)_3]$ complex. Pursuing this strategy, our group recently proposed a (SS)(P) fashion coordinating system, where the bidentate ligand is represented by a simple dimethyl-dithiocarbamate (DMTC), while a diphenyl phosphine derivative, that contains in its structure a carboxylic group suitable for the conjugation with a BAM, acts as monodentate ligand [48].

On the other hand the $[M(L_1)(L_2\text{-BAM})(CO)_3]$ complex can be obtained using a bidentate ligand conjugated to BAM (L_2-BAM) and a monodentate ligand L_1. Both cases are named [2+1] mixed ligand approach [49].

This new approach appears interesting for the versatility and controlled production of undesired isomers and, thus, appears to be promising for the future regarding preparation of the labelled compound in “one step” adding both ligands at the same time.

1.8 BIOLOGICALLY ACTIVE MOLECULES AS TARGETING AGENTS

In the past decay significant progresses have been made in the development of target-specific radiopharmaceuticals. Many biologically active molecules involved in several diseases, such as thrombosis, inflammation, neurological disorders and tumours, are well known. Moreover, their selectivity for a specific target and the consequent interaction mechanism were defined. Some of them are also commercially available, and can be used

as BAM for the design of new radiopharmaceuticals adopting the Paul Ehrlich's concept of the "magic bullet" [50]. Some examples are reported in Table 5.

Abbreviation	Full name	Biological effects	Disease
a-MSH	Melanocyte stimulating hormone	Melanogenesis	Melanoma
BB	Bombesin	Gut hormone release	Breast and prostate tumour
CCK	Cholecystokinin	Gallbladder contraction, exocrine, pancreatic excretion	Medullary thyroid cancer
CT	Calcitonin	Calcium homeostasis	Breast cancer
NT	Neurotensin	Vasoconstriction, raise in vascular permeability	Pancreatic tumour
SST	Somatostatin	Inhibition of hormone and exocrine secretion	Small-cell lung cancer, insulinoma
SP	Substance P	Hypotension, salivary secretion	Carcinoid
VIP	Vasoactive intestinal peptide	Vasodilatation, water and electrolyte secretion in the gut	Adenocarcinoma, pancreatic tumour
NHP	Human neutrophil peptide	Cell-cytokine interaction	Inflammation
UBI	Ubiquitin	Interaction peptide-bacteria	Infection
Annexin-V	Annexin-V	GPIIb/IIIa receptor interaction	Thrombosis

Table 5 Selected biologically active molecules for the design of target-specific radiopharmaceuticals

BAM has to be selected considering on the pathology and the chosen radionuclide (and its nuclear properties).

1.8.1 Small targeting molecules

Small peptides, peptidomimetics, and non-peptido compounds (mainly steroid hormones and neuro-transmitters) are excellent candidates for the development of new target-specific radiopharmaceuticals.

Recently, since the application of radiolabelled somatostatin analogues for imaging for receptor-positive tumour was successful, other regulatory peptides such as vasoactive

intestinal peptide (VIP), cholecystokinin (CCK), neurotensin, or substance P were intensively evaluated for a potential application both for imaging and therapy in nuclear medicine [51]. Steroid hormones and neurotransmitters (i.e. dopamine, serotonin, and cocaine derivatives) can be labelled to diagnose some types of tumours and neurological disorders. Antimicrobial peptides, such as human neutrophil peptide (NHP), interleukin-1 and –2, are currently employed for imaging of inflammation and/or infections. Some GPIIb/IIIa receptor-binding peptides, such as Annexin-V) are conjugated to BFCA for stabilising technetium and other radiometals for thrombus imaging.

If compared to the macromolecules, small targeting molecules have a lower molecular weight, which is expected to lead to a better penetration into the target tissue and to a faster blood clearance. Natural-peptide or peptidomimetics ligands exhibit high affinity to the targets usually in the nano- or subnanomolar range. It is crucial that radiolabelled analogues maintain their binding affinities. Because of the small size of manipulated molecules the attachment of BFCA-radiometal systems may interfere with the receptor or cause conformational changes in the binding motif leading to a loss of the biologically activity. Another important problem involves the rapid proteolysis or decomposition in plasma by endogenous enzymes, such as peptidase and protease, which can be reduced by modifying the biomolecules for example introducing unusual amino acids, or replacing the sensitive fragments. Despite this, an important advantage in studying this class of new potential radiopharmaceuticals is that small BAM can generally tolerate harsh reaction conditions during labelling and for chemical modification and, in addition, they can be readily synthesised.

1.8.2 Monoclonal antibodies

For a long time antibodies (Abs) were known to bind to antigens with very high affinity and specificity. Radiolabelling of fractions of antibodies (Polyclonal Abs) first took place in the 1950s and 1960s (targeting ferritin and human chorionic gonadotropin) [52]. In 1975 Georges Kohler and Cesar Mistein of the UK Medical Research Council's Laboratory of Molecular Biology fused myeloma cells to lymphocytes immunised with a specific antigen using polyethilenglycole (PEG). This procedure derived cell-secreted antibodies bound to antigen, generating individual specific monoclonal antibodies (MoAbs) [53]. From this

discovery MoAbs were used as vehicles to which radioactive isotopes could be attached with the accuracy to localise tumour and other diseased tissue targets.

An interesting strategy derived from the availability of MoAbs is represented by the Biotin/Avidin system for the tumour pretargeting approach. The method was developed to solve one of the major problems related to the use of radiolabelled MoAbs. The pharmacokinetic of these macromolecules in fact leads to a significant non-target uptake, causing low quality imaging in diagnostic and enhanced normal tissue toxicity in therapy, especially to the bone marrow. In addition, since the target accumulation is slow, short half-life elements cannot theoretically be employed.

The pretargeting approach is able to maintain high tumour uptake while providing a rapid clearance from the blood and the non-target organs. The majority of these studies employ the avidin (streptavidin)-biotin system, that is attractive since the K_a for avidin or streptavidin with biotin is approximately 10^{15}. The pretargeting design employs a multi-step approach wherein reagents were administered sequentially in a protocol defined to maximise the target uptake and minimise the non-target accumulation and the total body irradiation in general. In the first step a long-lived circulating non-radiolabelled avidin-MoAb or streptavidin-MoAb, with high affinity and specificity for antigens or over-expressed cancer cell receptors, is administered. After the calibrated time to localise and accumulate to the target (1-2 days), a “chase reagent” is injected in a second step in order to remove the unbound MoAb from the blood [54]. After one hour, the third step involves the administration of the radiolabelled biotin conjugate. Maximum tumour uptake and minimal radioactivity circulating with the blood is typically achieved after 1-3 hours, permitting the use of radioisotopes with short time-decay, such as technetium-99m. The activity is strongly bound to the target for a long time, thus allowing a good therapy effect or imaging for a long period, and the useless radiation dose is eliminated primarily via the kidneys.

1.9 PRELIMINARY STUDIES FOR THE DEVELOPMENT OF NEW ^{99m}Tc AND $^{186/188}$Re TARGET-SPECIFIC RADIOPHARMACEUTICALS

Since one of the most important aspects in radiochemistry is to know the structure of the prepared radiopharmaceutical, A BFCA-BAM system designed to strongly coordinate a radiometal has to be deeply studied before testing its potential diagnostic or therapeutic use.

A quick and accurate method would help radiochemists understand the fundamental chemistry at tracer level. It should be pointed out again that the ^{99m}Tc and $^{186/188}$Re concentration in the labelling mixture is very low (10^{-6}-10^{-7} and 10^{-11} M respectively) and at this concentration it is impossible to use classical analytical methods for complex characterisation (IR, UV, NMR, elemental analysis, mass and X-ray crystallography). Therefore, traditionally the characterization of a new radiopharmaceutical involves the synthesis of the corresponding ^{99}Tc or $^{185/187}$Re complex at the macroscopic level, since ^{99}Tc and $^{185/187}$Re are available in gram quantities. Rhenium, which possesses non-radioactive isotopes, is often used also for preparing technetium analogues for the similarities of their complexes as explained previously.

Complexes in quantitative level are synthesised both with BFCA alone and with the BFCA-BAM system. In this second case the synthesis is usually carried out only with small carrier molecule or small peptides, because with big BAM the characterisation is really complicated.

Finally an HPLC comparison experiment between the UV-trace (of the complex prepared at macroscopic level) and the Ray-trace (of the "hot" complex) at the same chromatographic conditions is carried out to demonstrate the structural analogies, always considering that the coordination chemistry for some chelating systems may differ at the macroscopic and tracer levels.

Another fundamental parameter is the labelling efficiency, defined as the ability of a BFCA to lead to high labelling yields towards the radioisotopes ^{99m}Tc/$^{186/188}$Re. BFCAs are tested for the labelling reactions first without the presence of BAM and then once conjugated to the carrier molecule to confirm the selectivity of the chosen systems. The performances are not expected to be lower than 90-95%, in order to avoid tedious purification procedures. There are several factors that influence the labelling efficiency of

a BFCA. These include the choice of the chelating system, its concentration and the reaction conditions such as temperature, viscosity, time and pH [49].

If the chelator concentration is fixed, the conditions used for the labelling are largely dependent upon the nature of donor atoms. For example, high pH and heating at 100 °C for 30 min is required for the successful ^{99m}Tc-labeling of N_3S triamidethiol and N_2S_2 diamidedithol at low concentrations (10^{-5}-10^{-6} M) while the N_2S_2 monoamidemonoaminedithiol can be labelled under milder conditions. For the N_2S_2 diaminedithiol, the ligand exchange with [^{99m}Tc]-glucoheptonate can be completed within 60 min at room temperature. The labelling efficiency of a BFCA is also affected by the presence of protecting groups on the donor atom(s) and the identity of the exchange ligand or coligand [55]. The use of protecting group(s) for thiol-containing chelators usually slows down the rate of radiolabelling [56], appropriate combinations of BFCA and exchange ligand (or coligand) must be assessed for the successful labelling of small biomolecules.

On the other hand, tricarbonyl species can be stabilised very efficiently using ligands (as hystidine) in micromolar concentrations, in less than 30 minutes at 98°C [51]. However mild conditions are preferred because many BAM may decompose at high temperature.

The radiolabelled product has to be tested through the quality control procedures. TLC is the most frequently used technique because it is simple and quick, usually taking only 10-15 min to carry out the whole procedure. Stationary phase can be paper strips, silica or RP-plates while the mobile phase is often comprised of an organic solvent (acetone, ethanol, acetonitrile, methanol or isopropyl alcohol) and saline (0.9% sodium chloride solution) or a buffer. In the labelling mixture, there are several labelled species: [^{99m}Tc/$^{186/188}$Re]permetallate, [^{99m}Tc/$^{186/188}$Re]colloid, the [^{99m}Tc/$^{186/188}$Re]-complex, eventually the [^{99m}Tc/$^{186/188}$Re]exchange ligand complex, and other radioimpurities. The first two species can be easily separated from the coordinates labelled compounds. However radiochemical purity (RCP) and the presence of different isomeric forms cannot be detected.

HPLC (Radio-HPLC) has recently become a routine quality control method for the most of the clinical and research radiopharmaceuticals. The advantage is determined by its capability to separate many radioactive compounds, even isomers such as epimers and diastereoisomers (optical isomers only by using chiral chromatographic conditions). This

method is in general enough precise but needs to calibrate the optimum conditions and it is not quick and cheap as TLC. Radio-HPLC also has its limitations. For example, the radio-HPLC cannot be used for the assessment of the metal-colloid formation. A TLC method is needed in combination with HPLC to assess both the radiolabelling yield and the RCP.

After these first preliminary studies the biological stability of the labelled compounds have to be tested using "challenging agents", such as amino acids, and *in vitro* systems, as human or rat serum. Finally a pharmacokinetic of the basic framework alone and with the presence of the BAM is explored using healthy animal models, basically mice, to determine the main excretion route and the eventual accumulation in non-target tissues.

REFERENCES

[1] (a) Cutler, C. S.; Lewis, J. S.; Anderson, C. J. *Adv. Drug Del. Rev*. **1999**, 37, 189-211. (b) Volkert, W. A., and Hoffman, T. J. *Chem. Rev*. **1999**, 899, 2269-2292

[2] O'Brien, H.A.; Burchiel, S.W.; Rodhes, B.A. *Overview of radionuclides useful for radioimaging, radioimmunotherapy*, Elsevier, Amsterdam, **1983**

[3] Keenan, A.M.; Harbert, J.C.; Larson, S.M. *J Nucl Med*, 1985, 26, 531-537

[4] (a) Jurisson, S.S.; Berning, D.; Jia, W.; Dangshe, M.A. *Chem Rev*, **1993**, 93, 137-1156. (b) Anderson, C.J.; Welch, M.J. *Chem Rev*, **1999**, 99, 2219-2234. (c) Neves, M.; Kling, A.;. Lambrecht, R.M *Appl Radiat Isot*, **2002**, 57, 657-664

[5] Weissleder, R.; Mahmood, U. *Molecular Imaging Radiology*, **2001**, 219, 316-333

[6] (a) Schwochau, K. *Technetium, Chemistry and Radiopharmaceutical Application*, Wiley-VCH, Weinheim, Germany, **2000.** (b) J. Steigman, W.C. Eckelman, *The chemistry of Technetium in Medicine*, Nuclear Science Series, National Academic Press, Washington D.C., **1992**

[7] Wessels, B.W. and Rogus, R.D. *Medical Phys*., **1984**, 11, 5, 638-645

[8] Fink-Bennet, D.M. and Thomas, K. *J Nucl Med Technol*, **2003**, 31, 2, 61-70

[9] Dillmann, R.O. *Cancer Invest*, **2001**, 19, 8, 833-841

[10] Reilly, R.M.; Gariepy, J. *J Nucl Med*, **1998**, 39, 6, 1036-1043

[11] (a) Technetium in Chemistry and Nuclear Medicine 1, E. Deutsch, M. Nicolini, H. N. Wagner, jr., Eds.; Cortina International, Verona (Italy), **1983**. (b) Technetium in Chemistry and Nuclear Medicine 2, M. Nicolini, G. Bandoli, U. Mazzi, Eds.; Cortina International, Verona (Italy) - Raven Press, New York (NY), **1986**. (c) Technetium and Rhenium in Chemistry and Nuclear Medicine 3, M. Nicolini, G. Bandoli, U. Mazzi, Eds.; Cortina International, Verona (Italy) - Raven Press, New York (NY), **1990**. (d) Technetium and Rhenium in Chemistry and Nuclear Medicine 4, M. Nicolini, G. Bandoli, U. Mazzi, Eds.; SGE Editoriali, Padova (Italy), **1995**. (e) Technetium, Rhenium and Other Metals in Chemistry and Nuclear Medicine 5, M.

Nicolini, U. Mazzi, Eds.; SGE Editoriali, Padova (Italy), **1999**. (f) Technetium, Rhenium and Other Metals in Chemistry and Nuclear Medicine 6, M. Nicolini, U. Mazzi, Eds.; SGE Editoriali, Padova (Italy), **2002**. (g) Technetium, Rhenium and Other Metals in Chemistry and Nuclear Medicine 7, U. Mazzi, A. Nadali, Eds.; SGE Editoriali, Padova (Italy) **2006**.

[12] Perrier, C. and Segrè, E. *J. Chem Phys*. **1937**, 5, 712-716, and **1939**, 7, 155-156

[13] Dilworth, J.R.; Parrott, S.J. *Chem Soc Rev*, **1998**, 27, 43-55

[14] Davidson, C.J.; Lock, L. in *Comprehensive Coordination Chemistry*, vol. 4, Eds. H.G. Wilkinson, R.D. Gillard, J.A. Mc Cleverty, Pergamon Press, Oxford **1987**

[15] Baldas, J.; Bonnyman, J.; Pojer, P.M.; Williams, G.A.; Mackay, M.F. *J Chem Soc Dalton*, **1982**, 2, 451-455

[16] (a) Verbruggen, A.M. *Eur J Nucl Med*, **1990**, 17, 346-364. (b) Delmon, L.I.; Moingeon, A.; Mahmood, A.; Davinson, A.; Jones, A.G. *Nucl Med Biol*, **1991**, 35, 47-59.

[17] (a) Cheeseman, E.H.; Blanchette, M.A.; Calabrese, J.C.; Ganey, M.V.; Maheu, L.J.; Morgan, R.A.; Walowitch, R.C.; Watson, A.D.; Williams, S.J.; Miller, S.J. *J Labelled Compd Radiopharm*, **1989**, 26, 421-423. (b) Walowitch, R.C.; Hill, T.C.; Garrity, S.T.; Cheeseman, E.H.; Burgess, B.A.; Oleary, D.H.; Watson, A.D.; Ganey, M.V.; Morgan, R.A.; Williams, S.J.; Miller, S.J. *J Nucl Med*, **1989**, 30, 1892-1901.

[18] (a) E. Deutsch, *Radiochim Acta*, **1993**, 63, 195-197. (b) N.N. Greenwood, A. Earnshaw, *Chemistry of the Elements*, Pergamon Press, New York (USA), **1993**.

[19] (a) A.P. Bernarducci, *Quart J Nucl Med*, **2003**, 47, 292-320. b) M.J.C. DeHoyos, B.J. Rubal, M.Y.C. Bradlley, *Invest Radiol*, **2004**, 39, 197-201.

[20] (a) J.F. Nijsen, G.C. Krijger, A.D. van Het Schip *Anticancer Agents Med. Chem.* **2007**, 7, 271–290 (b) A.I. Kassis, J. Adelstein Considerations in the selection of radionuclides for cancer therapy, in: M.J. Welch, C.S. Redvanly (Eds.), Handbook of Radiopharmaceuticals, Radiochemistry and Applications, Wiley & Sons, London, **2003**, pp. 767–793. (c) D.E. Milenic, M.W. Brechbiel, *Biol. Ther.* **2004**, 3, 361–370.

[21] I. Buchmann, D. Bunjes, J. Kotzerke et al. *Cancer Biother. Radiopharm.* **2002,** 17, 151–163

[22] G. Ferro-Flores, E. Torres-Garcia, L.Garcia-Pedroza et al. *Nucl.Med. Common.* **2005,** 26, 793–799

[23] M. Juweid, R.M. Sharkey, L.C. Swayne, et al. *J. Nucl. Med.* **1998,** 39, 34–42

[24] (a) P.O. Zamora, S. Gulhke, H. Bender et al. *Int. J. Cancer* **1999,** 65, 214–220. (b) C. Arteaga de Murphy, M. Pedraza-López, G. Ferro-Flores, et al. *Nucl. Med. Biol.* **2001,** 28, 319–326. (c) E.M.Molina-Trinidad, C.Arteaga deMurphy, G. Ferro-Flores et al *Int. J. Pharm.* **2006,** 310, 125–130.

[25] (a) A.Boschi, L. Uccelli, A.Duatti et al. *Nucl. Med. Commun.* **2004,** 25, 691–699. (b) T.Y. Luo, B.T. Hsieh, S.J.Wang, et al. *Nucl. Med. Biol.* **2004,** 31, 671–677. (c) C.J. Yoon, J.W. Chung, J.H. Park et al. *J. Vasc. Interv. Radiol.* **2004,** 15, 1121–1128.

[26] S. Jurisson, J.D. Lydon, *Chem Rev*, **1999**, 99, 2205-2218

[27] W.C. Eckelman, *J Nucl Med*, **1995**, 22, 3, 249-263

[28] R.K. Hom, J.A. Katzenellenbogen, *Nucl Med Biol*, **1997**, 24, 485-498.

[29] (a) Y. Arano, T. Uezono, H. Akizawa, M. Ono, K. Wakisaka, M. Nakayama, *J Med Chem*, **1996**, 39, 3451-3460. (b) R.W. Weber, R.H. Boutin, M.A. Nedelman, J.J. Lister, R.T. Dean, *Bioconjug Chem*, **1990**, 1,

431-437. (c) M.J. Abrams, M. Juweid, C.I. Tenkate, D.A. Schwartz, M.M. Hauser, F.E. Gaul, *J Nucl Med*, **1990**, 31, 2022-2028.

[30] R.K. Hom, D.Y. Chin, J.A. Katzenellenbogen, *J Org Chem*, **1996**, 61, 2624-2631

[31] Liu, S., and Edwards, S. D. *Chem. Rev.* **1999**, 99, 2235-2268

[32] B.A. Schubiger, R. Alberto, A. Smith, *Bioconjug Chem*, **1996**, 7, 165-179

[33] J. Fichna, A. Janecka, *Bioconjug Chem*, **2003**, 14, 3-17

[34] (a) Billinghurtst, M. W.; Abrams, D. N.; Lawson, M. S. *Appl. Radiat. Isot*. **1991**, 42, 607-612. (b) Ballinger, J. R., and Gulenchyn, K. Y. *Appl. Radiat. Isot.* **1991**, 42, 315-316.

[35]Hnatowich, D. J.; Chang, F.; Lei, K.; Qu, T.; Rusckowski, M. *Appl. Radiat. Isot.* **1997**, 48, 587-594

[36] S.R. Banerjee, K.P. Maresca, L. Francesconi, J. Valliant, J.W. Babich, J. Zubieta, *Nucl Med Biol*, **2005**, 32, 1-20

[37] Vanbilloen, H. P.; Bormans, G. M.; De Roo, M. J.; Verbruggen, A. M. *Nucl. Med. Biol.* **1995**, 22, 325-338

[38] R. Visentin, M.C. Giron, M. Bello, U. Mazzi, *Nucl Med Biol*, **2004**, 31, 655-662.

[39] R. Syhre, S. Seifert, H. Spies, A. Gupta, B. Johannsen, *Eur J Nucl Med*, **1998**, 25, 793–796.

[40] a) A. Marchi, R. Rossi, L. Magon, A. Duatti, R. Pasqualini, V. Ferretti, V. Bertolasi, *J Chem Soc Dalton Trans*, **1990**, 4, 1411-1416 b) A. Duatti, A. Marchi, V. Bertolasi, V. Ferretti, *J Am Chem Soc*, **1991**, 113, 9680-9682.

[41] A. Boschi, A. Duatti, L. Uccelli, *Top Curr Chem*, **2005**, 252, 85-115.

[42] a) R. Alberto, K. Ortner, N. Wheatley, R. Schibli, A.P. Schubiger, *J Am Chem Soc*, **2001**, 123, 3135–3136. b) R. Schibli, R. Schwarzbach, R. Alberto, K. Ortner, H. Schmalle, C. Dumas, A. Egli, P. A. Schubiger, *Bioconjug Chem,* **2002**, 13, 750-756.

[43] a) J.K. Pak, P. Benny, B. Spingler, K. Ortner, R. Alberto, *Chem Eur J*, **2003**, 9, 2053–2061. b) R. Schibli, K.V. Katti, C. Higginbotham, W.A. Volkert, R. Alberto, *J. Nucl Med Biol*, **1999**, 26, 711–716. c) J. Bernard, K. Ortner, B. Spingler, H.J. Pietzsch, R. Alberto, *Inorg Chem* **2003**, 42, 1014–1022 d) R. Alberto, *Eur J Nucl Med Mol Imaging*, **2003**, 30, 1299-1302.

[44] R. Waibei, R. Alberto, J. Willude, R. Finnern, R. Schibli, A. Stichelberger, *Nat Biotechnol*, **1999**, 17, 897-901.

[45] a) A. Egli, R. Alberto, L. Tannahill, R. Schibli, U. Abram, A. Schaffland, R. Waibel, D. Tourwe, L. Jeannin, K. Iterbeke, P.A. Schubiger, *J Nucl Med*, **1999**, 40, 1913-1917. b) R. LaBella, E. Garcia-Garagyoa, M. Bahler, P. Blauenstein, R. Schibli, P. Conrath, D. Tourwe, P.A. Schubiger, *Bioconj Chem*, **2002**, 13, 599-604.

[46] R. Schibli, R. LaBella, R. Alberto, L. Garcia-Garayoa, K. Ortner, U. Abram, *Bioconjug Chem*, **2000**, 11, 345– 351.

[47] a) T.W. Spradau, J.A. Katzenellenbogen, *Bioconjug Chem*, **1998**, 9, 765-772. b) M.B. Skaddam, F.R. Wust, S. Jonson, R. Syhre, M.J. Welch, H. Spies, *Nucl Med Biol*, **2000**, 27, 269-278.

[48] Riondato, M.; Camporese, D.; Martìn, D. *et al*., *Eur. J. Inorg. Chem.* **2005**, 20, 4048-4055

[49] R. Alberto, J.K. Pak, D. van Staveren, S. Mundwiler, P. Benny, *Biopolymers*, **2004**, 76, 324-333.

[50] P. Ehrlich, *The relationship existing between chemical constitution, distribution and pharmacological*

action, The collected papers of Paul Ehrlich, Pergamon, New York (USA), **1956**.

[51] L. Aloj, G. Morelli, *Curr Pharm Des*, **2004**, 10, 24, 3009-3031.

[52] D. Pressman, The development and use of radiolabeled antitumor antibodies, Cancer Res, 1980, 40, 2960-2964.

[53] G Kohler, C Milstein, Nature, **1975**, 256, 495-497.

[54] D.A. Godwin, C.F. Meares, M. Osen, *J Nucl Med*, **1998**, 39, 1813-1822

[55] Larson, S. K.; Solomon, H. F.; Caldwell, G.; Abrams, M. *J. Bioconj. Chem.* **1995**, 6, 635-642

[56] Rao, T. N.; Gustavsnov, L. M.; Srinivasan, A.; Kasina, S.; Fritzberg, A. R. *Nucl. Med. Biol.* **1992**, 19, 889-897

[57] R. Schibli, K.V. Katti, C. Higginbotham, W.A. Volkert, R. Alberto, *Nucl Med Biol*, 1999, **26**, 711-716

Part I

SOMATOSTATIN ANALOGUES

2

SST ANALOGUES LABELLING WITH ^{99m}Tc

2.1 INTRODUCTION

2.1.1 Clinical role of somatostatin

Somatostatin (somatotropin release-inhibiting factor, SRIF-14, Figure 1) is a cyclic tetradecapeptide, originally discovered as a hypotalamic neurohormone inhibiting growth hormone (GH) secretion [1], and firstly synthesized by Rivier [2]. The amino-terminally extended type, Somatostatine-28 (SRIF-28), was discovered in the gut [3], and higher molecular weights forms have been reported. SRIF-14 an 28 are predominantly produced by neurones and secretor cells in the central and peripheral nervous system, in endocrine pancreas and in small number in the thyroid, adrenals, kidneys and prostate [4-6].

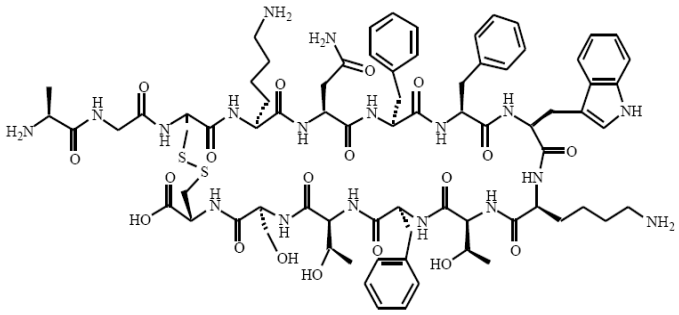

Fig. 1 Somatostatin (SRIF-14)

Its functions include inhibition of endocrine secretion as Growth Hormone (GH), insulin, glucagon, gastrin, cholecistokinin, Vasoactive Intestinal Peptide (VIP) and secretin, and of exocrine secretion as gastric acid, intestinal fluid and pancreatic enzymes [6]. Another action of sst is the inhibition of proliferation of various normal and tumour cells [7].

Somatostatin (sst) induces its biological effects through interaction with a family of specific transmembrane receptors (sstrs), expressed by a variety of normal and malignant tissues [7]. Five subtypes of structurally related, G-protein-coupled, human sst receptors have been cloned and characterized [8,9] and are located in pituitary, pancreas, gastrointestinal tract, thyroid and immune cells. Sstrs are also variably expressed in a variety of tumours such as gastroenteropancreatic (GEP) tumours, pituitary tumours, carcinoid tumours, small-cell lung tumours, prostate carcinoma, breast carcinoma, renal carcinoma and frequently nervous system tumours [10]. Signalling through SRIF receptors is complex; the binding of the ligand to SSTRs induces G_i-protein activation and signalling through various pathways, and is represented in Figure 2.

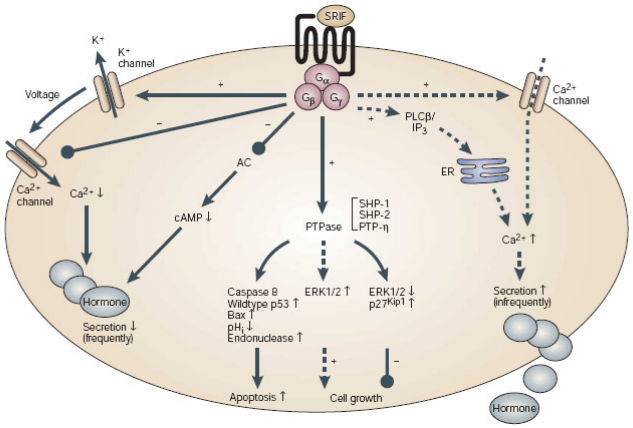

Fig. 2 SRIF receptor-mediated modulation of signaling cascades leading to changes in hormone secretion, apoptosis and cell growth [11]

The majority of cancer cells express more than one sstr subtype, $sstr_2$ being the most frequent one, followed by $sstr_1$, $sstr_3$, $sstr_4$ and finally by $sstr_5$. Recently, several laboratories found that sstr-expressing tumour frequently contain two or more sstr subtypes, and discovered that sstr subtypes might form homo/heterodimers to create a novel receptor with different functional characteristics, expand the array of selective sstr

activation pathway and subsequent intracellular signalling cascade [12]. The co-expression of multiple sstr subtypes in malignant and normal cells has recently been debated by Reubi *et al* [13], evaluating approximately 200 tumours for their receptors subtype protein expression by competition binding experiments, and the majority of the tested tumours predominantly expressed $sstr_2$ [14].

Regarding the molecular mechanisms involved in somatostatin antineoplastic activity, both indirect and direct effects via specific sstr expressed in target cells have been described. Direct action may result from blocking mitogenetic growth signal or inducing of apoptosis caused by interaction with sstr. Indirect effects may result from reduced or inhibited secretion of growth promoting hormones and growth factors that stimulate the growth of various type of cancer. Finally, inhibition of angiogenesis as well as influence on the immune system are important factors. Because of its dual role in inhibiting hormone release and cell growth, it was a logical step to evaluate sst as an anticancer drug for the treatment of neuroendocrine tumours (NET). Various studies demonstrated inhibitory effects of sst in patients with acromegaly, endocrine pancreatic tumours such as insulinomas and glucagonomas, and VIP-producing tumours [6]. However, the short half-life of sst in vivo (about 2-3 min) prevented its application in the clinic.

2.1.2 Somatostatin analogues in oncology

Because sst was found to have interesting properties with regard to potential use in cancer treatment, work was carried out by several laboratories to develop protease-resistant sst analogues. The availability of cloned receptor subtypes has enabled the detailed characterization of the binding properties of sst and sst analogues [15,16], and a large number of small peptide analogues were synthesized to overcome the therapeutic limitation of SRIF-14. Synthetic derivatives of somatostatin have similar activity to native somatostatin but with a longer half-life. Vale et al. synthesized a series of octa- and nona-peptide analogues, which all contained the Phe^{7}-D-Trp^{8}-Lys^{9}-Thr^{10} fragment found to be the essential pharmacophore of SRIF [17]. Of the many hundreds of somatostatin analogues synthesized, two are in common clinical use: octreotide and lanreotide. A third, RC-160 (vapreotide) has been well characterized in preclinical studies but is still in Phase II study (Figure 3) [18].

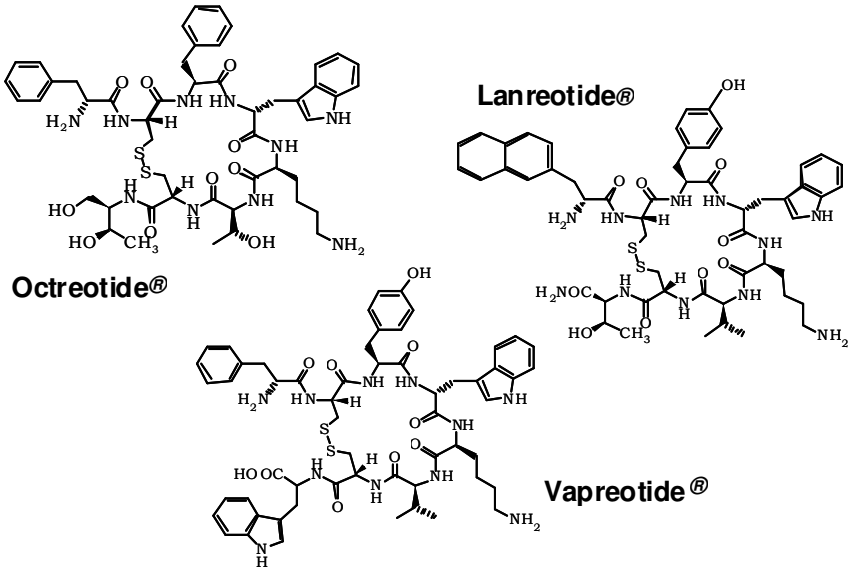

Fig. 3 SRIF analogues in clinical use

These analogues lack the key enzyme cleavage sites and are more stable than native somatostatin. As a result, they have relatively long half-lives, e.g. approximately 110 min for octreotide. Octreotide and Lanreotide are approved for treating pituitary adenomas and GEP tumours [19-21], and long-acting formulations are available thus reducing the administration to only once every 4 weeks. The binding affinity of the analogues compared with SRIF-14 and SRIF-28 are given in table 1 [22].

Compound	**$Sstr_1$**	**$Sstr_2$**	**$Sstr_3$**	**$Sstr_4$**	**$Sstr_5$**
SRIF-14	1.1	1.3	1.6	0.53	0.9
SRIF-28	2.2	4.1	6.1	1.1	0.07
Octreotide	>1000	2.1	4.4	>1000	5.6
Lanreotide	>1000	1.8	43	66	0.62
Vapreotide	>1000	5.4	31	45	0.7

Table 6. Binding affinities [23] (K_i) of clinically useful Somatostatin analogues at $sstr_{1-5}$ receptors

2.1.3 Radiolabelled somatostatin analogues

Radiolabelled somatostatin analogues are useful diagnostic tools to detect and localize small sst-expressing tumours, with particular utility in pointing primary and metastatic endocrine tumours. Furthermore, the demonstration of the efficient internalization of

receptor-ligand complexes into sst-positive cells formed the basis for the concept of targeted sst-mediated chemo- or radiotherapy of sst-expressing metastatic human cancer [7, 14].

Somatostatin receptor scintigraphy was introduced in the late 1980s, and after the development of [^{111}In-DTPA^{0}]octreotide this radiolabelled hormone analogue became the gold standard for staging sst-positive neuroendocrine tumours [24, 25]. Since then many improvements concerning the peptide and the radiolabelling were made. More recently, several novel chelator attachment at the N-terminus of sst analogues for labelling with radiometals were designed and studied in the clinic. In most cases, a bifunctional chelating agent (BFCA) as DTPA or DOTA was used. Nowadays, somatostatin analogues labelled with positron emitters are also available. The use of these compounds with an integrated positron emission tomography/computed tomography (PET/CT) camera provides an extremely valuable combination of physiological and anatomical information [26–28].

[^{111}In]-[DTPA d-Phe^{1}]-octreotide [29] was the first radiopeptide explored in patients which contains a chelator-bound radiometal. This radiopharmaceutical is now commercially available as OctreoScan and used routinely in the clinic for tumour imaging of sstr-expressing neuroendocrine tumours [24]. Other [^{111}I]-labelled heptadentate and octadentate [DTPA d-Phe^{1}]-octreotide analogues containing hydrolysable linker group were examined, with little advantage over OctreoScan. A major advantage was obtained with DOTA-octreotide analogues, which displayed more favourable *in vivo* distribution than OctreoScan and are more suitable for internal radiotherapy [30]. It has also been shown that sstr scintigraphy using this agent is the most sensitive method for localization of primary and metastatic diseases in endocrine pancreatic tumour and carcinoid insulinomas [31]. New conjugates may show higher sensitivity with regard to the localization of tumour and metastases. [^{111}I]-DOTA-TOC and [^{90}Y]-DOTA-TOC have shown to be effective targeting and therapeutic agent in animal model and patient [32]. To extend biological activity profile of radiolabelled somatostatin analogues, same authors investigate several radiopeptides. [^{111}In/^{90}Y- DOTA-1-Nal^{3}-octreotide] (^{111}In/^{90}Y- DOTA-NOC) was one of the most interesting peptide, it has improved affinity to $sstr_2$ and high affinity to $sstr_3$ and $sstr_5$ and potentially extend the spectrum of accessible tumours in diagnosis and internal radiotherapy [33]. ^{111}In,^{90}Y and ^{177}Lu are the most common radiometals used for diagnosis and therapy, but other radiometals such as ^{99m}Tc, ^{64}Cu and

^{68}Ga have been investigated. Several [^{64}Cu]-labelled somatostatin analogues were synthesized and showed favourable biodistribution in animal models and good performance in PET imaging in patients; however the use of ^{64}Cu relies on the availability of a cyclotron [34]. Another interesting positron emitter is ^{68}Ga which is produced by a $^{68}Ge/^{68}Ga$ generator available at most PET centres [35]. [^{99m}Tc]-labelled sst analogues have been studied in several laboratories because of the very favourable properties of this radionuclide, and three radiolabelling methods have been used: the direct labelling, the preformed chelate or prelabelling approach and the post-conjugation approach [36-39].

2.1.4 Aim of the project: ^{99m}Tc labelling of somatostatin dicarba-analogues

The current strategy to design technetium radiopharmaceuticals is focused on labelling receptor-binding molecules (i.e. peptides, monoclonal antibodies, steroid hormones, brain tracers and others). Transition metal radioisotopes must be incorporated into the biologically active molecule, in an appropriate oxidation state, by means of a conjugated chelating system in order to form an in vivo stable complex with the radionuclide, and maintain the receptor binding properties after labelling. This work is focused on the radiolabelling with ^{99m}Tc of new dicarba-analogues of octreotide. Sst analogues show, in most of the cases, the disulphide bridge of the parent somatostatin that can be subjected to the attacks of oxidizing and reducing agents used in the labelling reactions. This prompted us to search a more stable tether bridging the active motif of somatostatin, identified as the Phe-d-Trp-Lys-Thr sequence. At the same time, the new side-chain to side-chain closure had to preserve the conformation of this sequence in octreotide. D'Addona et coll. synthesized several new octreotide analogues, free from disulphur bridge, which showed an improved stability versus oxidative and reducing agents in vivo, therefore an improved stability to the radiolabelling procedures with Re and Tc. Moreover these analogues retain the pharmacophore region and their affinity for sst receptors 2 and 5. A first cyclic dicarba-analogous that contained a -CH=CH- bridge [40, 41], and more recently, three new unsaturated dicarba-analogues substituting respectively Thr^{10} with Phe and Tyr(Bzl) and Phe^{7} with 1-Nal were synthesized accordingly to the solid phase peptide synthesis technique. The general structure of these dicarba-analogues is represented in Figure 4.

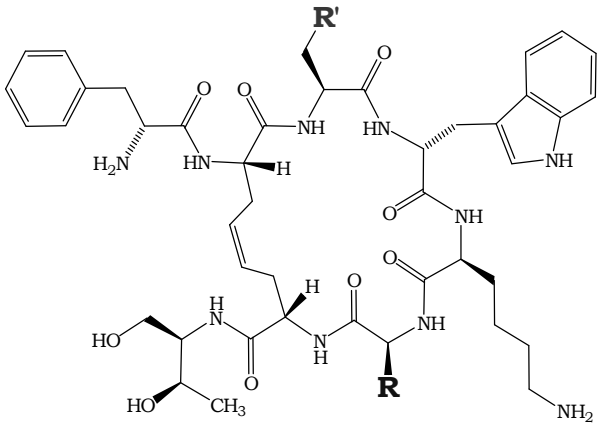

Fig. 4 General strucuture of new sst dicarba-analogues

Among them, the most selective for $sstr_5$ and so far the most promising, are here reported in Table 2.

	R	***R'***	***sst$_5$*** ***IC_{50}nM affinity***
1 (CIF)	CH_3-CH-(OH)-	C_6H_5-CH_2-	28 ± 1
2 (CIN)	CH_3-CH-(OH)-	$C_{10}H_8$-	8.7 ± 3.9

Table 7 IC_{50} nM affinities toward sst_5 receptors of CIF and CIN dicarba-analogues

To reach our objective, both dicarba-analogues where modified at the aminic terminal group introducing a BFCA, the N-[N-(3-Diphenylphosphinopropionyl)glycyl]cysteine (PN_2S). The PN_2S set is able to chelate ^{99m}Tc and $^{186/188}Re$ [42], and thanks to the carboxyl function of cysteine can be anchored to peptides or other biomolecules.

To achieve ^{99m}Tc-peptide labelling, two already known labelling procedures were adopted [43, 44]. The first labelling approach involves the formation of the $[^{99m}TcO]^{3+}$ core by using the $^{99m}TcO(gluconate)_2$ intermediate compound, and was performed on the second derivative (CIN-PN_2S), obtaining the complex reported in figure 5.

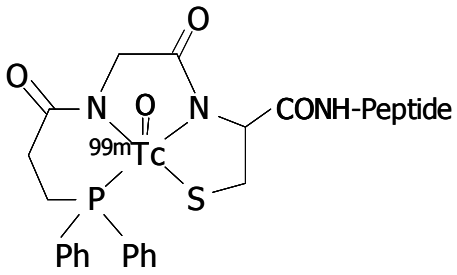

Fig. 5 Peptide-PN_2S complex with Tc-oxo core

The second approach was performed on the first derivative (CIF-PN_2S), modified with the same PN_2S bifunctional ligand, by using a (2+1) tricarbonyl approach developed by our group [43] starting from Tc tricarbonyl precursor, where the coordination vacancies can be occupied by an appropriate monodentate ligand and by a bidentate one, in a 2+1 mixed ligand approach. In this case, phosphine phosphorous linked to the peptide acts as monodentate ligand, while Dimetil-dithiocarbamate (DMTC) behaves as bidentate co-ligand, to produce the SS-P complex. The labelling reaction is reported in Scheme 1.

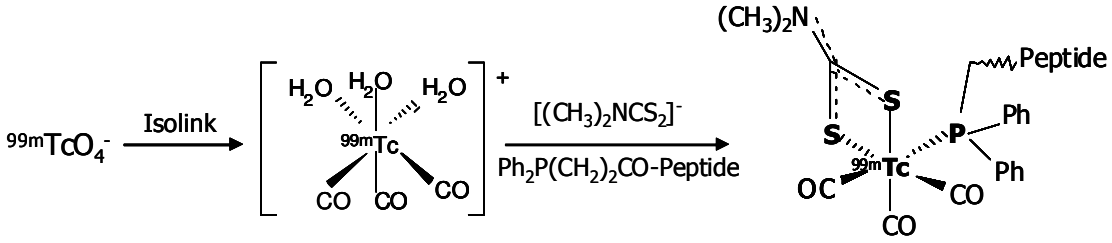

Scheme 2 Synthesis of Tc-tricarbonyl complex with the 2+1 mixed ligand approach

Sodium DMTC was chosen in the present study because it is stable, and commercially available, and is one of the simplest dithiocarbamates. This permits very small size complexes without any sterical competition with the phosphine or biomolecule in the tricarbonyl metal sphere. On the other hand, phosphine ligands are well known for their capability to form very stable and inert bonds with organometallic fragments.

2.2 EXPERIMENTAL SECTION

2.2.1 Materials and analytical methods

All chemicals and solvents were reagent grade and used without further purification. N,N-dimethyldithiocarbamate (DMTC) was provided by Fluka (Sigma-Aldrich, Milan, Italy), and sodium gluconate and $SnCl_2$ were purchased from Sigma-Aldrich (Milan, Italy). Solid-phase peptide synthesis of CIF-PN_2S (MW = 1381 Da) and CIN-PN_2S (MW = 1431 Da) were carried out under a nitrogen atmosphere by Dr. D. D'Addona et coll., Peptide synthesis research group (Prof. M. Ginanneschi), Dept. of Organic Chemistry, University of Florence (Italy) [41]. The syntheses of ^{99m}Tc-complexes were performed under an argon atmosphere using solvents degassed and tested for peroxides prior to use. Solvents for labelling and analyses and HPLC eluents were purchased from Fluka (Sigma-Aldrich, Milan, Italy) and Carlo Erba Reagenti (Div. Antibioticos, Milan, Italy); MilliQ water was obtained from a Millipore system (Millipore, Vimodrone, Milan, Italy). Solution pH was measured with pH indicator strips purchased from Carlo Erba Reagenti (Div. Antibioticos, Milan, Italy). $Na^{99m}TcO_4$ was eluted from a commercial Drytec Sorin $^{99}Mo/^{99m}Tc$ (General Electric, Carugate, Milano) using a 0.9% saline solution. The radioactive precursor *fac*-$[^{99m}Tc(H_2O)_3(CO)_3]^+$ was prepared using IsoLink kit purchased by Mallinckrodt Med. B.V. (Pettern, The Netherlands). Radioactive measurements were determined using a dose calibrator M2361 Messelektronik (Dresden, Germany) and a gamma counter with NaI detector (coupled to Thorn 9265 and Scalar Rate Meter Ludlum model 2200). All manipulations were carried out approved for low-level radioactivity use. Labelling efficiency and radiochemical purity (RCP) were assessed by RP-HPLC and expressed as percentage of injected activity. RP-HPLC analyses were performed on an Agilent LC 1100 chromatography system (Agilent Technologies, Waghaeusel-Wiesental, Germany) controlled by a quaternary Agilent LC 1100 programmable gradient pump. The analyses were monitored with an Agilent Diode Array and Multiple Wavelenghts detector set at 215 nm and at 254 nm, and with a GabiStar-γ-detector Raytest (Cinisello Balsamo, Milano, Italy). An Agilent C18 reversed phase column (Zorbax SB-C18, 5 μm, 250 mm x 4.6 mm, Agilent Technologies, Waghaeusel-Wiesental, Germany) was used, equipped with C18 precolumn (Agilent Technologies, Waghaeusel-Wiesental, Germany). Solvents used in the chromatographic analyses were MilliQ water with 0.1% trifluoroacetic acid (A) and

acetonitrile (ACN) with 0.05% trifluoroacetic acid (B). Two different elution methods were used:

Method A: RP-HPLC carried out at a flow rate of 1 ml/min. A gradient was followed starting with 0% solvent B for 3 min, rising to 40% B in 1 min and then to 85% B over 15 min, changing to 100% B in 2 min, held for 2 min and back to 0% B in 2 min.

Method B: RP-HPLC carried out at a flow rate of 1 ml/min, starting from 40% solvent B and changing to 85% B over 15 min, rising to 100% B in 1 min, held for 1 min and then back to 40% B in 1 min.

2.2.2 CIN-PN_2S labelling with $[^{99m}TcO]^{3+}$

Two steps reaction: 11 µl of a freshly prepared tin(II)-gluconate solution (1 µl 0.1 M $SnCl_2$ in 0.1 M HCl and 10 µl 0.01 M sodium gluconate in MilliQ water) were added to 0.5 ml eppendorf vial followed by $^{99m}TcO_4^-$ solution (100 µl, 50 MBq) and the resulting solution was incubate at room temperature for 15 minutes. Once assessed the absence of free $^{99m}TcO_4^-$, the solution was transferred in to a 0.5 ml eppendorf vial containing 100 µg of CIN-PN_2S (69 nmol) solubilised in 50 µl of EtOH and the reaction mixture was incubated at 70 °C for 30 minutes.

One step reaction: to a 0.5 ml eppendorf vial containing 100 µg of CIN-PN_2S (69 nmol) solubilized in 50 µl of EtOH, were added 10 µl of 0.01 M sodium gluconate in MilliQ water and 100 µl of $^{99m}TcO_4^-$ solution (50 MBq), followed by 1 µl of a freshly prepared 0.1 M $SnCl_2$ solution in 0.1 M HCl then the reaction mixture was incubated at 70 °C for 30 minutes.

All reactions were monitored using RP-HPLC method A.

2.2.3 CIF-PN_2S labelling with $[^{99m}Tc(CO)_3]^+$

Two steps reaction: to a eppendorf vial containing 50 µg of CIF-PN_2S (36 nmol) were added 15 µl of EtOH and 70 µl of the freshly prepared precursor *fac*-$[^{99m}Tc(H_2O)_3(CO)_3]^+$ solution (50 MBq) pH = 7 and incubated for 20 minutes at room temperature. Then 5.2 µl

of a DTCM solution in EtOH (1 mg/ml, 184 nmol) were added and the reaction mixture was heated at 50 °C for 30 min.

One step reaction: to a eppendorf vial containing 50 µg of CIF-PN_2S (36 nmol) dissolved in 15 µl of EtOH, were added first 5.2 µl of a DTCM solution in EtOH (1 mg/ml, 184 nmol) followed by 70 µl of the freshly prepared precursor *fac*-$[^{99m}Tc(H_2O)_3(CO)_3]^+$ solution (50 MBq), pH = 7, and then the reaction mixture was incubated at 50 °C for 30 min.

All reactions were monitored using RP-HPLC method B. Comparative *fac*-$[^{99m}Tc(H_2O)_3(CO)_3]^+$ labelling reactions with the only presence of dithiocarbamate or peptidic ligand were carried out in the same conditions and analysed by RP-HPLC.

2.3 RESULTS AND DISCUSSION

2.3.1 CIN-PN_2S labelling with $[^{99m}TcO]^{3+}$: $[(CIN\text{-}PN_2S)^{99m}TcO]$

The labelling reactions were performed by transchelation from $^{99m}TcO(gluconate)_2$ in a two-step chelator exchange synthesis, which involves the reduction from $99mTc^{VII}O4^-$ to $^{99m}Tc^{V}O^{3+}$ by a reducing the agent $SnCl_2$, and the formation of an intermediate complex with the chelating agent gluconate. ^{99m}Tc-gluconate is then able to react with the coordination set of interest (PN_2S) to give the final complex.

Due to its low solubility in aqueous solutions, the ligand was dissolved in degassed EtOH and the labelling reactions were performed with a small volume of $^{99m}TcO_4^-$ in saline solution in order to achieve a final mixture containing at least 30% EtOH. In order to optimize the formulation, the following parameters were examined: pH, temperature, reaction time, reagents concentration.

The amount of stannous chloride was the most important parameter: in fact higher amounts led to the formation of technetium colloid, while with lower amounts the reduction of the radioactive metal was not completely achieved. Temperature was also determining for the labelling yield, whose value increased with increasing heating. However, it was found that incubation at temperatures higher than 75°C produced decomposition of the labelled product. The presence of sodium gluconate was essential due

to high amounts of technetium colloid were found if the labelling reaction was carried out in absence of the exchange ligand.

The highest radiolabelling yield was obtained using the "one step" reaction, probably because the reducing environment, due to the $SnCl_2$ and to the argon atmosphere in the reaction vial, was preserved for a longer time.

Therefore in the optimized reaction to a vial containing 100 µg of CIN-PN_2S (69 nmol) solubilized in 50 µl of EtOH, were added 10 µl of 0.01 M sodium gluconate in MilliQ water and 100 µl of $^{99m}TcO_4^-$ solution (50 MBq), followed by 1 µl of a freshly prepared 0.1 M $SnCl_2$ solution in 0.1 M HCl. The reaction mixture was then incubated at 70 °C for 30 minutes. RP-HPLC analysis confirmed the formation of [CIN-$PN_2S^{99m}TcO$] (R_t = 12.4 min) with a high radiolabelling yield (70 ± 2.0%), but without production of a single defined compound (Figure 6).

HPLC retention times for $^{99m}TcO_4^-$ and [$^{99m}TcO(gluconate)_2$] were 3 and 2.4 minutes respectively.

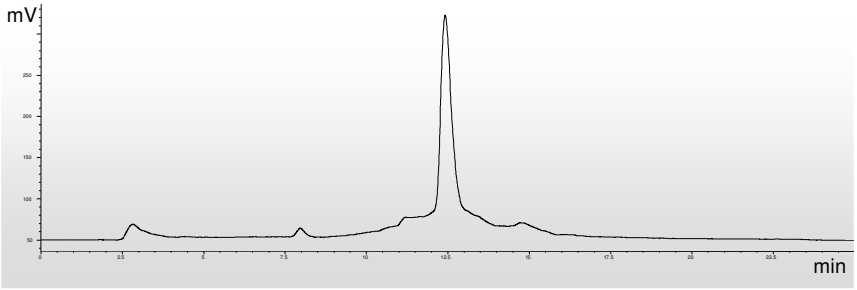

Fig. 6 HPLC γ-trace of the CIN-PN_2S labelling reaction

The reaction in fact led in 30 minutes to the formation of a major peak with R_t = 12.4 min (yield ~70%) and to minor broad peaks with a R_t between 11 and 12 min (yield 10%) and between 14 and 16 min (yield 8%) respectively. The same elution profile and the same molar ratio of the three species were detected after 24 hours at room temperature. Finally, the specific activity obtained in the labelling reaction was estimated to be 720 GBq/nmol .

In order to obtain a higher radiochemical purity, the reaction mixture was purified by means of analytic RP-HPLC isolating the radiolabelled compound with R_t = 12.4 min. The purification also allowed to separate the labelled peptide from the "cold" one, since it is eluted from the column with R_t = 7.1 min, therefore increasing the specific activity.

Collected fractions were dried under vacuum, and the labelled product was then dissolved in 160 µl of a saline/EtOH 70/30 solution, Finally, the purified product once re-injected in RP-HPLC showed a radiochemical purity higher than 93% (Figure 7), therefore it was possible to continue with stability studies.

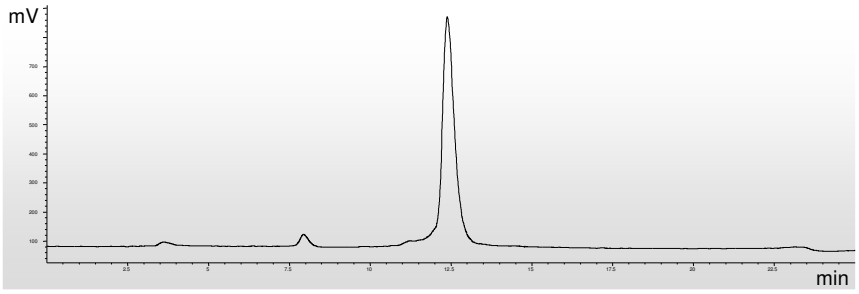

Fig. 7 HPLC γ-trace of the purified [CIN-PN_2S^{99m}TcO] complex

2.3.2 CIF-PN_2S labelling with $[^{99m}Tc(CO)_3]^+$: $[^{99m}Tc(CO)_3(DMTC)(CIF\text{-}PN_2S)]$

Instead of $[TcO]^{3+}$ core, technetium tricarbonyl core was used to labelling CIF-PN_2S moiety. Preparations of the radioactive complex were studied on no-carried-added conditions by ligand substitution from the precursor *fac*-$[^{99m}Tc(H_2O)_3(CO)_3]^+$ where the labile water ligands can be easily replaced by more stable ligands. DMTC [45] and phosphine ligands [46-48] were used to lead a *[2+1] mixed ligand approach* that involves a (SS)(P) coordination set. Diphenylphophines showed a lipophilic character even when linked to a hydrophilic molecule as CIF, therefore to assure their complete dissolution ligand solution was prepared using 20% EtOH.

The labelling reactions were studied, changing reaction conditions (reagents concentration and molar ratio, temperature, reaction time) in order to obtain the optimised protocol.

In order to have an unambiguously confirmation of the [2+1] targeted coordination set, comparative *fac*-$[^{99m}Tc(H_2O)_3(CO)_3]^+$ labelling reactions with the only presence of dithiocarbamate or peptidic ligand were carried out in the same conditions. The labelling reactions were analysed by HPLC to determine the retention times, whose were compared with the main peaks of the mixed ligand reactions. Ligands molar ratio appeared to be the

most critical parameter for the formation of the complex. Reactions of a 5:1 mixture of DMTC and phosphine ligands incubated at 70°C for 30 min gave the best results in terms of yields. In fact, higher molar ratios led to the formation of the complex between the tricarbonyl radioactive moiety and DMTC only, giving a unique peak at 9.6 min, while lower molar ratios led to the formation of the complex with the phosphine ligand alone, whose chromatogram shows a broad peak at 6.7 min. However, both labelling methods (*one step* or *two steps reactions*) led to the same radiolabelling yields: on one hand the one step synthesis is the most attractive method of preparing radiopharmaceuticals, on the other hand the two steps synthesis confirmed how the labile coordinated water molecule of the (SS) bicoordinate tricarbonyl complex was easily replaced by more stable phosphine ligand.

The optimised protocol therefore involves a one step reaction, where to a eppendorf vial containing CIF-PN_2S dissolved in 15 µl of EtOH, were added first DTCM in EtOH (5 equivalents) followed by 70 µl of the freshly prepared precursor *fac*-$[^{99m}Tc(H_2O)_3(CO)_3]^+$ solution. The pH was adjusted to 7, and then the reaction mixture was incubated at 50 °C for 30 min. RP-HPLC analysis shows that the labelling reactions led within 30 minutes to the formation of the single compound $[^{99m}Tc(CO)_3(DMTC)(CIF\text{-}PN_2S)]$ with R_t = 9.6 min (Figure 8), and with a quantitative radiolabelling yield (97%).

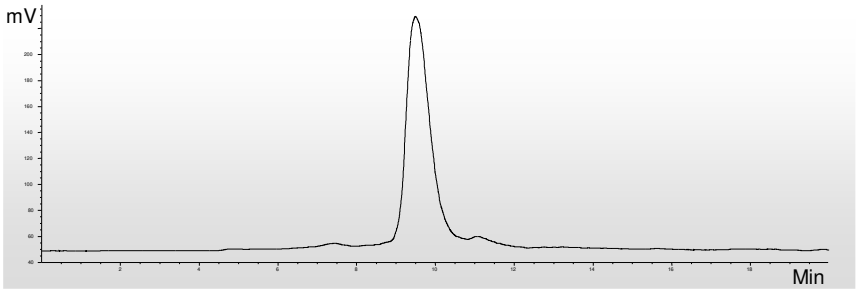

Fig. 8 HPLC γ-trace of the CIF-PN_2S labeling reaction

An irrelevant amount of unreacted dithiocarbammate-$[^{99m}Tc(CO)_3]$ intermediate, with R_t = 10.4 min, was evidenced in all cases while phosphine-$[^{99m}Tc(CO)_3]$ adducts, with R_t = 6.7 min, were not detected. The unreacted $^{99m}TcO_4^-$ and the by-products after addition of Isolink represented the main radioactive undesired products (≤ 2%). The specific activity

obtained for the [^{99m}Tc(CO)$_3$(DMTC)(CIF-PN$_2$S)] complex with the optimised protocol reported in the experimental section was estimated 1.38 TBq/mmol. Several experiments were carried out labelling lower amounts of peptide but maintaining the 5.1 molar ratio between DMTC an phosphinic ligand, however they did not lead to good yields. Therefore, it was assumed that the specific activity obtained when labelling 50 µg peptide was the higher we could achieve.

2.4 CONCLUSIONS

Sst dicarba-analogues were labelled with high yield with two different labelling approaches. For CIN-PN$_2$S derivative the formation of the complex with a ^{99m}technetium^{V}-oxo core was achieved either in a one step reaction or by formation at first of the ^{99m}TcO(gluconate)$_2$ intermediate compound, followed by peptide complexation. In both cases radiolabelling yields were good, but the complex needed further purification in order to achieve higher radiochemical purity and to continue with stability studies. The absence of a single defined compound in the labelling reaction is probably due to the formation of different isomers, as already observed for the PN$_2$S ligand alone [49]. The purification of the complex allowed us to obtain a higher specific activity, because retention times between the cold peptide and the radiolabelled product were very different.

The CIF-PN$_2$S derivative was labelled with a ^{99m}technetium tricarbonyl moiety and, as for the previous peptide, can be easily prepared in a one-step synthesis (useful in the design of a *commercial kit*) with good yields and don't need further purifications. Furthermore, this [2+1] integrated approach with a symmetric bidentate chelating agent also avoids the formation of stereoisomers, which are often detected using non-symmetric bidentate ligands or tridentate BFCA. The isomer formation influences the specific receptor binding because of the different metal-ligand orientation and may produce labelled species with different affinity for the same target, principally for small biomolecules [50]. From the perspective of developing a new drug, single and chemically stable products are essential for FDA approval [51]. Moreover, the amount of ethanol used in the peptide labelling reaction would decrease to less than 10 % after dilution when preparing injectable solutions for animal models or patients.

We concluded that the presented radiocomplexes were obtained easily and with good yields, and the following step is to test their stability and kinetic inertia in order to evaluate their application for the formulation of new radiopharmaceuticals.

REFERENCES

[1] Burgus, R.; Brazeau, P.; Vale, W. et al., Science, **1973**, 179, 77-79

[2] Rivier, J. Somatostatin: Total Solid Phase Synthesis. *J. Am. Chem. Soc*. **1974**, 96, 2986-2992

[3] Pradayrol, L.; Joernvall, H.; Mutt, V.; Ribet, *FEBS Letters*. **1980**, 109, 55-58

[4] Aluments, J.; Sundler, F.; Hakanson, R. *Cell Tissue Res.* **1977**, 185, 465-479

[5] Hokfelt, T.; Efendic, S; Hellerstrom, C. et al. *A. Acta Endocrinol. Suppl*. **1975**, 200, 5-41

[6] Reichlin, S. Somatostatin. *N. Engl.J.Med.* **1983**, 309, 1495-1501

[7] Patel, Y. C. *Front. Neuroendocrinol*. **1999**, 20, 157-198

[8] Hoyer, D.; Bell, G. I.; Berelowitz, M. et al. *Trends Pharmacol. Sci.* **1995**, 16, 86-88

[9] Reisine, T.; Bell, G.I. *Endocr. Rev*. **1995**, 16, 427-442

[10] Patel, J.C. *J. Endocrinol. Invest.* **1997**, 20, 348-367

[11] Weckbecker, G.; Lewis, I.; Albert, I.; Schmid, A. H.; Hoyer, D.; Bruns, C. *Nat. Rev*. **2003**, 2, 999-1017

[12] Froidevaux, S.; Ebarle, A. N. *Biopolymers Peptide Science*, **2002**, 66, 161-183

[13] Reubi, J. C.; Waser, B.; Schaer, J. C.; Laissue, J.A. *Eur. J. Nucl. Med.* **2001**, 28, 836-846

[14] Hofland, L.J.; Lamberts, S.V. *Endocr. Rev.* **2003**, 24, 28-47

[15] Bruns, C et al. Binding Properties of Somatostatin Receptor Suptypes. *Metab. Clin. Exp*. **1996**, *44*, 17-20

[16] Janecka, A.; Zubzycka, M.; Janecki, T. Somatostatin analogs. *J.Peptide Res.* **2001**, *58*, 91-107

[17] Vale, W.;.River, C.; River, J.; Brown, M. *Medicinal Chemistry V;* Eds Gotto, A. M. Jr; Peck, E. J. Jr; Boyd, A. E. **1977**, Elsevier Scientific, Amsterdam 25-62

[18] Bruns, C. ; Lewis, I.; Briner, U. et al. *Eur J Endocrinol* **2002**; 146: 707–716

[19] Lamberts, S. W. J.; van der Lay, A. J.; de Herder, W. W.; Hofland, L. J. *New Engl. J. Med.* **1996**, *334*, 246-254

[20] Karashima, T.; Cai, R. Z.; Shally, A. V. *Life Sci.* **1987**, *41*, 1011-1019

[21] Lamberts, S. W. J.; Krenning, E.P.; Reubi, J. C. *Endocrine Rev.* **1991**, *12*, 450-482

[22] Murfy, W. A.; Lance, V. A., Moreau, S.; Moreau, J.; Coy, D. H. *Life Sci.* **1987**, 40, 2515-2522.

[23] Patel, J. C.; Srikant, C. B. *Endocrinology*. **1994**, *135*,2814-2817

[24] Krenning, E.P.; Kwekkeboom, D.J.; Bakker, W.H. et al. *Eur. J. Nucl. Med* **1993,** 20, 716–731

[25] Kwekkeboom, D.J.; Krenning, E.P. and de Jong M. *Journal of Nuclear Medicine* **2000**, 41, 1704–1713

[26] Hofmann, M.; Maecke, H.; Borner, R. et al. *European Journal of Nuclear Medicine* **2001**, 28, 1751–1757

[27] Maecke, H.R.; Hofmann, M. & Haberkorn, U. *J. Nucl. Med.* **2005**, 46 (supplement 1) 172S–178S

[28] Wester, H.J.; Schottelius, M.; Scheidhauer, K. et al. *Eur. J. Nucl. Med Mol. Imaging* **2003**, 30, 117–122

[29] Bakker, W. H.; Albert, R.; Bruns, C. et al. *Life Sci.* **1991**, *49*, 1583-1591

[30] Froidevaux, S.; Heppeler, A.; Eberle, A. N. et al. *Endocrinology* **2000**, 141, 3304-3312

[31] Gibril, F.; Reynolds, J. C.; Doppman, J. L. et. al. A*nn. Inter. Med.* **1996**, 125, 24-26

[32] Otte, A.; Muller-Brand, J. ; Dallas, S.; Nitzshe, E.; Herrmann, R.; Maecke, H. *Lancet*. **1998**, 351, 417-418

[33] Wild, D.; Shmitt, J. S.; Ginj, M.; Maecke, H. R. et al. *Eur. J. Nucl. Med*. **2003**, 30, 1338-1347

[34] Sprague, J. E.; Peng, Y.; Sun, X.; Weisman, G. R. et al. *Clinical Cancer Research* **2004**, 10, 8674-8682

[35] Froidevaux, S.; Eberle, A. N.; Christe, M.; Sumanovski, L. et al. *Int. J. Cancer.* **2002**, 98, 930-937

[36] Pervez, S.; Mushtaq, A. M.; Arif, M. *Appl Radiat Isot* **2001**, 55, 647-651

[37] Du, J.; Hiltunen, J.; Marquez, M. ; Nilsson, S. ; Holmberg, A. R. *Appl Radiat Isot* **2001**, 55, 181-187

[38] Bangard, M.; Behe, M.; Guhlke, S. Et al. *Eur J Nucl Med* **2000**, 27, 628-637

[39] Decristoforo, C.; Melendez-Alafort, L.; Sosabowsky, J. K.; Mather, S.J. *J Nucl Med* **2000**, 41, 1114-1119

[40] Carotenuto, A.; D'Addona, D.; Rivalta, E. et al. *Letters in Organic Chemistry*, **2005**, 2 (3), 274-279

[41] D'Addona, D.; Carotenuto, A; Novellino, E. et al. *J Med Chem* **2008**, 51, 512-520

[42] Visentin, R.; Rossin, R.; Giron, M. C.; Dolmella, A.; Bandoli, G.; Mazzi U. *Inorg. Chem*. **2003**, 42, 950-959

[43] Riondato, M.; Camporese, D.; Martin, D.; Suades, J. et al. *Eur J Inorg. Chem*., **2005**, 20, 4048-4055

[44] Santimaria M., Blok D., Feitzma R.I.J., Mazzi U., Pauwels E.K.J., *J Nucl Med & Biol,* **1999**, 26, 251-258

[45] Gorshkov, N.I.; Schibli, R.; Schubiger, A.P.; Lumpov, A.A. et al. *J. Organomet. Chem.*, **2004**, 689, 4757-4763

[46] a) Kniess, T.; Correia, J.D.G.; Domingos, A.; Palma, E.; Santos, I. *Inorg. Chem.*, **2003**, 42, 6130-6135

b) Palma, E.; Correia, J.D.G.; Domingos, A.; Santos, I. et al. *J. Organomet. Chem.*, **2004**, 689, 4811-4819

[47] D.L. Nosco, A.J. Tofe, T.J. Dunn, L.R. Lyle, R.G. Wolfangel, M.J. Bushman, G.D. Grummon, D.E. Helling, M.E. Marmion, K.M. Miller, D.W. Pipes, T.W. Strubel, D.W. Wester in *Technetium and Rhenium in Chemistry and Nuclear Medicine*, 3; M. Nicolini, G. Bandoli, U. Mazzi, Cortina International, Verona, Raven Press, New York, **1990,** 381-392

[48] Smith, C.J.; Sieckman, G.L.; Owen, N.K.; Hayes, D.L. et al. *Cancer Research*, **2003**, 63, 4082-4088

[49] Visentin, R.; Giron, M. C.; Bello, M. and Mazzi, U. *Nucl Med Biol.* **2004**, 31, 655-662

[50] Wüst; Skaddan, M. B.; Leibnitz, P.; Spies, H. et al. *Bioorg. Med. Chem.*, **1999**, 7, 1827-1835

[51] Alberto, R. *Eur. J. Nucl. Med. Mol. Imaging* , **2003**, 30, 1299-1302

3

IN VITRO AND *IN VIVO* EVALUATION OF LABELLED SOMATOSTATIN ANALOGUES

3.1 INTRODUCTION

The synthesis of ^{99m}Tc labelled sst analogues was achieved easily and rapidly with good yields, using low concentration ligand in a one-step reaction, as reported in chapter 3. The following step is to study the metabolic stability and kinetic inertia of these complexes in order to evaluate their application for the formulation of new radiopharmaceuticals. The final complex must possess high solution stability to metal redox reactions and/or metal transchelation to native chelating ligands in biological systems. Thus, in vitro studies are performed in plasma or serum to assess the ^{99m}Tc labelled sst analogues metabolic stability and binding to plasma proteins, as fundamental analysis preceding animal studies. The aim of animal study is to evaluate both in vivo stability and pharmacokinetics of the radiometal-peptide complex. Labelled compounds pharmacokinetics following intravenous administration is one of the most important factors to consider in the development of a target-specific radiopharmaceutical. In fact, the radiometal-BFCA can seriously influence the biodistribution of conjugated low molecular weight biomolecules such as sst analogues. It should be reminded that in the design of new target specific radiopharmaceuticals the labelled compound must be able to achieve the highest target uptake with a diagnostically useful signal/noise ratio in the shortest period of time. Therefore a compromise between quick target site accumulation and fast blood clearance is the general aim of the much laboratory research.

This chapter describes the in vitro studies performed on [(CIN-PN_2S)^{99m}TcO] and on [^{99m}Tc$(CO)_3$(DMTC)(CIF-PN_2S)]. The stability and protein binding of the labelled compounds were tested before carrying out biodistribution studies in healthy mice, and only the tricarbonilic complex was stable enough to proceed with the in vivo study in order to determine the main excretion route, and the retaining of specificity of the sst analogous for its receptors after labelling.

3.2 EXPERIMENTAL SECTION

3.2.1 Materials and analytical methods

All chemicals and solvents were reagent grade, used without further purification and purchased as described in the previous chapter. Quality control and stability tests on the radiolabelled products were carried out by RP-HPLC, with instrument and elution methods already described in chapter 3. In addition, MicroSpin G-50 Columns were purchased from Amersham Biosciences (GE Healthcare, Milan, Italy). In vivo studies were performed with 5 weeks old female Balb/C mice (20-25 grams), purchased from the pound of the Department of Oncology (University of Padova, Italy). All animal experiments were carried out accordingly to the relevant national regulation.

3.2.2 Dilution stability

In order to determine the stability of ^{99m}Tc labeled sst analogues, both complexes were tested after dilution with phosphate buffer and saline solution. [CIN-PN_2S^{99m}TcO] was used after purification of the complex by means of RP-HPLC as described in chapter 3, while [^{99m}Tc$(CO)_3$(DMTC)(CIF-PN_2S)] was used without any further purification. 10 µL of complex solutions were diluted to a ratio 1:1, 1:10, and 1:100 with both saline solution (0.9 % NaCl) and phosphate buffer 0.1M (pH = 7). The solutions were incubated at room temperature at pH 7 and then samples were collected between 30 min and 24 h of incubation and analyzed by RP-HPLC.

3.2.3 Cysteine and histidine challenge

For both complexes, challenging assays were carried out adding 10 µL of a freshly prepared complex solution to 10 µL of cysteine in PBS buffer (pH = 7.4) with different concentration, in order to achieve a molar ratio of cysteine to radiolabelled complex between 5:1 and 500:1. All the reaction mixtures were then incubated at 37°C and radiochemical purity was analyzed 1 h later by RP-HPLC.

[^{99m}Tc(CO)$_3$(DMTC)(CIF-PN$_2$S)] was also tested toward ligand exchange and/or decomposition with histidine solutions. Histidine challenge was thus carried out adding 10 µL of a freshly prepared complex solution to 10 µL of histidine in PBS buffer (pH = 7.4) reaching a 100:1 molar ratio between challenging agent and radiolabelled complex.

4.2.4 Plasma stability

To evaluate the serum stability of [^{99m}Tc(CO)$_3$(DMTC)(CIF-PN$_2$S)], 20 µl of the labelled peptide reaction solution were diluted 1:10 either with normal human plasma and with phosphate buffer 0.1M (pH = 7) as a control, and incubated at 37 ^{o}C. 20 µl samples solutions were collected between 30 minutes and 24 hours of incubations, added to 35 µl of ACN to precipitate serum proteins and then centrifuged at 3000 x g (6500 rpm) for 5 minutes. The supernatant was then analysed by RP-HPLC using method B.

3.2.5 Protein binding

20 µL of a freshly prepared solution of [^{99m}Tc(CO)$_3$(DMTC)(CIF-PN$_2$S)] (10 MBq), without further purification, were added to 190 µl of normal human plasma and to 190 µl of PBS as a control, and the resulted mixture was shacked and incubated at 37°C. Selected samples of 20 µl at different time points (between 30 min and 24 hours) were processed using small sample size MicroSpin G-50 centrifugation columns. Columns were pre-spun at 3000 x g (6500 rpm) for 1 min, then the plasma sample was added and the column centrifuged again at 3000 x g (6500 rpm) for 2 minutes. The eluate was collected and the column (unbound activity) and eluate (protein bound activity) were counted separately in a gamma counter.

3.2.6 Biodistribution studies of [^{99m}Tc(CO)$_3$(DMTC)(CIF-PN$_2$S)]

The biodistribution of the radiolabelled peptide was studied in 4 healthy female Balb/C mice. Animals were treated with 2 µL (containing 0.8-1µg CIF-PN$_2$S, 0.72 nmoles) of a freshly prepared solution of [^{99m}Tc(CO)$_3$(DMTC)(CIF-PN$_2$S)] (3 MBq), diluted 1:50 with saline solution and filtrated on a 0.22 µm filter via tail vein injection, and then sacrificed after 2 hours by cervical dislocation. Selected tissues (thyroid, blood, heart, lung, stomach, liver, spleen, pancreas, kidney, adrenals, intestine, muscle and bone) were removed, weighed and counted in the gamma counter. The percentage of the injected dose (%ID) and of the injected dose per gram of tissue (%ID/g) for each tissue were calculated and presented as the means of 4 experiments. The %ID in whole blood was estimated assuming a whole-blood volume of a 6.5% of the total body weight.

3.3 RESULTS AND DISCUSSION

3.3.1 Dilution stability

To assess the stability of ^{99m}Tc labeled sst analogues toward aqueous dilution, both complexes were tested after dilution with phosphate buffer and saline solution. The results showed that the first complex, [CIN-PN$_2$S^{99m}TcO], rapidly undergoes to decomposition. In fact RP-HPLC analysis (method A) evidences reoxidation to ^{99m}TcO$_4^-$, determined by the retention times of the peaks. The radiochemical purity was lower than 32 % after 1 hour of incubation of the complex diluted 1:10 with both saline solution and phosphate buffer (Figure 1).

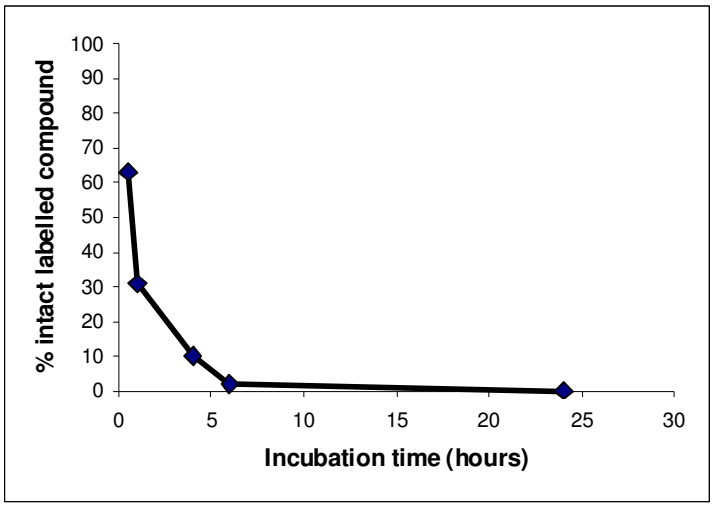

Fig. 1 Stability toward 1:10 dilution with PBS of [CIN-$PN_2S^{99m}TcO$]

The reason of this great instability can be explained by considering a possible oxidation of the phoshinic phosphorus (data confirmed by ESI mass-spectrometry analysis, m/z: 1447). In fact the PN_2S set was shown to be able coordinating the $[^{99m}TcO]^{3+}$ core even with a P^V [1] thus giving a complex where the metal is bound through the new (P)ON_2S set (Figure 2).

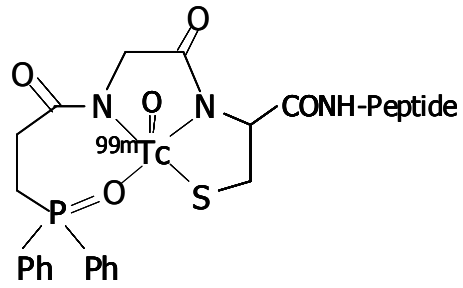

Fig. 2 $[^{99m}TcO]^{3+}$ core coordination by means of the (P)ON_2S set

For the second complex, $[^{99m}Tc(CO)_3(DMTC)(CIF\text{-}PN_2S)]$, results showed a good stability toward aqueous dilution. RP-HPLC analysis (method B) evidences a radiochemical purity higher than 75% after 6 hours incubation of the complex once diluted 1:100 with either saline solution or phosphate buffer (Figure 3).

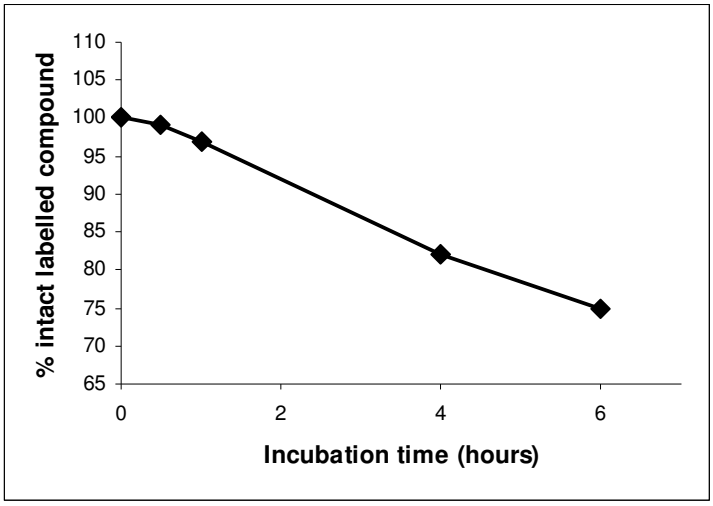

Fig. 3 Stability toward 1:100 dilution with PBS of [^{99m}Tc(CO)$_3$(DMTC)(CIF-PN$_2$S)]

The decomposition products are principally represented by re-oxidation to $^{99m}TcO_4^-$ and *fac*-[^{99m}Tc(H$_2$O)$_3$(CO)$_3$]$^+$ re-formation.

3.3.2 Cysteine and histidine challenge

The stabilities of the radioactive complexes were tested against ligand exchange and/or decomposition. The complexes were first challenged in cysteine in phosphate buffer solution (pH 7.4), incubated at 37°C and analysed by RP-HPLC [2,3]. Even in this case the first complex, [CIN-PN$_2$S^{99m}TcO], appeared not to be stable to transchelation while the [^{99m}Tc(CO)$_3$(DMTC)(CIF-PN$_2$S)] complex showed a good stability toward ligand exchange.

The results showed that after incubation with cysteine solutions the [CIN-PN$_2$S^{99m}TcO] complex undergoes to a rapid decomposition, and are summarized in Table 1.

Complex / Cysteine molar ratio	% intact labeled complex
1 : 5	73
1 : 50	65
1 : 500	29

Table 1 Cysteine challenge of [CIN-PN$_2$S^{99m}TcO] complex

More than 72% of radioactivity in fact dissociated from the complex when using the higher molar ratio of cysteine. The main degradation products are represented by technetium-oxo complex with this aminoacid (R_t = 7.6 min) or other products like re-oxidation of the metal core to $^{99m}TcO_4^-$ (R_t = 3.6 min) (Figure 4).

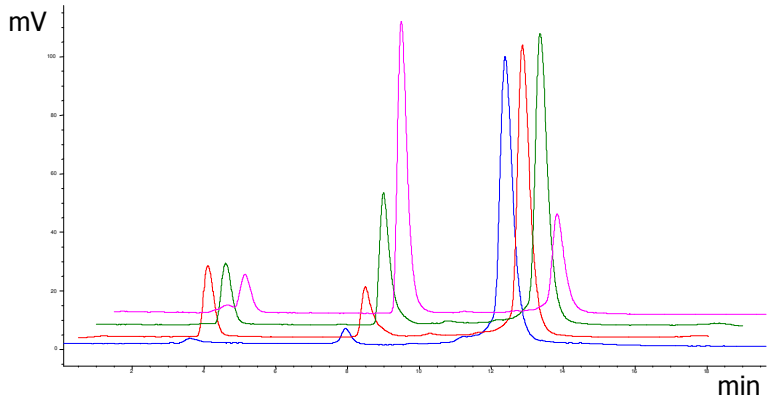

Fig. 4 HPLC γ-trace of [CIN-$PN_2S^{99m}TcO$] complex (blue), and cysteine challenge reactions 1:5 (red), 1:50 (green) and 1:500 (magenta)

The high instability of this complex against ligand exchange and toward dilution, as previously described, does not allow any further study.

Challenging assays for the second complex gave good results. [$^{99m}Tc(CO)_3$(DMTC)(CIF-PN_2S)] was incubated with cysteine and histidine solutions for 1 hour at 37°C. The results are summarized in Table 2, and no re-oxidation to $^{99m}TcO_4^-$ and *fac*-[$^{99m}Tc(H_2O)_3(CO)_3]^+$ re-formation was determined in an analysis of the retention time of the peaks, as reported in general for technetium tricarbonyl complexes.

Complex / Cysteine molar ratio	**% intact labelled complex**
1 : 5	96.4
1 : 50	92
1 : 500	91
Complex / Histidine molar ratio	**% intact labelled complex**
1 : 100	63

Table 2 Cysteine and histidine challenge of [$^{99m}Tc(CO)_3$(DMTC)(CIF-PN_2S)] complex

However a significant decomposition of the complex occurred using histidine, leading to 35% of radioactivity dissociated from labeled product (Figure 5).

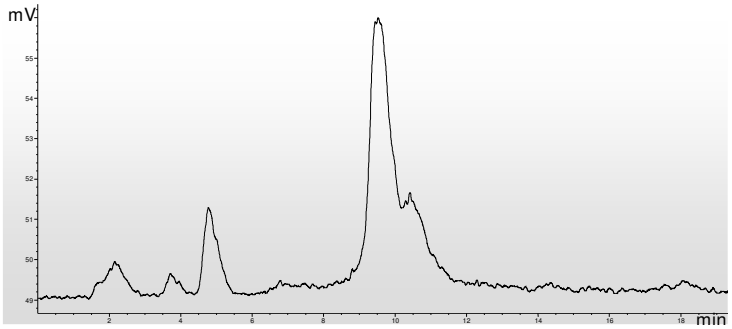

Fig. 5 HPLC γ-trace of [^{99m}Tc(CO)$_3$(DMTC)(CIF-PN$_2$S)] after 1 h incubation with histidine 1:100

Displacement of these amino acids, forming the corresponding technetium tricarbonyl complex or other products, is unlikely but it is relatively common, particularly with histidine, which is one of the most potent ligand systems for this moiety.

3.3.3 Plasma stability

The plasma stability was determined by incubation with normal human plasma up to 6 hours at 37°C. After incubation, ACN was added to the sample in order to precipitate the proteins, and the vial centrifuged. Investigation in human plasma of [^{99m}Tc(CO)$_3$(DMTC)(CIF-PN$_2$S)] revealed the great stability of the complex against metabolic decomposition, as reported in Figure 6.

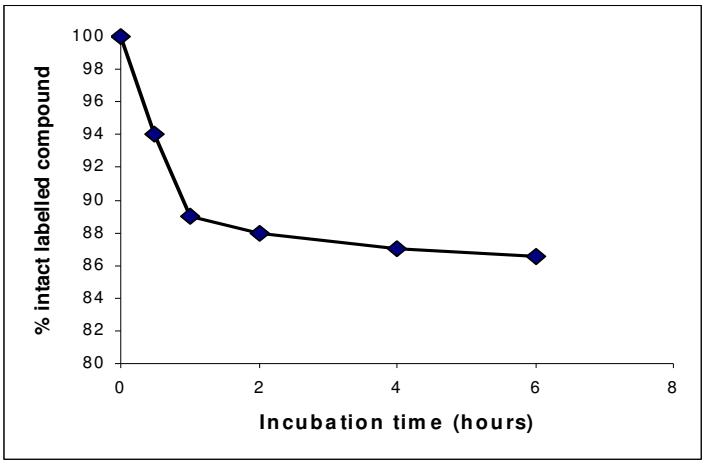

Fig. 6 Plasma stability for [^{99m}Tc(CO)$_3$(DMTC)(CIF-PN$_2$S)] complex

RP-HPLC analysis of the supernatant showed in all cases a major peak with the same retention time as the starting material corresponding to the labelled peptide that showed a radiochemical purity higher than 86% after 6 hours incubation. No re-oxidation to $^{99m}TcO_4^-$ and *fac*-$[^{99m}Tc(H_2O)_3(CO)_3]^+$ re-formation was determined (Figure 7).

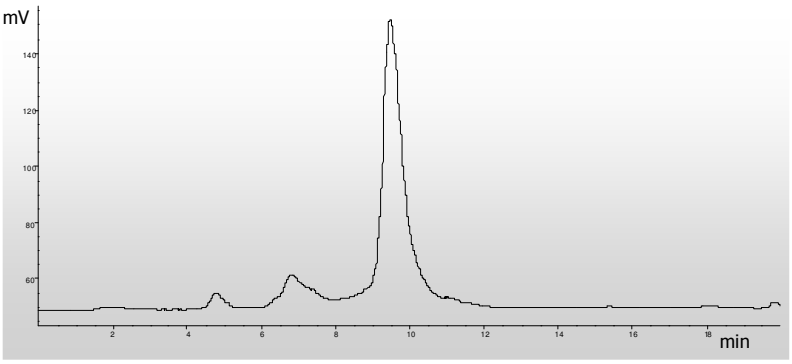

Fig. 7 HPLC γ-trace of $[^{99m}Tc(CO)_3(DMTC)(CIF\text{-}PN_2S)]$ complex after 6 h incubation with human plasma

3.3.4 Protein binding

Finally, the tricarbonyl complex was incubated in human plasma and the protein binding was determined between 15 minutes and 24 hours. The samples were added to small Sephadex G50 columns and centrifuged for 2 minutes. Under these conditions, the large molecular weight protein-bound complex elutes from the column, while un-bound, low molecular weight complexes remain in the column. The protein binding of the labeled peptide was calculated as a percentage of the total activity, and revealed that a low amount of radioactivity is associated with serum proteins (Figure 8), since after 24 hours incubation only about 22% of the activity eluted from the column.

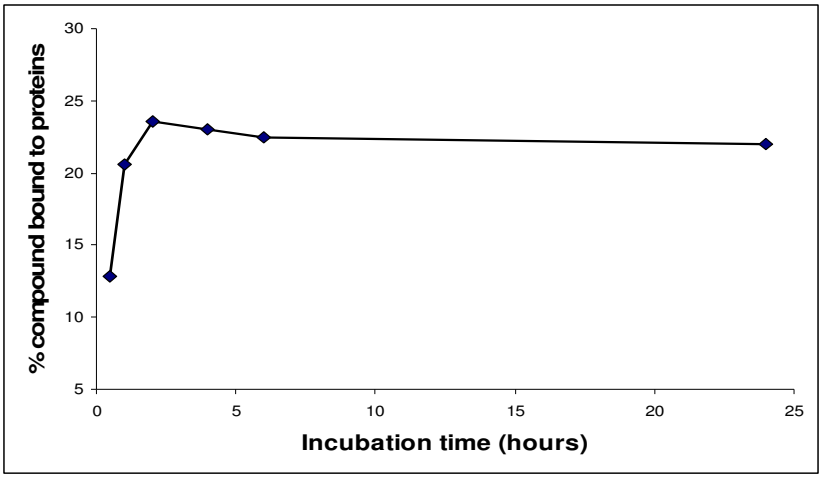

Fig. 8 Protein binding for $[^{99m}Tc(CO)_3(DMTC)(CIF\text{-}PN_2S)]$ complex

Aggregation with the biological components, due to the lipophilicity of the complex, and interaction with the histidine/cysteine residues naturally present in serum proteins may justify the observed results.

3.4.5 Biodistribution studies of [^{99m}Tc(CO)$_3$(DMTC)(CIF-PN$_2$S)]

For an initial evaluation of the in vivo behaviour of the radiolabelled complex, the experiment was settled injecting intravenously 4 healthy mice at the same time. Detailed information about the biodistribution and pharmacokinetics of the complex were obtained after the sacrifice of mice 2 h post injection, and counting the organs and the tissue activity (Table 3 and figure 9).

Table 3 Ex vivo data for [^{99m}Tc(CO)$_3$(DMTC)(CIF-PN$_2$S)] 2h post i.v. injection

Organs	% I.D. / organ	S.D.	% I.D. / gram	S.D.
Thyroid	0,09%	0,07%	0,56%	0,09%
Heart	0,15%	0,01%	1,62%	0,12%
Blood	0,17%	0,08%	2,09%	0,35%
Lung	2,03%	0,59%	22,77%	5,15%
Stomach	0,54%	0,41%	1,82%	1,13%
Spleen	11,17%	0,81%	136,07%	8,22%
Kidneys	0,74%	0,03%	3,53%	0,14%
Liver	19,47%	2,28%	22,86%	4,73%
Intestine	3,86%	0,35%	2,24%	0,20%
Muscle	0,10%	0,07%	0,41%	0,27%
Bone	0,06%	0,02%	2,80%	0,44%
Bladder	0,01%	0,01%	1,03%	0,48%
Pancreas	0,09%	0,06%	0,73%	0,11%
Adrenals	0,06%	0,01%	8,76%	1,26%

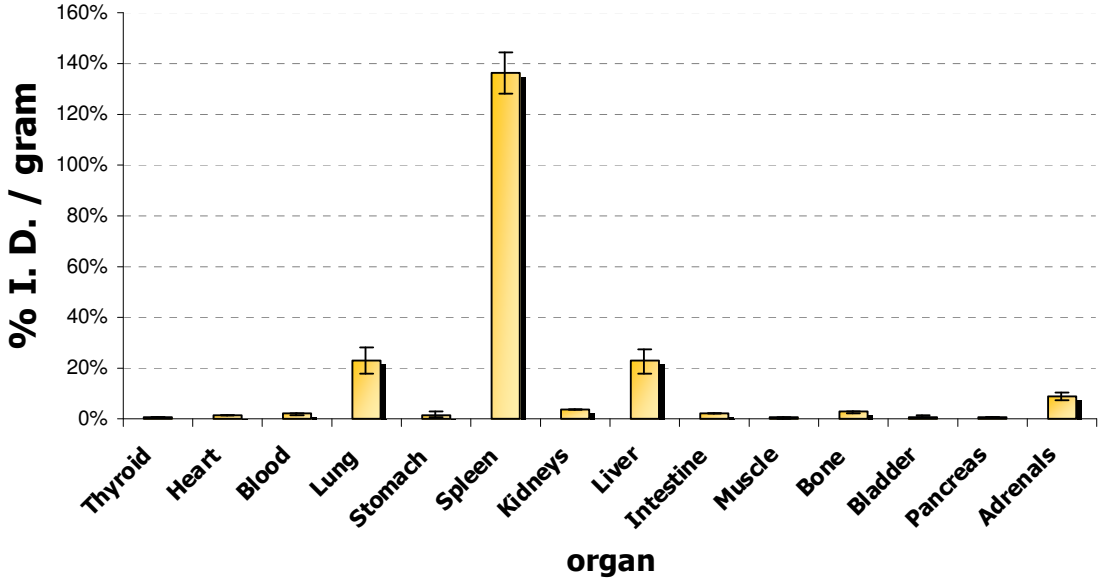

Fig. 9 % injected dose per gram of tissue for [^{99m}Tc(CO)$_3$(DMTC)(CIF-PN$_2$S)] 2h post i.v. injection

The presented data clearly showed the trend of [^{99m}Tc(CO)$_3$(DMTC)(CIF-PN$_2$S)] after injection, which was characterised by liver and spleen uptake. With regard to the high liver uptake and intestinal clearance, this patter of biodistribution is seen with very lipophilic complexes [4]. An efficient clearance via the hepatobiliary pathway determined its rapid removal from the bloodstream, and the spleen uptake can be justified with the complex binding to plasma proteins. However a small amount of radioactivity was found in lung, probably due to the formation of aggregates between the labelled complex and serum proteins. Pancreas and adrenals activities were finally evaluated: in fact, somatostatin receptor are overexpressed in these tissues in healthy animals. The results showed a high specific binding of the complex to sst receptors present in adrenals: the ratio between the activity found in adrenals and the activity present in blood is about 4, thus confirming the specificity of CIF for sst receptors even after labelling.

3.4 CONCLUSIONS

The ^{99m}Tc-oxo complex with the first sst analog showed a considerable decomposition and a great interaction with challenging agents such as cysteine, thus precluding any further biological study. This instability is probably caused by a partial oxidation of the phosphine phosphorus of the PN_2S set, that leads to a new coordination mediated by the phosphine oxide ligand ($(P)ON_2S$ set).

On the other hand, the results show that the carbonyl complex method provides an efficient means of preparing ^{99m}Tc-labelled peptides with high stability. Since the yield of the [^{99m}Tc$(CO)_3$(DMTC)(CIF-PN_2S)] complexation reaction is higher than 95%, the complex can be used without further purification, which is an advantage if considering that many ^{99m}Tc-labelled peptides need to be purified [5]. Experiments showed that [^{99m}Tc$(CO)_3$(DMTC)(CIF-PN_2S)] is stable to dilution and transchelation and, in addition, it shows a low protein binding. Stability studies evidenced that the complex is stable in serum and PBS over a 24 h period at 37°C with very low decomposition.

The primary aim in the design of a radiolabelled peptide is to maximize the uptake of radioactivity in the target (tumor) and to minimize the uptake and retention of activity in other tissues, which would otherwise increase their absorbed dose. In general, it is desirable to have low blood background and excretion through the kidneys rather than the hepatobiliary tract. Unfortunately, the in-vivo behaviour of [^{99m}Tc$(CO)_3$(DMTC)(CIF-PN_2S)] in animal models obtained from ex-vivo data showed clearance from the bloodstream and a rapid liver uptake, followed by elimination via the hepatobiliary route. Despite this behaviour, the activity found in adrenals demonstrated the complex to maintain the specificity to bind sst receptors. In fact the ratio between activity found in adrenals and activity found in blood was about 4,2. This result is lower than the one obtained in healthy mice with Octreoscan [6] and with other octreotide analogues labelled with ^{99m}Tc such as Demotate [7], but anyhow is promising for further investigation, such as receptor binding assays and biodistribution studies in AR42J tumour bearing mice, that are actually in progress.

To improve pharmacokinetics properties, some structural modification of the complex can be obtained modifying both the phosphine and the dithiocarbamate moieties thus reducing the lipophilicity of the complex. Water-soluble phosphines bearing a terminal

anchor group (COOH, NH_2, SH etc.) are commercially available and can substitute the diphenilphosphinopropionate moiety linked to the peptide. On the other hand, many dithiocarbamates and their coordination capability are well known [8], allowing the synthesis of hydrophilic derivatives able to improve hydrophilicity properties without increasing interactions with non-target organs.

REFERENCES

[1] Visentin, R.; Pasut, G.; Veronese, F. M. and Mazzi, U. *Bioconjug Chem* **2004**, 15, 1046-54

[2] Schibli, R.; La Bella, R.; Alberto, R.; Garcia-Garayoa, E.; Ortner, K. et al. *Bionjug Chem,* **2000**, 11, 345-351

[3] M.A. Stalteri, S. Bansal, R. Hider, S.J. Mather, *Bioconjug Chem*, **1999**, 10, 130-136

[4] Decristoforo, C. and Mather, S.J. *Nucl. Med. Biol.*, **1999**, 26, 389-386

[5] Decristoforo, C. and Mather, S.J. *Bioconjug Chem*, **1999**, 10, 431-438

[6] *Life Sciences*, **1991**, 49, 1593-1601

[7] Nikolopulou A.; Maina, T.; Sotiriou, P. et al. *J. Peptide Sci.* **2006**; 12, 124–131

[8] Carrer, A.; Suades, J.; Mazzi, U. *Inorg Chim Acta*, **2009** (submitted)

Part II

HYALURONIC ACID

4

^{188}Re-HA: LABELLING AND IN VITRO / IN VIVO EVALUATION

4.1 INTRODUCTION

4.1.1 Motivations to use of hyaluronic acid as tumour targeting agent

Hyaluronic acid (HA) is a linear polisaccharyde with a simple chemical structure (Fig. 1), formed by alternating D-glucuronic acid and N-acetyl-D-glucosamine units. It is one of the several glycosaminoglycan components and it is present in the cartilage scaffolding, the synovial fluid of joints and the extracellular matrix [1].

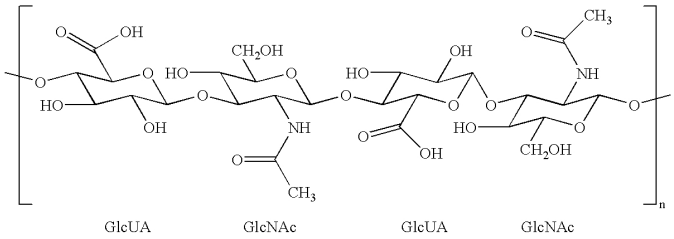

Fig. 1 Hyaluronic acid backbone

Acting as a signalling molecule in cell adhesion, growth, and migration, HA plays critical functions in cell motility, inflammation, wound healing and cancer metastasis [2].

It has been demonstrated that HA oligomers can bind to different cell types by interaction with several receptors. Among them, CD44 receptors are involved in pathologic cellular processes such as angiogenesis, tumour growth and metastasis progression [3,4], RHAMM receptors regulated HA cell motility [5], and HARE are responsible for receptor-

mediated uptake of HA in liver [6]. It was probed that HA could be internalized by the cells after been bound to these receptors and go through a lysosomial degradation [7].

Most human cancer cells (in particular epithelial, ovaric, colon and stomach tumours) were shown to overexpress CD44 receptors [8-14] with a high capacity to bind and internalize the HA moiety [15], Therefore, HA-drug bioconjugates could be used as tumor targeting, and this means that it is able to be concentrated on tumour cells with minimal uptake in normal cells. Recently HA has been conjugated to drugs such as Mitomycin C [16], Epirubicin [17] and Butyric acid [18-21], showing advantages in drug pharmacokinetic properties and controlled release [22, 23], and moreover markedly enhanced the selectivity for cancerous cells [24, 25].

On the other hand it has been demonstrated that beta-irradiation produces not only cellular death by DNA damage but also inhibits (*in vitro*) cancer cell growth by activation of apoptosis pathways in single cells at several levels, including the triggering of ligand/receptor pathways, mitochondrial activation and caspase activation [26, 27]**.** Consequently, the most promising results in radionuclide therapy are obtained using a combined-modality approach with a tumor targeting molecule labelled with a beta-emitting nuclide such as ^{188}Re.

4.1.2 Aim of the project: ^{188}Re-labeling of Hyaluronic acid

Some derivates of the tumour targeting agent hyaluronic acid (HA) were recently labelled with technetium-99m using a direct method, leading to a complex with high radiochemical purity [28]. The biodistribution studies in healthy mice of these radiolabelled complexes showed that 25 min after the intravenous administration, more than 80 % of the radiopharmaceutical was found in the liver and the spleen due to the lypophilicity of the complex and the selective binding of the hyaluronic acid to CD44 and HARE receptors [28].

Since the best results in cancer treatment has actually been obtained with the combined-modality therapy using tumor targeting molecule radiolabelled with beta emitting radionuclides, the aim of this work is to label the HA with ^{188}Re and to determine if it can be used as a therapeutic radiopharmaceutical. To reach our objective, the labelling reaction has been optimized and the stability studies on the radiolabelled complex were performed. Finally, biodistribution and pharmacokinetics of ^{188}Re-HA were evaluated.

4.2 EXPERIMENTAL SECTION

4.2.1 Materials and analytical methods

All chemicals and solvents were reagent grade and used without further purification. Hyaluronic acid (70 kDa) was obtained from BioChemika (Fluka, Sigma-Aldrich, Italy). $^{188}ReO_4^-$ was eluted from a commercial $^{188}W/^{188}Re$ generator (Polatom, Poland), and sodium gluconate and $SnCl_2$ were purchased from Sigma-Aldrich (Milan, Italy). ^{188}Re-HA complex was purified by size-exclusion chromatography using a Sephadex G-25 column Hi-Trap desalting, with a void volume of 1.5 ml, obtained from Supelco, Sigma-Aldrich (Milan, Italy). Labelling efficiency and radiochemical purity were analyzed using size exclusion HPLC chromatography and instant thin-layer chromatography (ITLC).

Size-exclusion HPLC analyses were carried out in a Waters chromatography system (Waters, Milford MA,USA), controlled by a binary Waters 510 programmable gradient pump and running Empower software. The analyses were monitored with a Waters 486 tunable absorbance detector set at 215 nm coupled to a Bioscan-γ-detector B-FC 3200 (Milano, Italy); a size-exclusion column Zorbax GF-250 was used (4 μm, 250 x 4.6 mm, Agilent Technologies, Waghaeusel-Wiesental, Germany) at a flow rate of 0.5 mL/min with 0.1M sodium phosphate solution at pH 7.0 as mobile phase. Pre-column filters were used at all times.

ITLC analyses was performed on silica gel impregnated fibre-glass sheets (Pall Italia s.r.l., Milano), running a sample of 1 μl on a 10 cm strips using as mobile phases acetone, saline solution, and a mixture (50/50) of 0.1 M sodium citrate solution at pH 5 and acetonitrile (ACN). Distribution of radioactivity on the strip was determined by cutting it into 1 cm pieces and each one was counted in a NaI-scintillation counter. Rf of ^{188}Re-HA is 0.0 in acetone and in saline solution and 1.0 in sodium citrate/ACN. The Rf of the labelled ^{188}Re-gluconate is 0.0 in acetone and 1.0 in both saline and sodium citrate/ACN, while free ^{188}Re-perrhenate migrates with the front in the three solvents (Rf = 1.0). Reduced hydrolysed ^{188}Re stays at the seeding point with the three solvents (Rf = 0.0).

Radioactive measurements were determined by using a calibrator M2361 Messelektronik (Dresden, Germany) and a gamma counter with NaI detector (coupled to Thorn 9265 and Scalar Rate Meter Ludlum model 2200). All manipulations were carried out approved for low-level radioactivity use.

In vivo studies were performed with 5 weeks old healthy female C57BL/6 black mice (20-25 grams), purchased from the pound of the Department of Oncology (University of Padua, Italy). All animal studies were done in compliance with guidelines set by the Padua University Animal Studies Committee.

4.2.2 Direct labelling of Hyaluronic Acid with ^{188}Re

The labelling reaction was at the beginning performed changing several parameters, such as the amount of stannous chloride (0.55, 1.1, and 2.2 mg), the temperature (25, 35, 50, 65, 80 and 90 ^{o}C), the incubation time (45, 75, 90, 110 and 130 min) and the addition of sodium gluconate as exchange ligand. Only one parameter was altered at a time, until we finally achieved the optimized protocol.

HA was then radiolabelled by adding 100 µl of ^{188}Re-perrhenate solution (20 MBq) and 60µl of 0.1M $SnCl_2$ solution in 0.1M HCl to a vial containing 1 mg HA. The pH of the reaction mixture was adjusted to 4 and the preparation was gently mixed and incubated at 65 °C for 90 minutes.

4.2.3 Purification of ^{188}Re-HA

^{188}Re-HA was purified by size-exclusion chromatography before starting the stability tests, using a Hi-Trap desalting column with a 1000-5000 Da cut-off and collecting samples of 0,5 mL. ^{188}Re-HA was quickly eluted with saline solution, fractions, while the Sephadex G25 resin retained ^{188}Re-perrhenate and other low-molecular weight species.

4.2.4 Dilution stability

In order to determine the stability of ^{188}Re-HA toward acqueous dilution, 50 µL of purified complex were diluted to a 1:10, 1:50, and 1:100 ratio with both saline solution (0.9 % NaCl) and phosphate buffer 0.1M. The solutions were incubated at room temperature at pH 7, collecting samples between 5 min and 72 h of incubation and analyzing them by size-exclusion HPLC and ITLC.

4.2.5 Cysteine challenge

Challenging assays were carried out adding 50 µL of a freshly purified ^{188}Re-HA solution to 50 µL of freshly prepared cysteine solutions in PBS buffer (pH = 7.4) with

different concentration, in order to achieve a molar ratio of cysteine to radiolabelled complex between 5:1 and 500:1. All the reaction mixtures were then incubated at 37°C and radiochemical purity was analyzed 1 h later by size-exclusion HPLC.

4.2.6 Serum stability and protein binding

To estimate the serum stability of ^{188}Re-HA a volume of 100 µl of the purified labelled product solution (3 mg/ml) was incubated at 37 ^{o}C with 1 ml of fresh human serum from healthy donors. Samples were collected at time intervals between 30 min and 24 hour, and analysed by size-exclusion HPLC. A shift on the radioactivity profile to a higher molecular weight indicates protein binding. Lower molecular-weight peaks, corresponding to longer retention-time in size-exclusion chromatography, indicate labelled catabolites or serum cysteine binding. The recovery of radioactivity was routinely determined.

4.2.7 Biokinetics studies of ^{188}Re-HA

The biodistribution studies of ^{188}Re-HA was determined by injecting healthy female C57BL/6 black mice with 50 µL (3 MBq) of the purified complex via the tail vein. The animals were then sacrificed by cervical dislocation after 0.5, 4, 24 and 72 hours post injection, and selected tissues (thyroid, blood, heart, lung, stomach, liver, spleen, kidney, intestine, muscle and bone) were excised and weighed. Each organ activity was then measured in a well-shaped scintillation detector. The radioactivity of the tissue samples was expressed as percentage of the injected activity per gram of tissue (% IA/g).

In order to derive ^{188}Re-HA time activity curves in each organ, the results of percentage of the injected activity per gram of tissue at different time points were used. Blood activity curve was used to establish the biokinetic model by fitting the data to a function with three exponential terms and extrapolated considering as the initial activity (t = 0) the initial injected activity to each animal.

4.3 RESULTS AND DISCUSSION

4.3.1 Radiolabelling yield

The labelling reaction of hyaluronic acid with Rhenium-188 was finally achieved with high yields, altering several parameters to optimize the formulation.

The reaction temperature had the most significant effect on the radiolabelling yields. Radiochemical purity increases directly with the temperature until it reaches 65°C, after that the radiolabelling yield remains relatively constant. ^{188}Re-HA yields increased proportionally with the incubation time reaching the maximum values after 90 min at 65°C (Figure 2).

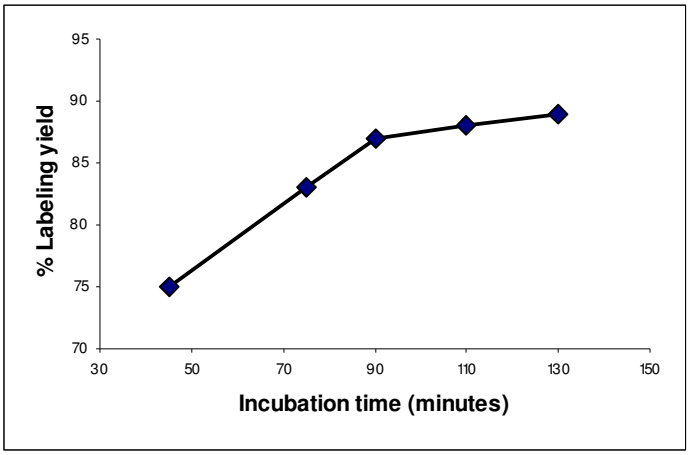

Fig. 2 Effect of the incubation time on the labelling yield of HA

The quantity of reducing agent ($SnCl_2$) had less influence probably because the reduction power of $SnCl_2$ was not high enough to produce other species than ^{188}Re(V)-compounds. Addition of sodium gluconate as exchange ligand decreases the radiochemical purity of the obtained product, probably because its chemical structure, similar to HA, acts as a competitor. The highest radiolabelling efficiency of ^{188}Re-HA (83 %, radiochromatogram in figure 3) was thus obtained after the addition of 100 µL (20 MBq) of ^{188}Re-perrhenate and 60 µL of 0.1 M $SnCl_2$ solution in HCl 0.1 M to a vial containing 1 mg HA. The pH was then adjusted to 4, and the reaction mixture was gently mixed and incubated at 65°C for 90 min.

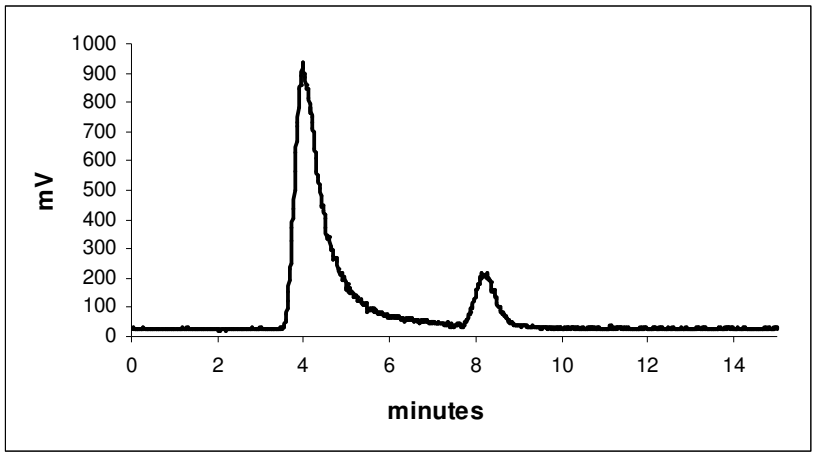

Fig. 3 HPLC γ-trace of the ^{188}Re-HA reaction mixture

4.3.2 Purification of ^{188}Re-HA

In order to evaluate the stability of the complex and to carry out the biological studies, the reaction mixture was purified using a Hi-Trap desalting column. ^{188}Re-HA was rapidly eluted with saline solution from the column in the first 2 ml fraction. The ^{188}Re-perrhenate was eluted with the 4 to 8 ml fractions, while the Sephadex G25 resin retained the reduced hydrolysed-^{188}Re. The purification was then confirmed by size exclusion HPLC (Fig. 4), where the radiochromatogram shows a unique peak corresponding to ^{188}Re-HA.

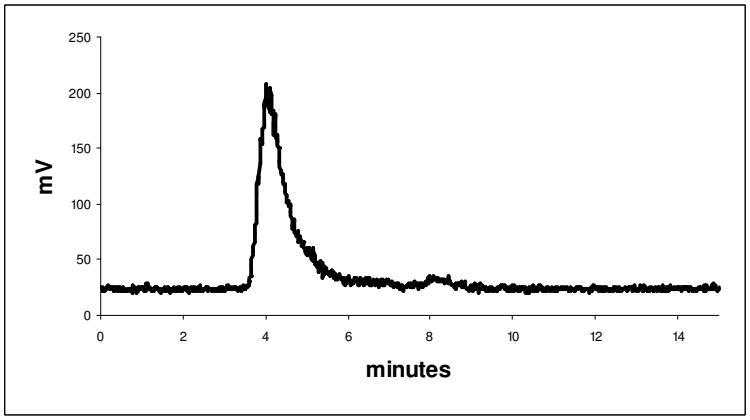

Fig. 4 HPLC γ-trace of the purified ^{188}Re-HA

4.3.3 Dilution stability

To determine the stability of ^{188}Re-HA toward aqueous dilution, a solution of the purified complex was diluted in saline solution and 0.1 M phosphate buffer. Size exclusion chromatography showed that the complex was stable once diluted to a ratio 1:50 and incubation for 1 h at room temperature. However the radiochemical purity decreased to 65 % after 24 h incubation (Figure 5).

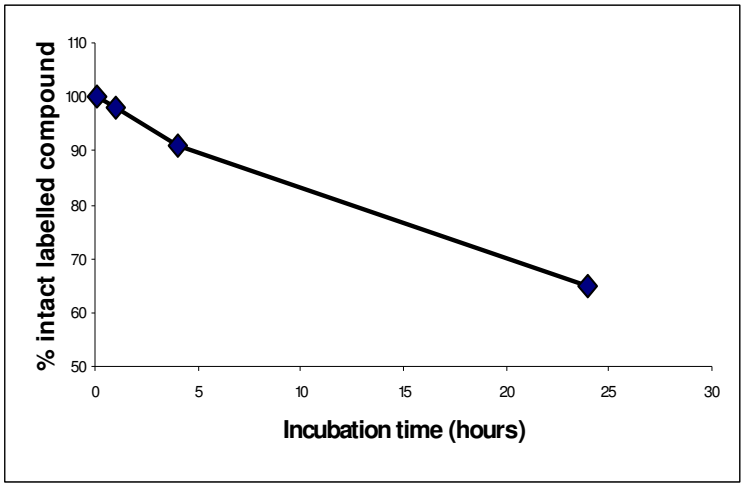

Fig. 5 Stability toward 1:50 dilution in PBS of ^{188}Re-HA

4.3.4 Cysteine challenge

The results evidenced that ^{188}Re-HA complex was quite stable in presence of cysteine since even after 1 h incubation with the highest concentration, both ITLC and HPLC showed less than 8 % of radioactivity was dissociated from the complex. Incubation of the radiolabelled complex with the higher amount of cysteine in fact did not lead to significant ligand exchange and/or decomposition, and since 500-fold molar excess of challenging agents are expected to well simulate an in vivo donor atom competition and redox reactions, the cysteine challenge proved the high stability of the ^{188}Re-HA complex.

4.3.5 Serum stability and protein binding

^{188}Re-HA stability test in human serum, showed radiochemical purity higher than 95 % after 1 h incubation at 37°C but decreased to 73% and 55% after 4 and 24 h respectively (Figure 6).

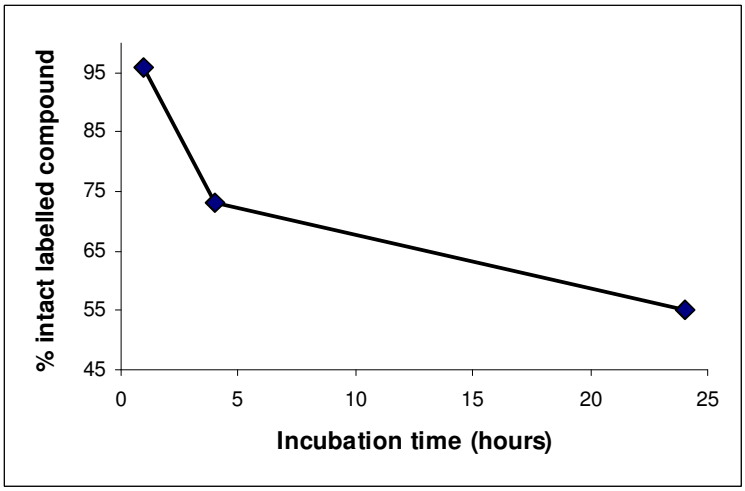

Fig. 6 Serum stability of ^{188}Re-HA

Only a slightly serum protein binding (2 %) was found over a period of 24 h by HPLC analysis, as reported in figure 7, where the UV serum chromatogram, with serum proteins peak at 6 minutes, is correlated to the γ-ray trace of ^{188}Re-HA (peak at 4 min). The two chromatograms overlay in a very little area, thus indicating that only 2% of activity is bound to serum proteins. At these conditions the perrhenate (peak at 8 min) was the only decomposition product formed. The HPLC recovery was higher than 98 % in all the cases.

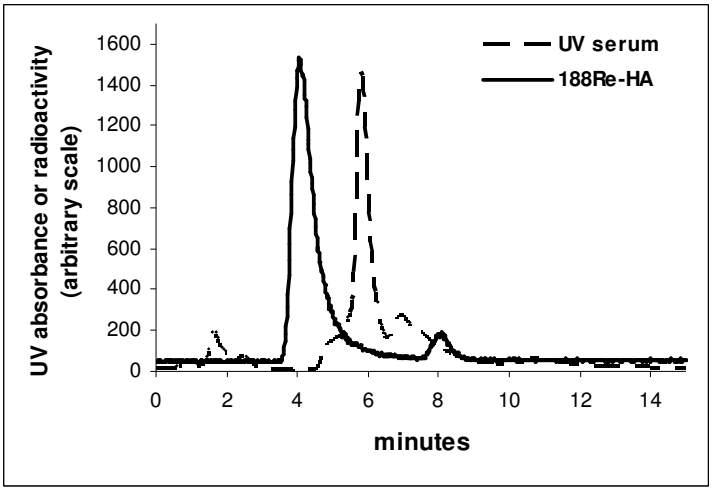

Fig. 7 Protein binding of ^{188}Re-HA**,** after 1 h incubation in human serum at 37 °C

4.3.6 Biokinetics studies of ^{188}Re-HA

Biodistribution studies were done in healthy female C57BL/6 black mice, a good model to implant different kinds of tumors necessary for the next step in the therapeutic studies. ^{188}Re-HA showed a fast blood clearance followed by a rapid accumulation in liver and spleen where it remained for at least 72 h, with a minimal uptake in other organs (Fig. 8).

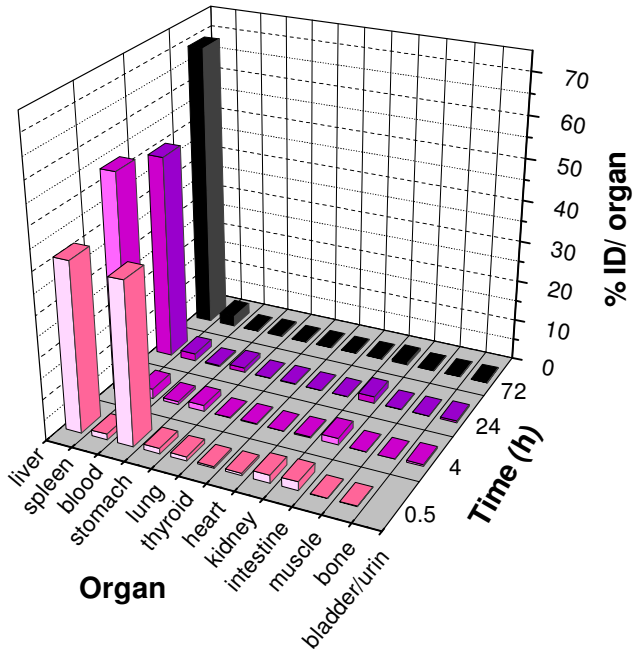

Fig. 8 Biodistribution at different time points of ^{188}Re-HA after i.v. administration

^{188}Re-HA activity found in blood at different time points was used to derive a blood activity curve, fitting data into a triexponential function (n = 5):

$$A(t) = 95.1e^{-1.96t} + 4.43e^{-0.647t} + 0.47e^{-0.028t}$$

Figure 9 shows the plot of ^{188}Re-HA clearance from the blood. The curve shows two main slopes which confirm a half-life of 21 min for the fast component ($T_{1/2}\alpha$ = ln2/1.96), and 1.07 h for the first slow component. The residence time calculated in blood was very low (36 min) as it could be prevented from the ^{188}Re-HA concentration in blood values after 24 and 72 h of injection.

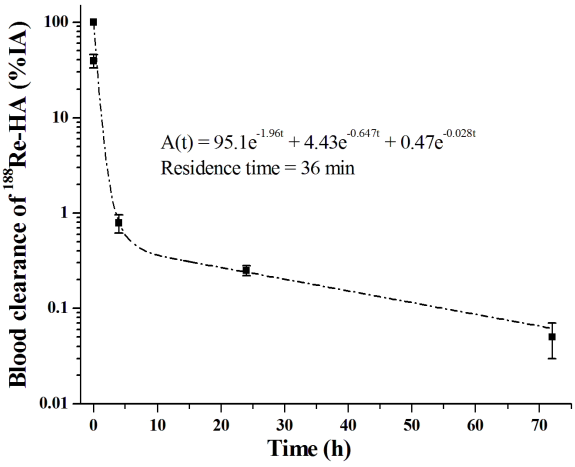

Fig. 9 Blood clearance of ^{188}Re-HA in healthy female C57BL/6 black mice

The rapid concentration of the ^{188}Re-HA in the main source organs, evident in Figure 10 plots, was attributable to the high molecular weight of the complex, that cannot undergo to renal excretion.

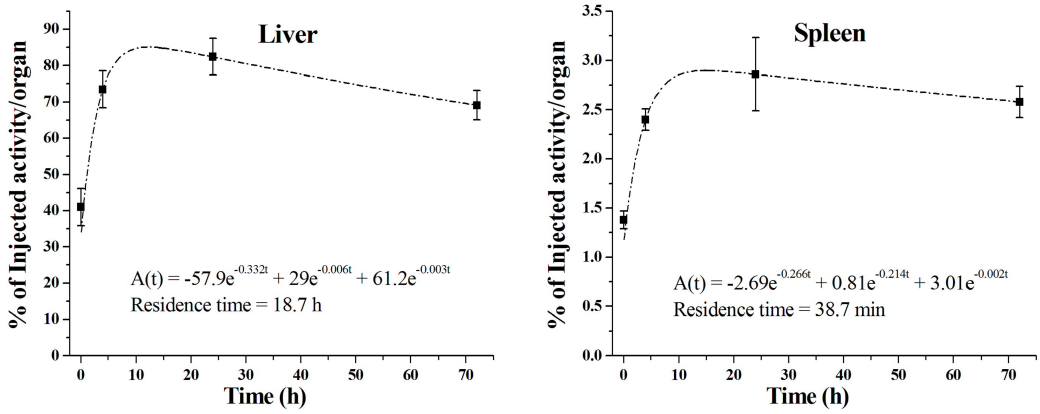

Fig. 10 Biokinetics of ^{188}Re-HA in the main sources organs liver and spleen of healthy female C57BL/6 black mice

Four hours after administration ^{188}Re-HA was almost totally removed from the blood by the liver polygonal cell. Due to the selective uptake via receptors present in the endothelial cells, it was concentrated in liver and spleen raising its maximum value after 24 hours with a concentration of 82.43% ± 5.05% and 2.86% ± 0.37% of the injected activity

respectively. The calculated residence times were 18.7 h for the liver and 38.76 min for spleen.

Figure 8 showed that there was minimal uptake in stomach and kidneys (less that 1% and 0.1% of the injected dose after 24 h and 72 h respectively), with residence times lower than 15 min. However HPLC analysis of mice urine demonstrated that activity was due to the free perrhenate obtained from the decomposition of the ^{188}Re-HA complex.

4.4 CONCLUSIONS

^{188}Re-HA complex was obtained easily and with high yields. The reaction temperature had the most significant effect on the radiolabelling yield, and this result can be explained by the fact that the HA solution is viscous at room temperature. Higher temperature makes the solution becoming more fluid, thus leading to a greater possibility of interaction between the metal present in the reaction mixture and the polymer coordination sites. However since the HA can degrade at temperatures higher than 80^{o}C, the incubation procedure was maintained at 65 ^{o}C.

It is difficult to determine the exact structure of the labelled complex with the use of a direct labelling method. However, knowing the functional groups that are present in the labelled molecule, a theoretical model can be proposed. It is widely known that the metal centre can be coordinated by the hydroxyl present on the carbohydrate skeleton and in some cases sugar derivatives like glucarate can be labelled with ^{99m}Tc and ^{188}Re with high stability [30,31]. This stability can be explained by the coordination of the metal core with both the hydroxyl and the carboxyl moieties present in the aldaric sugar derivatives. $ReO(O\text{-}COO)_2$ is the type of coordination proposed for the complex ^{188}Re(V)-hyaluronic acid. The structural characterization of the ^{188}Re-oligomers of D-glucuronic acid and of N-acetyl-D-glucosamine is currently underway to confirm this hypothesis.

Stability tests showed that ^{188}Re-HA was quite stable for one hour, afterwards the radiochemical purity slowly decreases. However biodistribution studies demonstrated that this time was enough to permit the ^{188}Re-HA reaching the target organs: liver uptake of the injected compound takes place very rapidly since activity is almost completely concentrated in liver after 4 hours. Weigel *et al.* [5] demonstrated that hyaluronic acid

binds to HARE receptors present in the liver and the interaction is followed by internalization and degradation of the polymer. It was assumed the ^{188}Re-HA complex undergoes the same metabolic pathway being internalized by the cell, but once there the hyaluronic backbone is degraded while rhenium-188 can not escape from the cell, thus increasing the activity in the liver. Since thyroid, kidneys and stomach radioactive residence times were lower than 15 min (2.2, 4.8, and 14.2 respectively) and after the first hours there was not more radioactivity concentration in these organs that indicate the formation of perrhenate (unique decomposition product). Therefore we presume that ^{188}Re-HA was very stable in-vivo although the in-vitro stability was not very high.

In conclusion, ^{188}Re-HA showed to be stable enough, and furthermore to possess adequate biodistribution and pharmacokinetics parameters, to be used in the treatment of primary and secondary liver tumors. Therefore it seems to be a promising candidate to take forward for preclinical trials. The results of its therapeutic efficacy on animals with induced liver cancer are reported in chapter 5.

REFERENCES

[1] Hascall, V. C.; Laurent, T. C. *Hyaluronan: structure and physical properties*. Copyright Glycoforum. **1998**

[2] Toole, B.P. *Nat. Rev.Cancer*, **2004**, 4, 528-539

[3] Marhaba, R.; Zoller, M. *J Mol Histol.* **2004**, 35, 211-231

[4] Makrydimas, G.; Zagorianakou, N.; Zagorianakou, P.; Agnantis, J. N. *In Vivo* **2003**, 17, 633-640

[5] Nedvetzki, S.; Gonen, E.; Assayag, N.; Reich, R. et al. *Proc Natl Acad Sci USA* **2004**, 101, 18081-18086

[6] Weigel, J.A.; Raymond, R.C.; McGary, C.; Singh, A.; Weigel, P.H. *J Biol Chem* **2003**, 278, 9808-12

[7] Knudson, W.; Chow, G.; Knudson, C. B. *Matrix Biol.* **2002**, 21, 15-23

[8] Greiner, J.; Ringhoffer, M.; Taniguchi, M. et al. *Exp Hematol* **2002**, 30,1029-1035

[9] Greiner, J.; Ringhoffer, M.; Taniguchi, M. et al. *Int J Cancer* **2003**, 106, 224-31

[10] Borland, G.; Ross, J.A.; Guy, K. *Immunology* **1998**, 93: 139–148

[11] Lesley J, English NM, Gal I, Mikecz K, Day AJ, Hyman R. *J Biol Chem* **2002**, 277, 26600–26608

[12] Lesley J, Hascall VC, Tammi M, Hyman R. *J Biol Chem* **2000**, 275, 26967–26975

[13] Nanashima, A.; Yamaguchi, H.; Tanaka, K.; Shibasaki, S. et al. *Surg Today* **2004**, 34, 913–919

[14] Stern, R.; Shuster, S.; Wiley, T.S.; Formby, B. *Exp Cell Res* **2001**, 266, 167–176

[15] Luo, Y.; Ziebell, M. R.; Preswitch, G. D.; *Biomacromolecules* **2000**, 1, 208-218

[16] Kozobolis, V.P.; Christodoulakis, E.V.; Tzanakis, T. et al. *J Glauc* **2002**, 11, 287–293

[17] Akima, K.; Ito, H.; Iwata, Y.; Matsuo, K. et al. *J Drug Target* **1996**, 4, 207–215

[18] Coradini, D.; Pellizzaro, C.; Abolafio, G.; Bosco, M. et al. *Invest New Drugs* **2004**, 22, 207–217

[19] Coradini, D.; Zorzet, S.; Rossin, R.; Scarlata, I. et al. *Clin Cancer Res* **2004**, 10, 4822–4830

[20] Liao, Y. H.; Jones, S. A.; Forbes, B.; Martin, G.P.; Brown, M. B. *Drug Deliv.* **2005**, 12 327-342

[21] Brown, M. B.; Jones, S. A. *J Eur Acad Dermatol Venereol.* **2005**, 19, 308-318

[22] Liu, N.F.; Lapcevich, R.K.; Underhill, C.B.; Han, Z.Q. et al. *Cancer Res* **2001,** 61, 1022–1028

[23] Speranza, A.; Pellizzaro, C.; Coradini, D. *Anti-Cancer Drugs* **2005**, 16, 373–379

[24] Luo, Y.; Prestwich, G.D. *Bioconjugate Chem* **1999**, 10, 755–763

[25] Luo, Y.; Prestwich, G.D. *Bioconjugate Chem* **2001**, 12, 1085–108

[26] Lambert, B.; Bacher, K.; De Keukeleire, K. et al *J Nucl Med* **2005**, 46, 1326-1332

[27] Paeng, J.C.; Jeong, J.M.; Yoon, C.J. et al. *J Nucl Med* **2003**, 44**,** 2033-2038

[28] Melendez-Alafort, L.; Riondato, M.; Nadali, A. et al. *J Label Comp Radiopharm* **2006**, 49, 939-50

5

^{188}Re-HA: THERAPEUTIC EVALUATION

5.1 INTRODUCTION

5.1.1 Current therapies for hepatocellular carcinoma

Hepatocellular carcinoma (HCC) is the most common type of primary liver cancer, and is one of the most prevalent causes of cancer-related deaths [1]. Even if the major risk factors for HCC development have been well defined, primary and secondary liver cancer is still characterized by an overall poor prognosis and patient survival has not been improved during the last three decades [2]. Tumour detection often takes place late, and since more than 80% of patients who present with HCC are suffering from underlying diseases, such as hepatitis B and C, and alcohol-induced cirrhosis, therapeutic possibilities are limited [3]. Surgery, by either hepatectomy or liver transplantation, is the only type of curative treatment but if considering the degree of liver dysfunction, the tumour load and often the late detection, the vast majority of patients are not eligible for surgery [4]. Therefore, only palliative nonsurgical treatment could be given using ablative therapies, which destroy tumour by the injection of chemical substances, radiation, or heating or cooling [5]. For multifocal HCC, transarterial chemo-embolisation is generally accepted, and survival advantages have been identified [6] in patients with well-compensated cirrhosis.

A number of new treatment options have thus been developed and clinically introduced. Radioembolization is one example, carried out by injection of radiolabelled lipiodol into the hepatic artery. In these locoregional treatments liver malignancies are passively targeted because, unlike the normal liver, the blood supply of intrahepatic tumours is

almost uniquely derived from the hepatic artery. The embolic agent lipiodol labelled with Iodine-131 have shown encouraging results in the treatment of HCC, improving the survival of HCC-bearing rats [7]. However, ^{131}I-lipiodol is expensive, has a high gamma energy, a short beta (i.e., cytotoxic) range, and requires hospitalisation for radioprotection purposes for several days after its administration in humans.

Recently Rhenium-188 (^{188}Re) has emerged as a versatile therapeutic radionuclide since it can be cheaply produced from a Tungsten-188 generator [8], and showed better physical and chemical properties such as: higher-energy beta-ray emission with a consequently greater cytotoxic range, that could improve response rate particularly in larger tumours, a 155-keV g ray suitable for gamma camera imaging, and a relatively short half-life (17 hours), minimizing radioprotection issues and thus not requiring hospitalization [9, 10].

Lipiodol has been labelled with ^{188}Re using 4-hexadecyl-1,2,9,9-tetramethyl-4,7diaza-1,10-decanethiol (HDD), ^{188}Re-(S2CPh)(S3CPh)(2) complex (SSS) and bis-(diethyldithiocarbamato)nitrido rhenium-188 (^{188}ReN-DEDC) to obtain ^{188}Re-HDD/lipiodol, ^{188}Re-SSS/lipiodol and ^{188}ReN-DEDC/lipiodol with a high radiochemical yield [11-13]. However experimental results after the ^{188}Re-SSS-lipiodol treatment in HCC-bearing rats did not show any therapeutic effect. In vitro stability studies in human plasma demonstrated that ^{188}ReN-DEDC/lipiodol release ~15% of the activity within three half-lives and biodistribution studies in Wistar rats showed just one-third of total activity in the liver 6 h after intraportal venous injection, declining to 2% retention at 72 h [13]. In addition some unexplained spleen and bone marrow uptake was observed 20 h post injection in patients that produce a grade 4 myelosuppression in one patient [14]. Only ^{188}Re-HDD/lipiodol after preliminary studies in humans confirmed a good tolerance and gave some promising results [15-17]. Even so it was found that it can produce lung toxicity as well as mild and transient side effects in about 50 % of patients treated [10]. These observations show the necessity to explore a different therapy for the hepatocellular carcinoma.

5.1.2 Aim of the project: therapeutic evaluation of ^{188}Re-HA on induced HCC

Some derivates of the tumour targeting molecule hyaluronic acid (HA) were recently labelled with technetium-99m using a direct method leading to a complex with high radiochemical purity [18, 19]. The biodistribution studies in healthy mice of these

radiolabelled complexes showed that 25 min after the intravenous administration, more than 80 % of the radiopharmaceutical was found in the liver and the spleen due to the size of the complex and the selective binding of the hyaluronic acid to CD44 and HARE receptors [19].

In the previous chapter, HA was directly labelled with ^{188}Re and the obtained complex once injected in vivo was stable enough to allow biodistribution studies in healthy mice. These experiments showed that liver uptake of the injected compound takes place very rapidly and is almost complete, and once there the activity remains in the liver. Since the best results in cancer treatment has actually been obtained by means of the combined-modality therapy using tumour targeting molecules radiolabelled with beta emitting radionuclides. Consequently, ^{188}Re-HA hepatic specific capture may turn in a promising opportunity to treat primary and secondary liver tumours. Our objective is to evaluate the therapeutic effect of ^{188}Re-HA complex in animal models with induced liver cancer, in order to establish if it can be used as a hepatocellular carcinoma therapeutic agent.

5.2 EXPERIMENTAL SECTION

5.2.1 Materials and analytical methods

All chemicals and solvents were reagent grade, used without further purification and purchased as described in the previous chapter. In addition diagnostic kits for hepatic enzymes AST and ALT were purchased from Sclavo Diagnostics (Siena, Italy).

5.2.2 Dosimetry estimation

Before starting with therapeutic experiments in mice with induced liver cancer, the maximum tolerated liver dose, dosimetry and toxicity of ^{188}Re-HA were estimated in healthy mice.

Initially biodistribution studies were carried out by injecting healthy female C57BL/6 black mice with the radiolabelled complex via the tail vein, as reported in the previous chapter. Animals were then sacrificed at 0.5, 4, 24 and 72 hours post injection, and selected tissues were excised and weighed, measuring each organ activity and expressing the resulting value as percentage of the injected activity per gram of tissue (% IA/g). Then for

each organ a time-activity curve was calculated, in order to determine the pharmacokinetic of the radiolabelled complex.

The current method of dosimetry is based on the medical internal radiation dose (MIRD) formalism [8, 20–22]. In brief, it considers a mean dose for a given target organ due to some source-target configuration.

Following the MIRD method [23], activity is the number of disintegrations per unit time, and when integrated over the time it gives the total number of decays or cumulated activity in the source organ ($\tilde{A}_h$). This parameter was calculated for organs of interest starting from the biokinetic data, integrating the area under the time-activity curves (reported in the previous chapter) and it was expressed per unit of initial activity (MBq h/MBq).

$$\tilde{A}_h = \int_{t=0}^{t=\infty} A_h \, dt$$

The source organ has to be defined to calculate the absorbed dose in the target organs. The beta dose to the target organ (r_k) from a source organ (r_h) considering the self–organ and the cross organ absorbed fractions can be obtained from the following equation

$$\tilde{D}\,(r_k \leftarrow r_h) = \tilde{A}_h \, S(r_k \leftarrow r_h)$$

Where $\tilde{D}\,(r_k \leftarrow r_h)$ is the mean absorbed dose to a target organ from a source organ and S is a dose Factor that can be calculated with the following equation.

$$S(r_k \leftarrow r_h) = \frac{K \sum_i \Delta_i \, \phi_i \, (r_k \leftarrow r_h)}{m_k}$$

Where

K = unit conversion constant

Δ_i = the equilibrium dose constant for radiation i, that in this case is the average energy of beta-particle emission (0.766 for ^{188}Re)

m_k = the mass of the target organ.

$\phi_i(r_k \leftarrow r_h)$ = is the absorbed fraction in the target organ r_k for radiation i emitted in the source organ r_h, that is the fraction of the energy of radiation i emitted in the source organ

that is absorbed in the target organ and depend on the properties of the i-type emission and the size, shape and separation of the source and target organs.

S values were calculated as reported by Miller *et al* [24], using the beta-absorbed fractions in mouse model calculated by two Monte Carlo radiation transport codes MCNP4C and PEREGRINE. Total mean absorbed dose $\tilde{D}(r_k)$ to target organ r_k was then calculated by addition of the absorbed dose contributions from all the source organs r_h.

$$\tilde{D}(r_k) = \sum_h [\tilde{A}_h \, S(r_k \leftarrow r_h)]$$

The unit of absorbed dose is the gray (Gy)=J/kg

5.2.3 Maximum tolerated liver dose in mice

The maximum-tolerated dose (MTD), it means the highest dose that a normal organ can withstand was calculated using seven groups of five healthy female C57BL/6 black mice, and correlated to the injected activity. The animals were injected in the tail vein with 200 µl of ^{188}Re-HA solution (0.3 mg HA/ml) with activities of 37, 18.5, 12.6, 9.2, 7.4, 4.7, or 2.3 MBq thus forming activity treated groups 1, 2, 3, 4, 5, 6, and 7 respectively. Then the mice from all the groups were set up in the initial toxic phase for 45 days, and survival and weight variations were monitored. Finally the absorbed dose (in Gy) for each organ was calculated using the average radiation absorbed dose value obtained from the dosimetry estimation.

5.2.4 Bone marrow toxicity

Bone marrow toxicity was evaluated using five groups, each one with five healthy female C57BL/6 black mice. The animals were injected with gamma-ray activities of 1.85, 3.7, 7.4, 11.1 and 18.5 MBq of radiolabelled complex in 200 µl solution (0.3 mg HA/ml) via the tail vein.

Before the treatment (basal level) and 1, 3, 7, 14 and 28 days after the administration of ^{188}Re-HA, blood samples from retroorbital sinus were collected in heparinized tubes. For each sample, White blood cells (WBC) were counted with an optical microscope after double lysis of red blood cells (RBC). The decrease of WBC was expressed as percentage with respect to the basal level, and was calculated as:

$$Decrease\,\% = -\frac{\left(WBC_i - WBC_{basal}\right)}{WBC_{basal}}\,x\,100$$

where:

WBC_i = aversge of WBC counting at the day *i* after treatment

WBC_{basal} = average of WBC counting before the treatment

5.2.5 Liver toxicity

Liver toxicity of ^{188}Re-HA was studied using the same blood samples collected for bone marrow toxicity. On heparinized plasma obtained from each blood sample, ALT and AST levels were measured by means of GPT (ALT) Uni-UV and GPT (AST) Uni-UV diagnostic kits. Results are expressed with the Enzymatic International Unit per litre (U/L), defined as enzyme activity that can provide the conversion of 1 μmole substrate in 1 minute.

5.2.6 Therapeutic efficacy evaluation

In order to evaluate the therapeutic effect of ^{188}Re-HA several experiments in C57BL/6 black mice were carried out, using the M5076 tumour cell line, a fibrosarcoma that rapidly metastatizes in the liver after intravenous inoculation. For each experiment one of the group of mice was not treated, and used as a positive control.

1. The first experiment was performed by inoculation of 20000 M5076 cells / mouse in 3 groups each one of six mice. After four days, two groups were treated with an i.v. injection of ^{188}Re-HA with γ-ray activities of 7.4 MBq and 12.6 MBq respectively. Animals were sacrificed 18 days after tumour induction.

2. In the second experiment 50000 M5076 cells / mouse were inoculated into 3 groups of six mice. After seven days, two groups were treated with 2.2 MBq and 4.4 MBq of ^{188}Re-HA respectively, and all animals were sacrificed 21 days after tumour induction.

3. For the third experiment, the number of inoculated cells was 10000 / mouse in 3 groups of six mice: 7 days later two of them received 1.1 MBq or 2.2 MBq of ^{188}Re-HA respectively. Animals were sacrificed 28 days after tumour induction.

4. The fourth experiment was carried out by inoculating 300 M5076 cells / mouse into 4 groups of mice. Two of them were treated 15 days later with 2.2 MBq and 3.7 MBq of ^{188}Re-HA respectively, one of them was treated twice with 2.2 MBq after 15 and 30 days from the inoculation. The aim of this experiment was to evaluate the impact of the therapy on the survival, and then animals were observed for 30 days from the first therapeutic treatment and then sacrificed. However animals presenting very strong diseases or deep suffering were sacrificed before the end of the experiment if necessary.

The presence of liver metastasis was studied histologically after animal sacrifice, comparing the eventual regression of the tumour with positive controls in all the cases. All the results were analyzed by the Mann-Whitney test.

5.3 RESULTS AND DISCUSSION

5.3.1 Dosimetry estimation

The mass of each organ was measured, and the total number of disintegrations or cumulated activity in the source organs (MBq h/MBq) per each MBq of the injected complex (Table 1) was determined using the area under the time-activity curves for each organ, obtained from the biodistribution data at 4 different times.

Source organs (r_h)	Mass (m) (Kg)	Accumulated activity ($\tilde{A}$) MBq.s/MBq
Thyroid	1.05E-04	129.60
Heart	1.15E-04	51.48
Lung	1.50E-04	91.44
Stomach	1.75E-04	856.80
Spleen	9.00E-05	2325.60
Kidney	2.63E-04	286.92
Liver	1.05E-03	67320.00
Intestine	1.21E-03	1234.80
Bone	1.10E-04	28.01

Table 1 Organs mass (m) and accumulated activity of the source organs (r_h) per each MBq of injected ^{188}Re-HA

The mean absorbed dose for each target organ from each source organ is reported in table 2, as well as the total mean radiation absorbed dose for each organ that was obtained by addition of all the source organs contributions.

Table 2 Radiation absorbed dose contributions of each source organ to each of the target organs (Gy/MBq) and the average absorbed dose of each organ obtained by addition of the contributions from all the source organs, per MBq of ^{188}Re-HA injected in healthy female C57BL/6 black mice (n=5)

Target organ (r_k)	**Source Organ (r_h)**									**Absorbed dose (Gy/MBq)**
	Thyroid	**Heart**	**Lung**	**Stomach**	**Spleen**	**Kidney**	**Liver**	**Intestine**	**Bone**	
Thyroid	3.81E-02	0.00E+00	0.00E+00	0.00E+00	0.00E+00	0.00E+00	0.00E+00	0.00E+00	0.00E+00	3.812E-02
Heart	0.00E+00	2.85E-02	9.71E-03	0.00E+00	0.00E+00	0.00E+00	4.71E-02	0.00E+00	0.00E+00	8.533E-02
Lung	0.00E+00	1.32E-02	2.61E-02	1.02E-01	0.00E+00	0.00E+00	4.09E-01	0.00E+00	0.00E+00	5.500E-01
Stomach	0.00E+00	0.00E+00	1.20E-03	3.93E-01	9.85E-01	6.42E-03	1.18E-01	8.30E-02	0.00E+00	1.586E+00
Spleen	0.00E+00	0.00E+00	0.00E+00	4.14E-02	1.20E+00	4.81E-03	0.00E+00	0.00E+00	0.00E+00	1.246E+00
Kidney	0.00E+00	0.00E+00	0.00E+00	3.12E-02	3.93E-01	6.94E-02	1.18E-01	1.88E-03	0.00E+00	6.130E-01
Liver	0.00E+00	2.63E-03	3.66E-03	6.24E-02	0.00E+00	1.28E-02	5.57E+00	1.63E-03	0.00E+00	5.654E+00
Intestine	0.00E+00	0.00E+00	0.00E+00	3.48E-02	0.00E+00	2.41E-02	4.56E-01	1.08E-01	0.00E+00	6.222E-01
Bone	0.00E+00	0.00E+00	0.00E+00	0.00E+00	0.00E+00	0.00E+00	0.00E+00	0.00E+00	9.58E-03	9.580E-03

5.3.2 Maximum Tolerated liver dose in mice

The absorbed dose (in Gy) per each organ of the seven groups of mice was calculated using the average radiation absorbed dose data obtained previously from the dosimetry estimation, and is here reported in table 3, related to the corresponding injected activity. As expected, liver is the organ that receives the highest absorbed dose, followed by stomach and spleen.

Organ	Injected Activity (MBq)						
	37.0	**18.7**	**12.6**	**9.2**	**7.4**	**4.7**	**2.3**
Thyroid	1.41	0.71	0.48	0.35	0.28	0.18	0.09
Heart	3.16	1.60	1.08	0.79	0.63	0.40	0.20
Lung	20.35	10.28	6.93	5.06	4.07	2.58	1.26
Stomach	58.70	29.67	19.99	14.60	11.74	7.46	3.65
Spleen	46.12	23.31	15.71	11.47	9.22	5.86	2.87
Kidney	22.68	11.46	7.72	5.64	4.54	2.88	1.41
Liver	209.21	105.74	71.25	52.02	41.84	26.58	13.01
Intestine	23.02	11.63	7.84	5.72	4.60	2.92	1.43
Bone	0.35	0.18	0.12	0.09	0.07	0.05	0.02

Table 3 Absorbed dose (in Gy) for each organ of the seven groups of healthy female mice (n=5) injected with ^{188}Re-HA

Animals from the first and second groups, which received 37 and 18.7 MBq of ^{188}Re-HA, died after 3 and 7 days of the injection respectively. Therefore the Liver-MTD in mice should be lower than 100 Gy. Animals from groups 3 to 7 survived the 45 days period proposed by the study, and were then sacrificed.

5.3.3 Bone marrow toxicity

Bone marrow is the most sensitive tissue to beta-irradiation damage, due to its high cellular proliferation level. This is the reason why conventional radiotherapy or beta-emitting radionuclides administration are often associated with decreased circulating WBC

levels, and can lead to neutropenia and leukaemia. Therefore, bone marrow toxicity was studied evaluating leucocytes levels in the blood stream.

The results are summarized in figure 1, and showed that WBC levels were markedly reduced in the first 3 days after treatment; however they tend toward basal levels in 15 to 30 days.

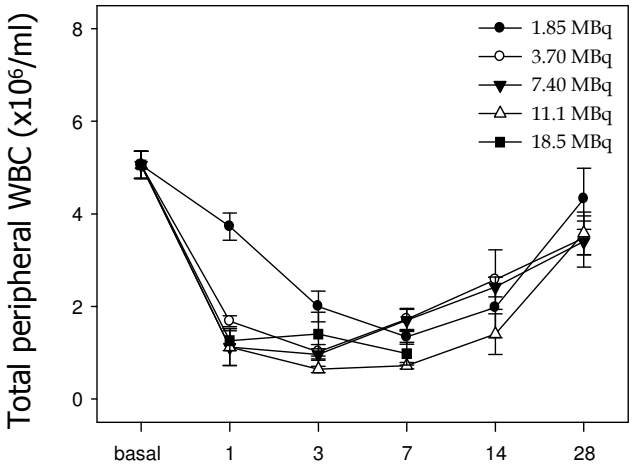

Fig. 1 WBC levels at different time points after treatment with ^{188}Re-HA

Only for the first group, the one that received the higher activity, there was no recovery since all animal died after 7 days.

5.3.4 Liver toxicity

Since ^{188}Re-HA accumulates primarily in the liver, hepatic toxicity was analyzed evaluating liver enzymes levels in the blood stream. Liver enzymes under normal circumstances reside within hepatic cells, but when liver is injured they are spilled into the blood. Concentration of liver enzymes in to the plasma samples (Figure 2) confirmed that a liver absorbed dose higher than 105 Gy, obtained after injection of 18.5 MBq of ^{188}Re-HA, produced a hepatic dysfunction that can cause death after 1 week.

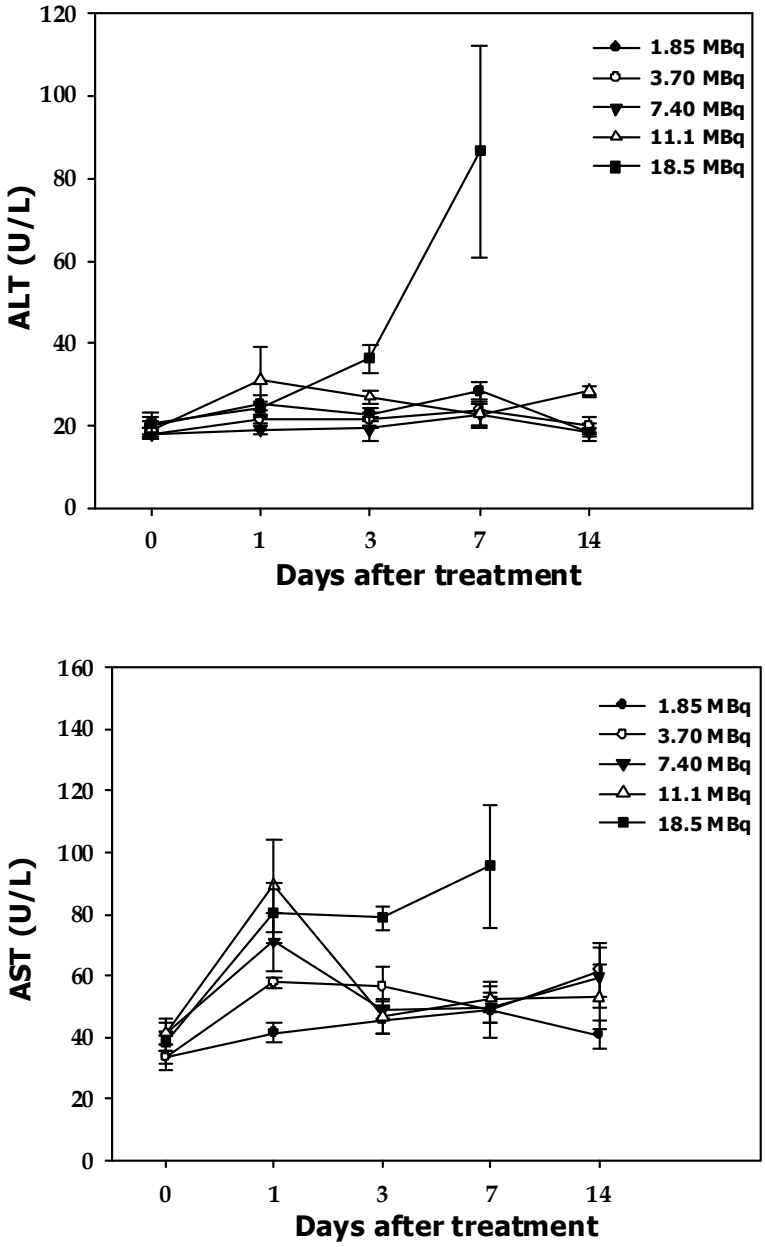

Fig. 2 ALT and AST levels at different time points after treatment with ^{188}Re-HA

The injection of 7.4 and 1.8 MBq of ^{188}Re-HA produces a liver dose of 41.84 and 10.18 Gy respectively that resulted in a mild or low liver toxicity as demonstrated by the levels of AST and ALT which increased immediately after the treatment but returned to normal values after 2 weeks, indicating non-hepatocyte injury. Consequently MTD in mice was estimated to be ~40 Gy.

5.3.5 Therapeutic effect

To evaluate the *in vivo* effect of ^{188}Re-HA toward liver metastatizing cancer, four experiment were carried out. Among them, the first 3 experiments concerned the study of tumour regression on M5076 induced metastasis, the fourth experiment evaluated the impact of the treatment on survival. For the first experiment, treated mice were sacrificed after 18 days from tumour induction, and excised organs were analysed. Results evidenced a high therapeutic effect on treated livers with respect to the positive controls (Figure 3).

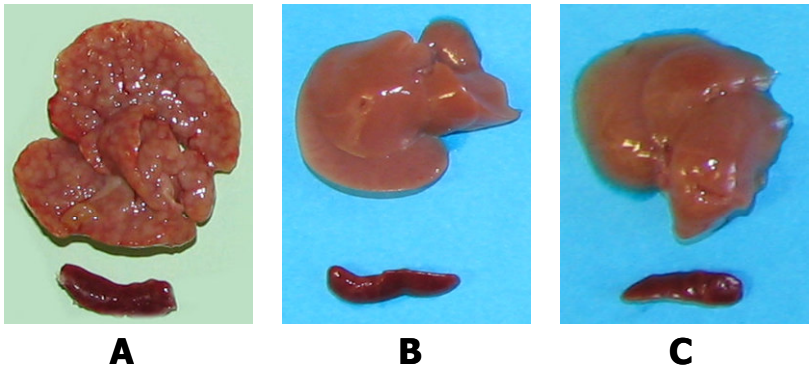

Fig. 3 Liver and spleen of mice inoculated with 20000 M5076 cells and treated 4 days later with B) 7.4 MBq and C) 12.6 MBq of ^{188}Re-HA. A) untreated

This effect is supported also by organ (liver and spleen) weights, which are very different between treated mice and untreated positive controls: untreated mice showed hefty organs, while treated animal organs where similar in size and weight to those of healthy mice (Figure 4).

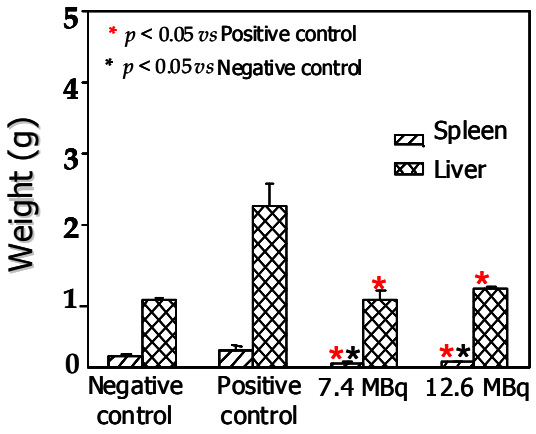

Fig. 4 Liver and spleen weight average of treated animals *vs* positive and negative controls

The encouraging result obtained from the first experiment prompted us to evaluate if mice with higher number of metastasis treated with lower activities would produce an alike therapeutic effect. Experiment 2 showed that despite the increased number of inoculated cells, the lower activities used and the longer time (21 days after) from the tumour induction to the treatment, the anti-neoplastic effect was comparable to the previous experiment. This result was evidenced by the almost total absence of metastasis in treated animals with respect to positive controls (Figure 5).

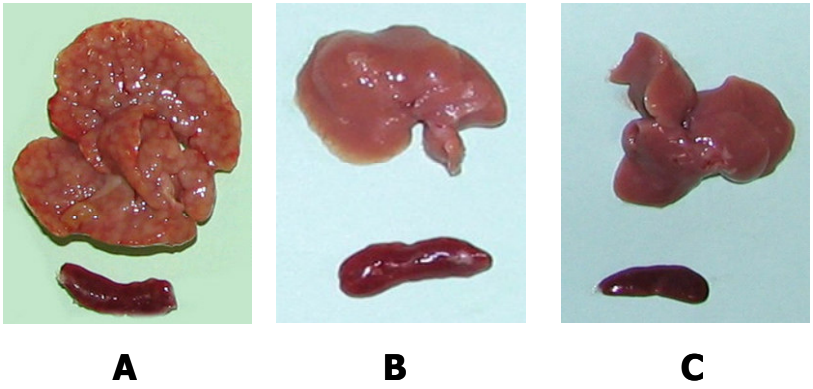

Fig. 5 Liver and spleen of mice inoculated with 50000 M5076 cells and treated 7 days later with B) 2.2 MBq and C) 4.4 MBq of ^{188}Re-HA. A) untreated

Even in this case, organs weight of animals with tumour treated are comparable to those of healthy mice (Figure 6).

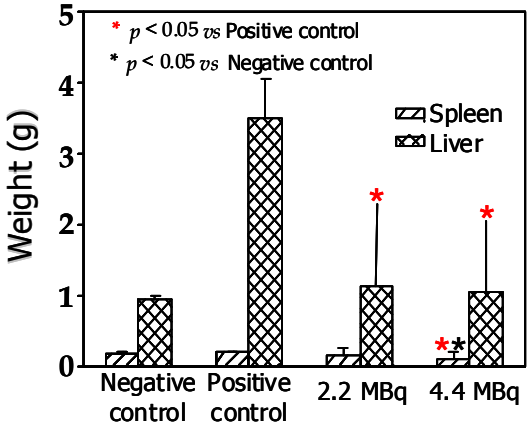

Fig. 6 Liver and spleen weight average of treated animals *vs* positive and negative controls

Since the second experiment gave good results even with reduced activity, we decided to study the effect of single or double treatments with lower activities. The analysis of untreated positive controls livers of the third experiment showed a great concentration of metastasis, that were significantly reduced in both size and number after treatment with 1.1 and 2.2 MBq of ^{188}Re-HA, and the histological studies of each group are reported in Fig. 7.

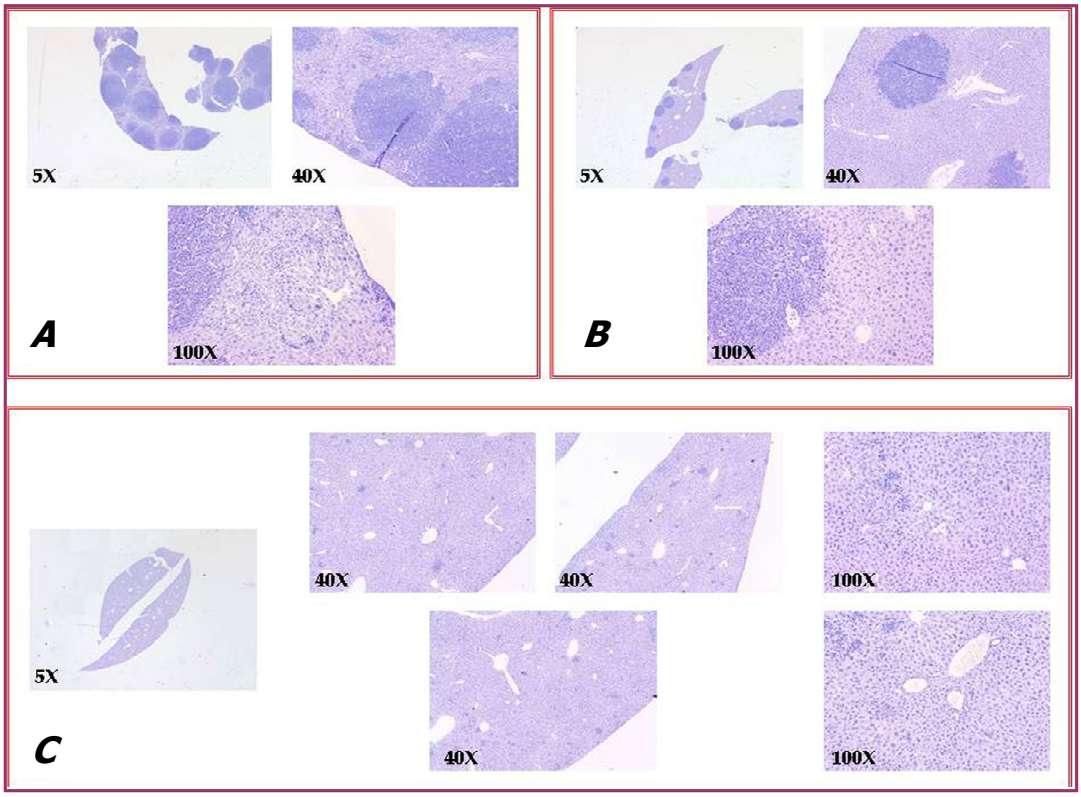

Fig. 7 Histological study on liver and spleen samples of mice: positive control (A), treated with 1.1 MBq (B) and with 2.2 mBq (C) of ^{188}Re-HA

Untreated animals showed an high number of metastasis that appear as blue zone in the histological section. The number of metastasis decreased after treatment with 1.1 MBq of ^{188}Re-HA (B), and metastasis almost disappeared after treatment with 2.2 MBq (C). Therefore, it was proved that even a low amount of activity in a single administration leads to a therapeutic effect. Since tumour diagnosis often occurs late in patients, the next step was to evaluate if similar treatments could improve the survival on mice with tumour sites when if they are treated with the radiolabelled complex after longer time from the tumour

induction. The results of all the fourth experiment pointed out that all the mice treated once or twice with ^{188}Re-HA showed a dramatic increase in survival, as reported in figure 8.

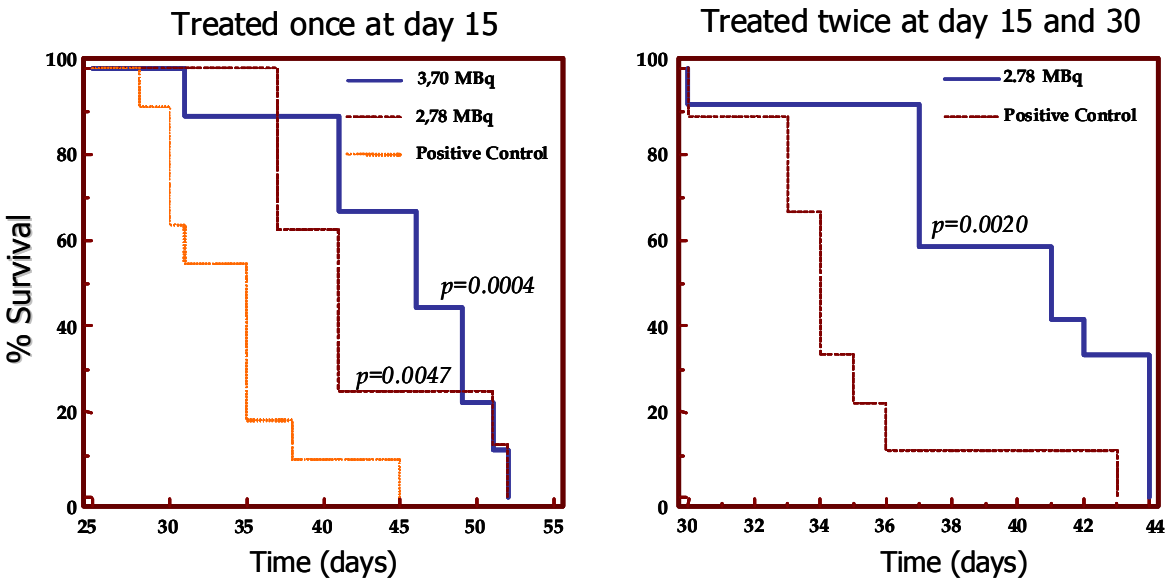

Fig. 8 Effect on survival of ^{188}Re-HAon C57BL/6 injected with 300 M5076 cells / mouse

However, in order to determine the most efficient therapeutic activity and the role of multiple treatments on tumour regression, several experiments have to be done.

5.4 CONCLUSIONS

Actually, the best results in cancer treatment are obtained using the combined-modality therapy employing a beta emitting radionuclide [25, 26]. The rationale of this strategy is due to the capacity of beta-irradiation to produce not only cellular death by DNA damage as in the case of the gamma- or X-ray irradiation, but also inhibiting (*in vitro*) cancer cell growth by activation of apoptosis pathways in single cells at several levels [27, 28]. Therefore, tumour responses applying the combined therapy are higher than the responses with the chemotherapy or radiotherapy using an external gamma-ray source. Our objective when labelling HA with ^{188}Re, is to join the HA effect as tumour targeting molecule, to the

DNA damage as result of ^{188}Re direct irradiation, and also the cytotoxicity caused by the activation of apoptosis pathways to obtain a more effective anticancer drug.

The dosimetry data showed that stomach absorbed dose in mice was very high despite the low uptake and short residence time of ^{188}Re-HA in this organ, due to the small size of the mice the nearby target organs (liver and spleen) provide a high contribution of absorbed dose as shown in table 3. However entering the experimental value of accumulated activity in each organ and using "S"-human values of the adult male phantom it was possible to obtain the absorbed dose estimated for human in Gy/GBq [29]. The results showed that the absorbed dose in stomach in the human model was reduced to the 13% of the dose in mouse model due to the Re-188 β-ray (with a maximum tissue penetration of 11 mm) will be almost completely absorbed within the liver and spleen increasing just it's self irradiation, as result of the larger organs size and greater distance between organs in human model.

Concentration of liver enzymes in to the plasma samples confirmed that dosimetry data were calculated in the correct way since we found that the MTD in mice was ~40 Gy, and this value correlated to the human liver MTD reported (from 20 to 45 Gy) [30].

Using the respective absorbed doses in organ per unit, it was calculated that administering an activity of 7 GBq in human the mean absorbed dose to the liver (including tumour), spleen, thyroid, stomach, lung and bone marrow would be ~31, 11, 5, 1.5, 0.12 0.02 Gy respectively. These data show that this activity is able to produce therapeutic effect in liver but at the same time is safe to the other organs since all of them received a dose much lower than the maximum tolerated absorbed doses.

Moreover, ^{188}Re-HA was obtained with a labelling yield higher than 90 % and, once purified, injected with radiochemical purity ~100% much better in comparison with the labelling yield of ^{188}Re-HDD/lipiodol [15, 16, 31] that approximately reaches 70 %, and which synthesis using activities higher than 7.0 GBq routinely was not feasible.

The biodistribution studies of ^{188}Re-HDD/lipiodol reported by Lamber *et al* [15], showed that 42% of the injected activity was eliminated by the renal clearance within 46 h, indicating that the complex was degraded resulting in perrhenate or other hydrophilic products. In order to reduce the uptake of free perrhenate in thyroid or stomach, patients received 1 gr of sodium perclorate [32]. Additionally, it was found lung uptake justified by the nature of the ^{188}Re-HDD/lipiodol and/or arteriovenous shunting. In contrast,

biodistribution studies, reported in the previous chapter showed that < 80 % of ^{188}Re-HA remained in the liver and less that 5 % was eliminate by renal clearance in 24 h and ^{188}Re-HA can be administered by a simple intravenous injection, quite the opposite for ^{188}Re-HDD/lipiodol where well-trained personal is needed since it has to be administrated through the hepatic artery under fluoroscopic control in order to increase the uptake on the cancer cells. Moreover, due to the high liver residence time of ^{188}Re-HA without lung uptake is possible to administer the same absorbed dose to the liver with half of the activity of ^{188}Re-HDD/lipiodol maintaining all other organs under the maximum tolerated absorbed doses, as confirmed by dosimetry data.

^{188}Re-HA therapeutic effect on animal models with induced liver cancer prove to be able of reduce metastasis size and increase survival in mice. However further investigations have to be carried out to determine the optimal activity and the best administrations way (single or multiple) for HCC treatment.

In conclusion ^{188}Re-HA has many advantages over Re-188-HDD/lipiodol for hepatocellular carcinoma therapy and following adequate preclinical studies showed to be a good candidate to take forward for clinical trials.

REFERENCES

[1] Raoul, J.L. Natural history of hepatocellular carcinoma and current treatment option. *Semin. Nucl. Med.* **2008**, 38, S13-S8

[2] Llovet, J.M. Updated treatment approach to hepatocellular carcinoma. *J. Gastroenterol.* **2005**, 40, 225-35

[3] Borgia, B. and Neri, D. Therapeutic approaches to hepatocellular carcinoma. *Drug Future* **2008**, 33, 75-83

[4] Blum HE. Treatment of hepatocellular carcinoma. *Best Pract. Res. Clin. Gastroenterol.* **2005**, 19, 129-45

[5] Gish, R.G. and Baron, A. Hepatocellular carcinoma (HCC): Current and evolving therapies. *IDrugs* **2008**, 11, 198-203

[6] Llovet, J.M.; Bruix, J. *Hepatology* **2003**, 37, 429–42

[7] Garin, E.; Rakotonirina, H.; Lejeune, F. ; Denizot, B. et al. *Nucl. Med. Commun* **2006,** 27, 363-9

[8] Knapp, F.F. *Cancer Biother Radiopharm* **1998,** 13, 337–49

[9] Jeong, J.M. and Knapp, F.F.R. *Semin. Nucl. Med.* **2008**, 38, S19-S29

[10] Lambert, B. and de Klerk, J.M.H. *Nucl. Med. Commun.* **2006**, 27, 223-9

[11] De Ruyck, K.; Lambert, B.; Bacher, K. et al. *J. Nucl. Med*. **2004,** 45, 612-8

[12] Garin, E.; Denizot, B.; Noiret, N. et al. *Nucl. Med. Commun.* **2004**, 25, 1007-13

[13] Boschi, A.; Uccelli, L.; Duatti, L. et al. *Nucl. Med. Commun.* **2004**, 25, 691-9

[14] Duatti, A.; Uccelli, L.; Pasquali, M. et al. *Eur J Nucl Med Mol Imaging* **2006**, 33, S105-S

[15] Bernal, P.; Raoul, J.L.; Stare, J. et al. *Semin. Nucl. Med.* **2008**, 38, S40-S5

[16] Bernal, P.; Raoul, J.L.; Vidmar, G. et al. *Int. J. Radiat. Oncol. Biol. Phys.* **2007**, 69, 1448-55

[17] Lambert, B.; Bacher, K.; Defreyne, L. et al. *Eur. J. Nucl. Med. Mol. Imaging* **2006**, 33, 344-52

[18] Coradini, D.; Zorzet, S.; Rossin, R. et al. **2004**, 10, 4822-30

[19] Melendez-Alafort, L.; Riondato, M.; Nadali, A. et al. *J. Label. Comp. & Radiopharm.* **2006**, 49, 939-50

[20] Raoul, J.L.; Guyader, D.; Bretagne, J.F. et al. *Hepatology* **1997**, 26, 1156–61

[21] Leung, W.T.; Lau, W.Y.; Ho, S. et al. *J Nucl Med* **1994,** 35, 1313–8

[22] Risse, J.H.; Grünwald, F.; Kersjes, W. et al. *Cancer Biother Radiopharm* **2000**, 15, 65–70

[23] Stabin, M. *Physics in Medicine and Biology* **2006**, 51, R187-R202

[24] Miller, W.H.; Hartmann-Siantar, C.; Fisher, D. et al. *Canc Biother Radiopharm* **2005**, 20, 436-49

[25] Ferro-Flores, G.; Torres-Garcia, E.; Garcia-Pedroza, L. et al. *Nucl. Med. Commun.* **2005**, 26, 793-9

[26] Kaminski, M.S.; Tuck, M.; Estes, J. et al. *New England Journal of Medicine* **2005**, 352, 441-9

[27] Antoccia, A.; Banzato, A.; Bello, M. et al. *Nucl. Instrum. Methods Phys. Res. Sect. A-Accel. Spectrom. Dect. Equip.* **2007**, 571, 471-4.

[28] Friesen, C.; Lubatschofski, A.; Kotzerke, J. et al. *Eur. J. Nucl. Med. Mol. Imaging* **2003,** 30, 1251-6

[29] Stabin, M.G.; Sparks, R.B. and Crowe, E. *J. Nucl. Med.* **2005**, 46, 1023-7

[30] Kassis, A.I. and Adelstein, J. Considerations in the selection of radionuclides for cancer therapy. In: Welch MJ, Redvanly CS, eds. Handbook of Radiopharmaceuticals, Radiochemistry and Applications. London: Wiley & Sons; **2003**, p. 767-793

[31] Bernal, P.; Raoul, J.; Vidmar, G. et al. *Eur. J. Nucl. Med. Mol. Imaging* **2006**, 33, S215-S

[32] Sundram, F.; Chau, T.C.M.; Onkhuudai, P. et al. *Eur. J. Nucl. Med. Mol. Imaging* **2004**, 31, 250-7

6

LOW AND HIGH MW HAs : LABELLING WITH ^{188}Re

6.1 INTRODUCTION: AIM OF THE PROJECT

Recently low molecular weight anticancer drugs as Mitomycin C, Epirubicin and Butyric acid have been linked to polymers such as hyaluronic acid (HA), which provide advantages in drug solubility, stabilization, localization and controlled release and at the same time markedly enhanced the selectivity for cancerous cells and suppress their undesirable cytotoxic side-effects.

The knowledge that polymers with different MW often present diverse biodistribution pathways and the encouraging results obtained with hyaluronic acid labelled with ^{188}Re in the treatment of induced liver cancer in mice (reported in chapter 5) prompted us to investigate if other HAs with different molecular weights could be suitable for the production of therapeutic radiopharmaceuticals. Since the linear PEG (70 kDa), was eliminated for renal clearance due to the glomerular filtration, it was supposed that PEGs with lower size (5 or 10 kDa) will be excreted via the urinary pathway too. Therefore, the aim of this work was to study the biodistribution of low molecular weight HAs, in order to establish if they could be used on bladder cancer treatment after conjugation with some antitumoural agents.

Contemporarily, high molecular weights HAs were studied to determine if they can provide advantages in drug pharmacokinetics with respect to the polymer (70 kDa) used in the previous chapter.

To reach our objective, HAs with high (200, 500 kDa) and low (5, 10 kDa) MW were directly labelled with ^{188}Re, then stability studies were performed on all the resulting products, followed by the biodistribution studies of ^{188}Re-HA complexes on healthy mice.

6.2 EXPERIMENTAL SECTION

6.2.1 Materials and analytical methods

All chemicals and solvents were reagent grade, used without further purification and purchased as described in chapter 5. Liophilized low molecular weight (LMW, 5 and 10 kDa) and high molecular weight (HMW, 200 and 500 kDa) hyaluronic acids were obtained from Fidia Farmaceutici (Abano Terme, Italy). $^{188}ReO_4^-$ was eluted from a commercial $^{188}W/^{188}Re$ generator (Polatom, Poland). Sephadex G-25 column Hi-Trap desalting, with a void volume of 1.5 ml, obtained from Supelco, Sigma-Aldrich (Milan, Italy) was used to purify by size-exclusion chromatography ^{188}Re-HA complex. Labelling efficiency and radiochemical purity were analyzed using size exclusion HPLC chromatography and instant thin-layer chromatography as described in chapter 5. Biodistribution studies were performed on 5 weeks old healthy female Balb/c mice (20-25 grams), purchased from the pound of the Department of Oncology (University of Padua, Italy).

6.2.2 Direct labelling of Hyaluronic Acid with ^{188}Re

In order to optimize the labelling protocol for each HA derivative, labelling reactions were performed changing : the amount of stannous chloride (0.55, 1.1, 1.65 mg), the temperature (25, 50, 65 and 80 ^oC), the incubation time (30, 60, 90, 120 and 150 min) and the final volume of the labelling reaction (160, 240 and 290 µl). Only one parameter was altered at a time. Each labelling reaction was carried out with degassed solvents and freshly prepared reducing agent solutions. Reactions were monitored by size-exclusion HPLC, where the free perrhenate has a R_t = 8.1 min. while labelled complexes give a broad peak with R_t = 4.2 min. The best protocols for each HA derivative are reported below:

5 kDa HA: 100 µl perrhenate (15 MBq) eluted from the generator and 60 µl of 0.1 M $SnCl_2$ solution (in 0.1 M HCl) were added to a vial containing 1 mg HA. The reaction mixture was gently stirred and left at room temperature for 60 minutes.

10 kDa HA: 1 mg of polymer was solubilised in 100 µl saline solution (0.9 %) containing $^{188}ReO_4^-$ (15 MBq) and then added of 60 µl of 0.1 M $SnCl_2$ solution. The reaction mixture was then gently mixed and incubated at 50°C for 90 minutes.

200 kDa HA: 150 µl perrhenate (20 MBq) eluted from the generator and 90 µl of 0.1 M $SnCl_2$ solution were added to a vial containing 1 mg HA, and the reaction mixture was incubated at 50°C for 120 minutes.

500 kDa HA:, 200 µl of $^{188}ReO_4^-$ (20 MBq) eluted from the generator and 90 µl of 0.1 M $SnCl_2$ solution were added to 1 mg liophilized polymer. Then the reaction solution was heated at 65°C for 150 minutes.

6.2.3 Purification of ^{188}Re-HA

When radiolabelling yields were lower than 90%, ^{188}Re-HA complex was purified by size-exclusion chromatography before starting the stability tests, using a Hi-Trap desalting column with a 1000-5000 Da cut-off and collecting samples of 0,5 ml fractions. ^{188}Re-HA was quickly eluted with saline solution, while the Sephadex G25 resin retained ^{188}Re-perrhenate and other low-molecular weight species.

6.2.4 Dilution stability

In order to determine the stability of ^{188}Re-HA toward aqueous dilution, 50 µL of purified complexes were diluted to a 1:10, 1:50, and 1:100 ratio with both saline solution (0.9 % NaCl) and phosphate buffer 0.1M. The solutions were incubated at room temperature at pH 7, collecting samples between 30 min and 6 h of incubation and analyzing them by size-exclusion HPLC and ITLC.

6.2.5 Cysteine challenge

Challenging assays were carried out adding 50 µL of a freshly purified ^{188}Re-HA solution to 50 µL of freshly prepared cysteine solutions in PBS buffer (pH = 7.4) with different concentration, in order to achieve a molar ratio of cysteine to radiolabelled complex between 5:1 and 500:1. All the reaction mixtures were then incubated at 37°C and radiochemical purity analyzed 1 h later by size-exclusion HPLC.

6.2.6 Biodistribution studies of ^{188}Re-HA complexes

The biodistribution studies of ^{188}Re-HA were determined by injecting healthy female Balb/c mice with 100 µL (3 MBq) of the purified complex via the tail vein. The animals were then sacrificed by cervical dislocation 2 hours post injection, and selected tissues (thyroid, blood, heart, lung, stomach, liver, spleen, kidney, intestine, muscle and bone) were excised and weighed. Each organ activity was then measured in a well-shaped scintillation detector and the radioactivity of the tissue samples was expressed as percentage of the injected activity per organ of tissue (% IA/organ).

6.3 RESULTS AND DISCUSSION

6.3.1 Direct labelling of Hyaluronic Acid with ^{188}Re

In chapter 4 was evidenced that addition of the exchange ligand sodium gluconate, decreases the radiochemical purity of the obtained complex, therefore labelling reactions were performed in absence of this agent. Each derivative labelling reaction was monitored by size-exclusion HPLC, and radiolabelling yields was expressed as percentage of activity bound to the polymer respect to the injected one.

The final volume of the labelling reaction was an important parameter, since the high molecular weight polymers gives solutions with high viscosity. Greater volumes make the solution becoming more fluid, thus allowing a higher possibility of interaction between the metal present in the reaction mixture and the polymer coordination sites. Therefore, in order to achieve good labelling yields, reaction mixtures had to be as fluid as possible and HMW hyaluronic acids required higher reaction solution volumes. Consequently, to reach the same viscosity level in all reactions, HA 500 kDa was labelled using a final volume of 290 µl, HA 200 kDa with 240 µl while for LMW HAs volumes of 160 µl were enough.

Other factors were examined to obtain the optimised labelling protocol for each derivative, and are here summarized.

For the first polymer, 5kDa HA, the radiolabelling reaction leads to the formation of the complex quickly and easily at 25°C. The temperature had great influence on the radiolabelling reaction, since it was found that increasing temperature the radiolabelled complex was broken up producing free perrhenate. This fact can be explained if

considering that increasing temperature leads to an increase of the oxidative processes, whose result is the re-oxidation of the rhenium^{V}-oxo core to the higher oxidation state $Re^{VII}O_4^-$ that is more stable. The amount of reducing agent was also critical, because higher quantities of stannous chloride led to the formation and precipitation of Re-colloids. It is well known in fact that Sn(II) can lead to significant problems, such as the formation of the insoluble colloids $Re^{IV}O_2$ and $Sn^{IV}O_2$. . Analogous considerations can be done for the 10 kDa HA derivative, even if in this case the labelling yields reached a maximum when the reaction was incubated at 50°C. Higher incubation temperatures led to decomposition of the radiolabelled complex, as already observed for the first compound.

For the third product, 200 kDa HA, a higher amount of stannous chloride and higher incubation temperature with respect to the previous derivatives were required. Moreover, the reaction reached its maximum radiolabelling yields (49%) after 2 hours incubations (Figure 1), then the complex undergoes decomposition giving as product free perrhenate.

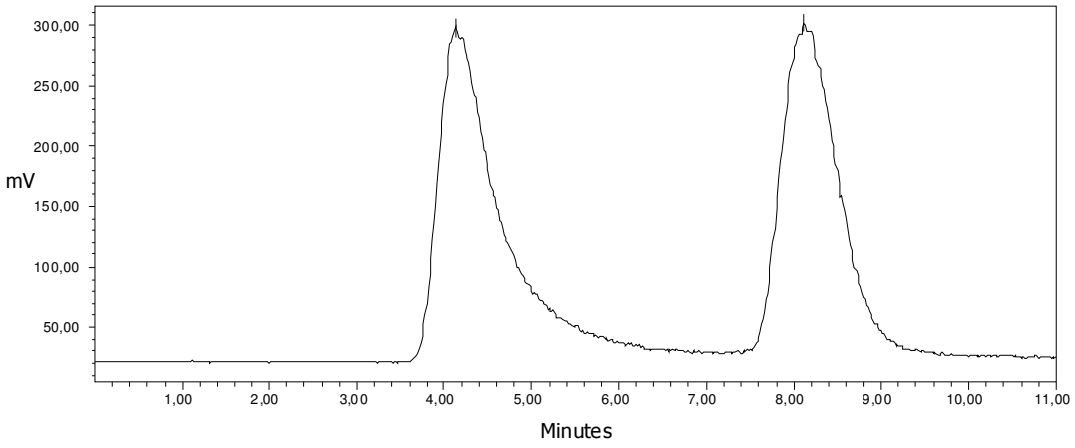

Fig. 1 HPLC γ-trace of the ^{188}Re-HA 200 kDa reaction mixture

The last compound, HA 500 kDa, reacted in the same conditions of the 200 kDa, except for the incubation time that was prolonged to 150 min.

The radiolabelling yields for the four derivatives are summarized in Table 1.

Hyaluronic acid	Radiolabeling yields
5 kDa	98 %
10 kDa	77 %
200 kDa	49 %
500 kDa	86 %

Table 1 ^{188}Re-labeling yields of HAs with different MW

Radiolabelling yields decreased with the increasing of the polymer molecular weights, and this is probably related to the tri-dimensional conformation assumed in solution by HA, resulting in a lower accessibility of the coordination sites present in its backbone. However, HA 500 kDa reached satisfying labelling yields. An explanation of this behaviour is possible if assuming that, despite the 3D conformation of the polymer in solution, the larger size of this hyaluronic acid provides enough coordination sites for the metal core on its surface.

6.3.2 Purification of ^{188}Re-HA

The Stability studies were carried out for the first complex, ^{188}Re-HA 5 kDa, without any further purification, since the labelling reaction gives a product quite pure (98 %). In order to evaluate the stability and to perform the biological studies of the other three complexes, the radiolabelled products were purified using a Hi-Trap desalting column. ^{188}Re-HA was rapidly eluted with saline solution from the column in the first 2 ml fraction. The ^{188}Re-perrhenate was eluted with the 4 to 8 ml fractions, while the Sephadex G25 resin retained the reduced hydrolysed-^{188}Re. The purification was then confirmed by size exclusion HPLC where the elution profile shows a unique peak corresponding to ^{188}Re-HA. Figure 2 reports as example the radiochromatogram of ^{188}Re-HA 200 kDa after purification.

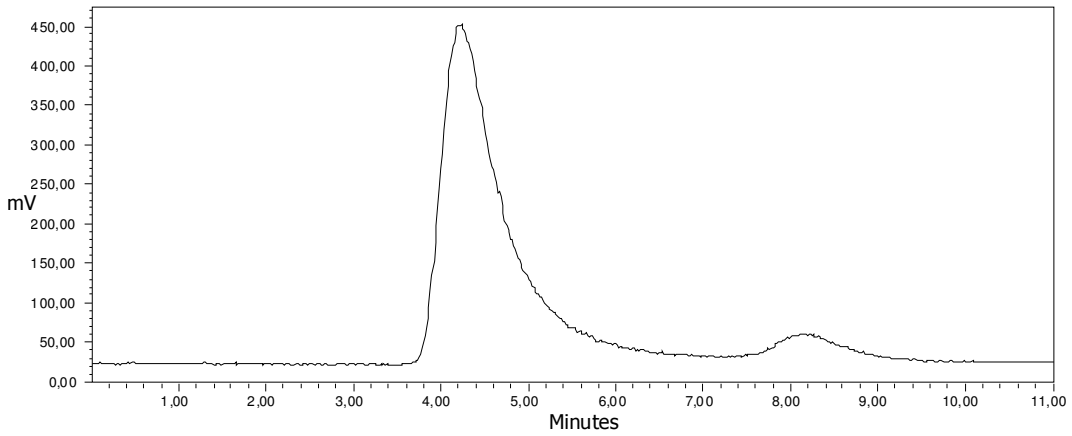

Fig. 2 HPLC γ-trace of the ^{188}Re-HA 200 kDa purified complex

6.3.4 Dilution stability

To determine the stability of ^{188}Re-HA complexes toward aqueous dilution, a solution of the purified complex was diluted in saline solution and 0.1 M phosphate buffer. Size exclusion chromatography showed that the smaller complex was completely unstable, since the radiochemical purity was lower than 45% once diluted to a ratio 1:10 and incubation for 1 h at room temperature. The unique decomposition product was represented by rhenium that re-oxidized to perrhenate. Therefore, any further study on this derivative was precluded.

The second complex, ^{188}Re-HA 10 kDa, showed higher stability toward dilution with respect to the first one. Unfortunately, even in this case radiochemical purity decreased to 52% once diluted to a ratio 1:50 with both saline solution and PBS, and incubation for 1 h at room temperature, thus precluding further investigations. On the other hand, the larger two complexes showed a good stability once diluted to 1:50 in PBS, as summarized in Figure 3.

This behaviour can be explained if considering that the polymer can fold on itself, thus protecting the metal core bound to its coordination site. Therefore larger polymer seem to stabilize the metal centre better than the small polymer do, as a result of the higher probability of folding on themselves.

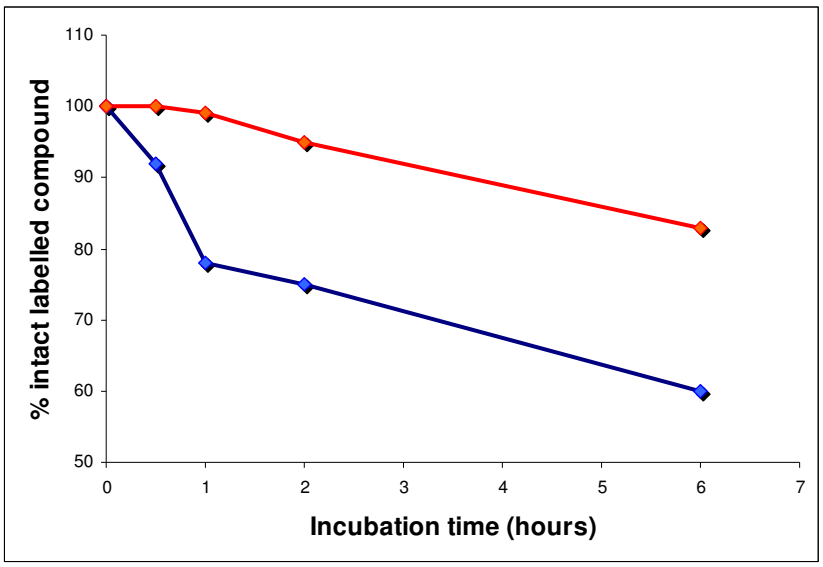

Fig. 3 Stability toward 1:50 dilution in PBS of ^{188}Re-HA 200kDa (blue) and 500 kDa (orange)

In all cases, the only degradation product found was $^{188}ReO_4^-$ due to the rhenium^V-oxo that when it is not stabilized by an appropriate coordination set, tends to re-oxidize to perrhenate.

6.3.5 Cysteine challenge

Challenging conditions were harsh and expected to well simulate an in vivo donor atom competition and redox reactions. The results evidenced that ^{188}Re-HA complexes were quite stable in presence of cysteine since even after 1 h incubation with the highest challenging agent concentration, both ITLC and HPLC showed less than 10 and 5 % of radioactivity dissociated from the 200kDa and 500 kDa complex respectively. Therefore, cysteine challenge proved the high stability of these ^{188}Re labelled HAs, since it did not lead to significant ligand exchange and/or decomposition.

6.3.6 Biodistribution studies of ^{188}Re-HA complexes

Biodistribution studies were done in healthy female Balb/C mice to investigate the *in vivo* behaviour of high molecular weights ^{188}Re-HA complexes and compared it with the 70 kDa radiolabelled compound used for therapeutic experiment in chapter 5, in order to establish if larger polymers can exhibit advantageous properties.

Each experiment was carried out on 4 animals, which were sacrificed 2 hours post injection. The radioactivity present in each tissue samples was expressed as percentage of the injected activity per organ, and is here reported in figure 4 and 5.

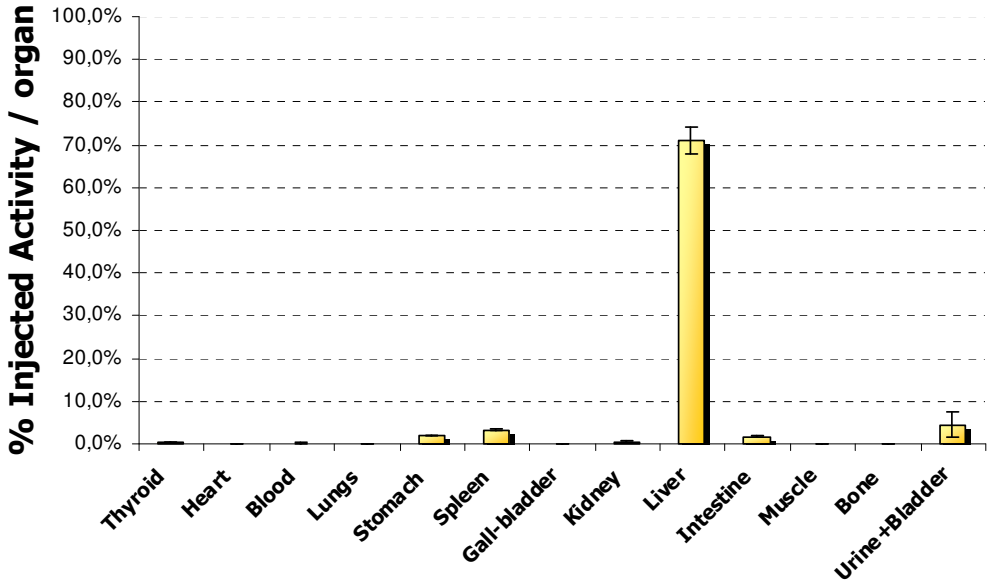

Fig. 4 Biodistribution of ^{188}Re-HA 200 kDa 2h post injection (n=4)

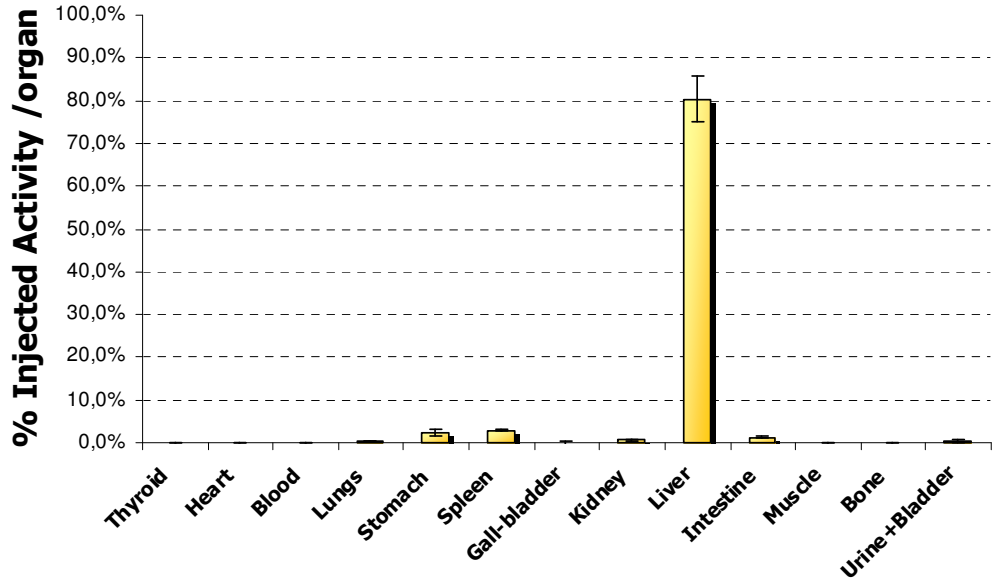

Fig. 5 Biodistribution of ^{188}Re-HA 500 kDa 2h post injection (n=4)

Collected *ex-vivo* data showed that for both polymers the activity is concentrated in liver 2 hours after the administration of the radiolabelled complex. It was found that liver uptake increases with the increasing of radiolabelled complex size. The correlation to liver concentration data obtained with the 70 kDa HA reported in chapter 5 (40% and 50% ID/organ after 30 min and 4h of administration respectively), confirms that these HAs complexes undergo a higher hepatic concentration. Moreover, an irrelevant amount of activity was found in thyroid, stomach, kidneys and intestine, where perrhenate the unique decomposition products is concentrated, thus confirming the *in vivo* stability of both complexes.

6.4 CONCLUSIONS

An easy method to radiolabel HAs with different MW using Re-188 was found. The reaction temperature seems to have the most significant effect on the radiolabelling yields of all the products. It was found that compounds with high molecular weights needed higher reaction temperatures to reach satisfying labelling yields. This fact is related to the viscosity of HA solutions at room temperature. An increase in the temperature makes the solution becoming more fluid, enhancing the possibility of interaction between the metal and the polymer coordination sites.

Stability tests showed a great difference in the results obtained. ^{188}Re-HA complexes with high molecular weights were stable for one hour, afterwards the radiochemical purity slowly decreases. In contrast the low molecular weight complexes undergo a rapid decomposition when diluted both with PBS and saline. This instability can be related to the number of coordination sites for the metal present on the HA backbone (hydroxyl and carboxyl moieties of the aldaric sugar derivatives), which is widely lower for small polymers with respect to the larger ones. Moreover, a larger polymer can fold thus protecting the metal core bound on itself.

Biodistribution studies demonstrated that, as expected, both HMW ^{188}Re-HAs reach the target organ showing to be almost completely concentrated in liver 2 hours after injection. As previously reported, this behaviour can be related to the fact that hyaluronic acid binds to HARE receptors present in the liver and the interaction is followed by internalization

and degradation of the polymer [1]. It was assumed the ^{188}Re-HA complex undergoes the same metabolic pathway being internalized by the cell, but once there the hyaluronic backbone is degraded while rhenium-188 can not escape from the cell. Moreover, there was very little radioactivity concentration in thyroid, kidneys and stomach that indicates the formation of perrhenate (the only decomposition product).

In particular biodistribution studies evidenced that the larger polymer leads to higher liver capture (80% and 71% of injected activity for 200 and 500 kDa respectively) when compared to the ^{188}Re-HA 70kDa studied in chapter 4 (59.7% 2h post injection). This specific uptake can lead to higher target to background ratios, thus reducing irradiation related toxicity to other organs.

In conclusion, HMW HAs labelled with ^{188}Re showed to be as stable as ^{188}Re-HA (70kDa) with a higher liver uptake 2 h after injection, however further investigations have to be carried out to determine if their pharmacokinetics and *in vivo* behaviour offers any advantages with respect to the ^{188}Re-HA (70kDa).

REFERENCES

[1] Nedvetzki, S.; Gonen, E.; Assayag, N.; Reich, R. et al. *Proc Natl Acad Sci USA* **2004**, 101, 18081-18086

7

GENERAL CONCLUSIONS

Lately, research in nuclear medicine focused on the production of less expensive tracer and therapeutic agents. In this contest, the use of technetium-99m and rhenium-188 can be of great importance. ^{99m}Tc and ^{188}Re are in fact readily available at lower cost than other radioisotopes, such as iodine-123. Moreover, routine clinical trials can take advantage of the easy supplying of ^{99}Mo/^{99m}Tc and ^{188}W/^{188}Re generators in nuclear medicine departments.

The goal of this doctoral work was to label biologically active molecules with ^{99m}Tc and ^{188}Re in order to obtain target specific radiopharmaceuticals suitable for the diagnosis or treatment of tumours.

In the first part of the present work (chapter 2 and 3), new somatostatin dicarba-analogues (CIN and CIF) were labelled with ^{99m}Tc in high yields, using two different indirect labelling approaches. For the first derivative, modified with PN2S chelating agent, the formation of the complex with a ^{99m}technetium^{V}-oxo core was achieved with good radiolabelling yields. However, the complex needed further purification in order to achieve a higher radiochemical purity. Unfortunately, stability tests showed a considerable decomposition of the ^{99m}Tc-oxo complex and a great interaction with challenging agents such as cysteine, thus precluding any further biological study.

The second derivative, modified with the same PN2S moiety, was easily labelled with a ^{99m}technetium tricarbonyl approach in a one-step synthesis (useful in the design of a *commercial kit*) with good yields and without needing further purifications. Stability studies evidenced that the complex is stable to dilution and transchelation and, in addition, it shows a low protein binding. Finally, biodistribution studies showed high liver uptake,

followed by excretion via the hepatobiliary route. Despite this behaviour, the activity found in adrenals demonstrated the complex to maintain the specificity to bind sst receptors. Therefore, biodistribution data indicate that this sst analogous labelled with ^{99m}technetium tricarbonyl is promising for further investigation, such as receptor binding assays and biodistribution studies in AR42J tumour bearing mice, that are actually in progress.

The second part of the present work focused on the direct labelling with ^{188}Re of the tumour targeting agent hyaluronic acid. ^{188}Re-HA complex was obtained easily and with high yields, and stability tests showed that it was quite stable for one hour, as reported in chapter 4. However biodistribution studies demonstrated that this time was enough to permit the ^{188}Re-HA reaching the target organs: liver uptake of the injected compound takes place very rapidly since activity is almost completely concentrated in liver after 4 hours. This behaviour is probably related to the interaction of the complex with HARE receptors present in the liver. Moreover, since after the first hours there was not more radioactivity concentration in thyroid, kidneys and stomach that indicate the formation of perrhenate, we presume that ^{188}Re-HA was very stable in-vivo although the in-vitro stability was not very high. This labelled compound seems therefore to be a promising candidate to take forward for preclinical trials.

Chapter 5 reports dosimetry and therapeutic efficacy studies of ^{188}Re-HA on animals with induced liver cancer. Our objective when labelling HA with ^{188}Re, was to join the HA effect as tumour targeting molecule, to the DNA damage as result of ^{188}Re direct irradiation, and also the cytotoxicity caused by the activation of apoptosis pathways to obtain a more effective anticancer drug. The dosimetry data obtained in mice were then processed entering the experimental value of accumulated activity in each organ and using "S"-human values of the adult male phantom, obtaining thus the absorbed dose estimated for humans in Gy/GBq. The results showed that the absorbed dose in stomach in the human model was highly reduced with respect to the mouse model, and Re-188 β-ray irradiation will be almost completely absorbed within the liver and spleen increasing just it's self irradiation, as result of the larger organs size and greater distance between organs in human model. Concentration of liver enzymes in to the plasma samples confirmed that dosimetry data were calculated in the correct way since we found that the MTD in mice was ~40 Gy, and this value correlated to the human liver MTD reported from 20 to 45 Gy. Consequently, 7 GBq in human of ^{188}Re-HA administered in human would be able to

produce therapeutic effect in liver but at the same time it would be safe to other organs, since all of them received a dose much lower than the maximum tolerated absorbed doses.

Besides, ^{188}Re-HA can be administered by a simple intravenous injection, quite the opposite for ^{188}Re-HDD/lipiodol already used in clinical trials for the treatment of liver cancer. Lipiodol in fact needs well-trained personal for its administration, since it has to be injected through the hepatic artery under fluoroscopic control in order to increase the uptake on the cancer cells.

Finally, the ^{188}Re-HA therapeutic effect on animal models with induced liver cancer was proven since it was able to reduce metastasis both in number and dimensions, and it increased survival of mice. Therefore, ^{188}Re-HA seems to be a promising agent for the treatment of hepatocellular carcinomas showing also many advantages over Re-188-HDD/lipiodol, and is a good candidate to take forward for clinical trials.

Chapter 6 reports the labelling with ^{188}Re and biodistribution studies of hyaluronic acids with different (5, 10, 200 and 500 kDa) molecular weights. The aim of this work was to study the biodistribution of low molecular weight HAs, in order to establish if they could be used on bladder cancer treatment after conjugation with some antitumoural agents. Despite the good labelling yields obtained with 5 and 10 kDa HAs, the obtained compound showed high instability toward dilution and transchelation. This instability can be related to the number of coordination sites for the metal present on the HA backbone, which is widely lower for small polymers with respect to the larger ones. However, any further study could be carried out on these compound.

Contemporarily, HAs with high molecular weights were studied to determine if their *in vivo* behaviour could provide advantages in drug pharmacokinetics with respect to the polymer (70 kDa) previously reported. HAs 200 and 500 kDa were therefore labelled easily and with good yields, and the radiolabelled products showed good stability *in vitro.* Moreover, biodistribution studies evidenced that the larger polymer leads to higher liver capture when compared to the ^{188}Re-HA 70kDa studied in chapter 4. This specific uptake can lead to higher target to background ratios, thus allowing to reduce irradiation related toxicity to other organs. In conclusion, further investigations have to be carried out on the HMW HAs labelled with ^{188}Re to determine their pharmacokinetics in order to establish if their *in vivo* behaviour offers such an advantages with respect to ^{188}Re-HA 70kDa for their use as radiopharmaceuticals.